

**EVALUATION OF STONE DETERIORATION  
PROBLEMS OF ANAVARZA ARCHAEOLOGICAL  
SITE FOR THE PURPOSE OF CONSERVATION**

**A Thesis Submitted to  
the Graduate School of Engineering and Sciences of  
İzmir Institute of Technology  
in Partial Fulfillment of the Requirements for the Degree of**

**DOCTOR OF PHILOSOPHY**

**in Architectural Restoration**

**by  
Emre İPEKÇİ**

**November 2021  
İZMİR**

## ACKNOWLEDGMENT

I would like to express my sincere appreciation to all the people involved during this special experience. First of all, I would like to express my deepest gratitude to my supervisors Prof. Dr. Hasan Böke, Assoc. Prof. Dr. Rozelin Aydın and Assoc. Prof. Dr. Barbara Lubelli for their precious support, guidance and enthusiasm. I specially thank to Prof. Dr. Hasan Böke for his scientific and moral support during this study.

I am grateful to the doctoral committee members; Prof. Dr. Başak İpekoğlu and Prof. Dr. Alper Baba for their time and valuable contributions during this study, and I am also thankful to Assoc. Prof. Dr. Ali Akın Akyol and Assist. Prof. Dr. Funda Gençer for their attendance to my thesis defense seminar and their comments. I also thank to the Center for Materials Research at the İzmir Institute of Technology for SEM-EDS analyses.

I would like to thank to the Scientific and Technological Research Projects Funding Program (TUBITAK 1001) for supporting this study. I also would like to thank the Council of Higher Education for the one-year scholarship (YÖK/YUDAB) to make research abroad.

I would like to thank to my colleagues for all the fun and unforgettable memories that we have had at the Material Conservation Laboratory and at the Faculty of Architecture.

My special thanks to my dear friends Fulya Atarer, Keziban Çelik, Tuğçe Pekdoğan and mijn vriend Paul van Santen for their endless support, friendship and love.

And finally, I would like to thank to my beloved parents Nurgül İpekci, Ali İpekci and my sister Merve İpekci for their endless patience, support, encouragement and love.

# ABSTRACT

## EVALUATION OF STONE DETERIORATION PROBLEMS OF ANAVARZA ARCHAEOLOGICAL SITE FOR THE PURPOSE OF CONSERVATION

Archaeological sites, which are significant components of the cultural heritage, should be conserved as a whole with all their architectural and material characteristics following a multidisciplinary approach. In this study, the weathering processes of the standing and recently excavated limestones used in Anavarza archaeological site (Adana, Turkey) that was included in the UNESCO World Heritage Tentative List were investigated for planning the excavation works and necessary preservation measures. For this purpose, chemical, mineralogical, petrographic, microstructural properties, soluble salt content, moisture transport properties and bacterial distribution of limestone samples taken from weathered surfaces and sound stones were determined by using XRD, FT-IR, SEM-EDS, TG/DTA, polarizing microscope, IC, gravimetric methods and advanced molecular techniques.

The main weathering problem observed on the limestones is microbiological colonization. Results of mineralogical and petrographic analysis indicated that sound limestones were mainly consisted of calcite and quartz minerals, whereas, standing surfaces of the limestones were consisted of calcite, quartz, calcium oxalate (whewellite) and clay minerals. The chemical analysis indicated that the amount of SiO<sub>2</sub>, Al<sub>2</sub>O<sub>3</sub> and FeO on both standing and recently excavated surfaces are higher than the sound inner parts of the limestones due to presence of clays that promote the formation of biological growths. Microbiological results showed that bacterial communities on the standing, recently excavated surfaces and sound inner parts of the limestones are different.

The results of this study showed that the excavations should be carried out with remedial treatments to prevent further weathering of limestones in open air conditions.

**Keywords:** Anavarza, Archaeological Site, Limestone, Stone Deterioration

## ÖZET

### ANAVARZA ANTİK KENTİ TAŞ BOZULMA PROBLEMLERİNİN KORUMA AÇISINDAN DEĞERLENDİRİLMESİ

Kültürel mirasın önemli bileşenleri olan arkeolojik alanlar, multidisipliner bir yaklaşım gözetilerek tüm mimari ve malzeme özellikleriyle bir bütün olarak korunmalıdır. Bu çalışmada, UNESCO Dünya Mirası Geçici Listesi'nde yer alan Anavarza arkeolojik alanında, toprak üstünde kalan ve kazısı yeni yapılan kireçtaşlarında görülen bozulma ve nedenleri, kazı çalışmalarının planlanması ve gerekli koruma önlemlerinin alınması amacıyla araştırılmıştır. Bu amaçla bozulma görülen taş yüzeylerden ve sağlam taşlardan alınan kireçtaşı örneklerinin kimyasal ve mineralojik kompozisyonları, petrografik ve mikroyapısal özellikleri, çözünür tuz içeriği, nem taşıma özellikleri ve bakteri kolonizasyonu; XRD, FT-IR, SEM-EDS, TG/DTA, polarize mikroskop, IC, gravimetrik yöntemler ve ileri moleküler teknikler kullanılarak belirlenmiştir.

Anavarza arkeolojik alanı'nda kireçtaşlarında gözlenen temel bozulma türü biyolojik kolonizasyonlardır. Sağlam kireçtaşları temelde kalsit ve kuvars minerallerinden oluşurken, toprak üstünde kalan taş yüzeyleri kalsit, kuvars, kalsiyum oksalat (whewellite) ve kil minerallerinden oluşmaktadır. Hem toprak üstünde kalan hem de kazısı yeni yapılan kireçtaşı yüzeylerinde tespit edilen toplam SiO<sub>2</sub>, Al<sub>2</sub>O<sub>3</sub> ve FeO miktarı, kireçtaşının sağlam iç kısımlarından daha fazladır. Taş yüzeylerinde ince silt ve kil mineralleri ile birlikte yoğun biyolojik kolonizasyonlar bulunmaktadır. Deneysel sonuçlar, kireçtaşlarının toprak üstünde kalan, ve kazısı yeni yapılan yüzeylerinde ve sağlam iç kısımlarında farklı bakteri topluluklarının geliştiğini göstermiştir.

Bu çalışmanın sonuçları, açık hava koşullarında kireçtaşlarının daha fazla bozulmasını önlemek için kazıların iyileştirici koruma yöntemleriyle yapılması gerektiğini göstermiştir.

**Anahtar Kelimeler:** Anavarza, Arkeolojik Alan, Kireçtaşı, Taş Bozulması

# TABLE OF CONTENTS

LIST OF TABLES .....	viii
LIST OF FIGURES .....	ix
CHAPTER 1. INTRODUCTION .....	1
1.1. Problem Definition.....	1
1.2. Aim and Significance of the Study .....	1
1.3. Content of the Study .....	2
1.4. Study Area .....	3
1.4.1. Geographical and Meteorological Characteristics.....	3
1.4.2. The Ancient City of Anavarza.....	5
CHAPTER 2. STONE WEATHERING.....	11
2.1. Introduction.....	11
2.2. Stone Weathering.....	12
2.2.1. Weathering in natural environments.....	13
2.2.2. Salt deterioration.....	14
2.2.3. Atmospheric pollution .....	16
2.2.4. Biodeterioration .....	17
2.2.4.1. Biodeterioration mechanisms .....	18
2.2.4.2. Biofilms .....	19
2.2.4.3. Thriving microorganisms on stones .....	21
2.2.4.4. Bacterial colonization.....	21
2.3. Stone Conservation .....	23
2.3.1. Conservation Measures in Archaeological Sites .....	26
CHAPTER 3. METHODS .....	28
3.1. Site Survey .....	28
3.1.1. Visual observation .....	28
3.1.2. On site investigation .....	34
3.2. Sampling .....	35

3.3. Laboratory Investigation .....	39
3.3.1. Determination of Mineralogical Composition of Stone and Soil Samples .....	40
3.3.2. Determination of Chemical Composition of Stone and Soil Samples .....	41
3.3.3. Determination of Petrographic and Microstructural Properties of Stones .....	41
3.3.4. Determination of Soluble Salts .....	43
3.3.5. Determination of Moisture Transport Properties of Stones from the Historic Quarry .....	45
3.3.6. Determination of Bacterial Communities .....	48
 CHAPTER 4. RESULTS AND DISCUSSION.....	51
4.1. Mineralogical Composition of Stone and Soil Samples .....	51
4.1.1. Sound Inner Cores of Stone Samples .....	51
4.1.2. Weathered Surfaces of Stone Samples .....	52
4.1.3. Soil Samples .....	55
4.2. Chemical Composition of Stone and Soil Samples .....	55
4.2.1. Sound Inner Cores of Stone Samples .....	56
4.2.2. Weathered Surfaces of Stone Samples .....	56
4.2.3. Soil Samples .....	59
4.3. Petrographic and Microstructural Properties of Stone Samples .....	59
4.3.1. Sound Inner Cores of Stone Samples .....	60
4.3.2. Weathered Surfaces of Stone Samples .....	63
4.4. Soluble Salts of Stone and Soil Samples .....	68
4.5. Moisture Transport Properties of Stones .....	73
4.5.1. Moisture Transport Properties of Stones from the Historic Quarry .....	74
4.5.2. Moisture Transport Properties of Stones from the Site .....	77
4.5.3. Comparison of the Moisture Transport Properties of Stones from the Historic Quarry and the Site.....	79
4.6. Bacterial colonization of stones .....	80
4.6.1. Distribution on the phylum level .....	81
4.6.2. Distribution on the class level .....	85

4.6.3. Distribution on the genus level.....	86
4.7. General Evaluation of Deterioration of the Limestones in Anavarza...	89
 CHAPTER 5. CONCLUSIONS .....	 92
 REFERENCES .....	 95
 APPENDICES	
APPENDIX A. MINERALOGICAL COMPOSITIONS OF LIMESTONES (XRD PATTERNS) .....	104
APPENDIX B. MINERALOGICAL COMPOSITIONS OF LIMESTONES (FT-IR SPECTRUMS) .....	115
APPENDIX C. CHEMICAL COMPOSITIONS OF LIMESTONES (TGA CURVES) .....	126
APPENDIX D. SOLUBLE SALTS OF STONES (IC RESULTS) .....	137
APPENDIX E. SOLUBLE SALTS OF STONES (CONDUCTIVITY RESULTS)...	138
APPENDIX F. CHEMICAL COMPOSITIONS OF SOILS (EDS RESULTS) .....	139
APPENDIX G. MICROBIOLOGY RESULTS .....	140

## LIST OF TABLES

<b><u>Table</u></b>	<b><u>Page</u></b>
Table 1. Anamnesis, diagnosis and therapeutical steps.....	24
Table 2. State of preservation of assets classification (SP) (CEN 2021) .....	25
Table 3. Preservation condition class (PC) (CEN 2021).....	25
Table 4. Risk class (RC) with description of risk of loss (CEN 2021) .....	26
Table 5. Sample codes with indication of sampling location and damage.....	37
Table 6. Table showing the places where the scraped/chipped stone samples collected .....	38
Table 7. Analysis methods used in the research.....	40
Table 8. Weight losses (TG/DTA) and oxide composition (SEM/EDS) of stones .....	57
Table 9. Mean values and standard deviation (in parentheses) of major oxide compositions of soils (9 samples) (%) .....	59
Table 10. HMC and IC results of the samples from Alakapı .....	69
Table 11. Distribution of the bacteria phylum and classes.....	88



# LIST OF FIGURES

<b><u>Figure</u></b>	<b><u>Page</u></b>
Figure 1. The map showing the location of Anavarza.....	3
Figure 2. The air photo showing the ancient city of Anavarza surrounded by calcareous rocks .....	4
Figure 3. Average values of temperatures and maximum temperatures (°C) and average values of rainfall (mm) measured in 1991-2020 in Adana .....	5
Figure 4. Plan of the ancient city of Anavarza (Source: Gough 1952).....	6
Figure 5. The image showing the traces of processing in the quarry near the amphitheater area .....	7
Figure 6. The image of the triumphal arch (Alakapı) and the colonnaded road.....	7
Figure 7. The image of the triumphal arch (Alakapı).....	8
Figure 8. Stone columns on the colonnaded road.....	8
Figure 9. The image of the triumphal arch (Alakapı) in 1905.....	9
Figure 10. The images of the triumphal arch (Alakapı); in 2018 (A), during the restoration works in 2019 (B) and after restoration in 2020 (C).....	9
Figure 11. Deterioration on limestones in the forms of black crust, yellow patina, loss of cohesion, biological colonization, cracks .....	10
Figure 12. Biological colonization on the stones.....	10
Figure 13. Interactions between stone material, environmental conditions and biofilm, 1: Atmosphere and substrate interaction, 2: Atmosphere and biofilm interaction, 3: Interaction between metabolic compounds and substrate, 4: Physicochemical interaction between biofilm and substrate, 5: Physical forces due to microbial growth.....	20
Figure 14. Soiling on the excavated and black crust on the standing parts of stone surfaces.....	29
Figure 15. Yellow patina and black crust observed on the stone surfaces. ....	29
Figure 16. Exfoliation and spalling observed on stone surfaces.....	30
Figure 17. Scaling and hair cracks observed on stone surfaces.....	30
Figure 18. Crumbling and erosion observed on stone surfaces. ....	30
Figure 19. Scratch observed on stone surfaces.....	30
Figure 20. Thriving micro-organisms (lichens, algae, bacteria etc.) observed on stone surfaces .....	31

<b><u>Figure</u></b>	<b><u>Page</u></b>
Figure 21. Mapping of the weathering forms of stones used in the triumphal arch (Alakapı).....	32
Figure 22. Mapping of the weathering forms of stones used in the colonnaded road ....	33
Figure 23. Photo and thermal image of the standing parts and the excavated parts of the stone surfaces.....	34
Figure 24. Figure showing where the samples were collected .....	36
Figure 25. Figure showing the sample code .....	36
Figure 26. Thin section samples .....	42
Figure 27. Samples covered with epoxy resin and cut cross section samples .....	43
Figure 28. Powder samples for HMC measurements .....	44
Figure 29. Specimens for water absorption measurement .....	46
Figure 30. Sealed specimens for drying rate measurements.....	47
Figure 31. Cultivation of samples in R2A liquid medium.....	48
Figure 32. Growth of samples in R2A liquid medium .....	49
Figure 33. Growth of samples in R2A solid medium.....	49
Figure 34. X-ray diffraction (XRD) pattern and FT-IR spectra of sound limestone (A.in.2, A.in.3) (C: calcite, Q: quartz) .....	52
Figure 35. X-ray diffraction (XRD) pattern and FT-IR spectra of standing part of the column 3, sample C3.st.2 (C: calcite, Q: quartz, Wh: Whewellite, A: Amorphous substances (Aluminosilicates), O-H: Oxygen-Hydrogen bands, C-H: Carbon-Hydrogen bands).....	53
Figure 36. X-ray diffraction (XRD) pattern and FT-IR spectra of recently excavated part of the column 7, sample C7.ex.1 (C: calcite, Q: quartz, O-H: Oxygen-Hydrogen bands, C-H: Carbon-Hydrogen bands).....	54
Figure 37. X-ray diffraction (XRD) pattern and FT-IR spectra of the standing surfaces (sample A.st.3) of limestones (C: calcite, Q: quartz, Wh: Whewellite, G: Gypsum, O-H: Oxygen-Hydrogen bands, C-H: Carbon-Hydrogen bands) .....	55
Figure 38. XRD graphic of the soil (C7.so.1) (C: Calcite, Q; Quartz, An: Anorthite, M: Muscovite) .....	55
Figure 39. Total % amounts of clays (Al <sub>2</sub> O <sub>3</sub> , SiO <sub>2</sub> and FeO) of samples from inner cores and weathered surfaces .....	58
Figure 40. TGA curve of the standing surface of stone sample (C2.st.1) .....	58

<b><u>Figure</u></b>	<b><u>Page</u></b>
Figure 41. TGA curves of all stone samples.....	59
Figure 42. The stone samples for petrographic analysis.....	60
Figure 43. Macroscopic and microscopic images of sample C2.in.1 .....	60
Figure 44. Macroscopic and microscopic images of sample C3.in.1 .....	60
Figure 45. Macroscopic and microscopic images of sample C4.in.1 .....	61
Figure 46. Macroscopic and microscopic images of sample C9.in.1 .....	61
Figure 47. Macroscopic and microscopic images of sample C5.in.1 .....	62
Figure 48. SEM images of the sample C3.st.1, C3.st.2 and C3.st.3 .....	64
Figure 49. SEM image and EDS results of the intersection of the standing stone sample from the 3 <sup>rd</sup> column.....	65
Figure 50. SEM images of the deterioration layers on standing stone sample from the 3 <sup>rd</sup> column.....	65
Figure 51. SEM image and EDS mapping of the intersection of the standing stone sample from the 3 <sup>rd</sup> column.....	66
Figure 52. SEM image of the intersection of the standing stone sample from the 6 <sup>th</sup> column (C6.st.1), (M: microbiological formation, S: stone inside) .....	66
Figure 53. SEM images of the standing surface (C7.st.1) and the recently excavated surface (C7.ex.1) of the 7 <sup>th</sup> column .....	67
Figure 54. SEM image and EDS mapping of the intersection of the recently excavated part of the 7 <sup>th</sup> column (C7.ex.1) .....	68
Figure 55. Sample locations on the Alakapı .....	70
Figure 56. Ion content and HMC graphics of the sample A.st.3 and A.st.2 .....	71
Figure 57. Salt diagram of the sample A.st.3.....	72
Figure 58. Salt diagram of the sample A.st.2.....	73
Figure 59. Water absorption by capillarity of the limestones from the historic quarry.....	75
Figure 60. Stone samples after water absorption test, Q1 and Q3.....	75
Figure 61. Porosity of stone samples from the historic quarry .....	76
Figure 62. Drying rate properties of the limestones from the historic quarry .....	76
Figure 63. Water absorption by capillarity of the limestones from the site (C3, C8-1, C8-2).....	77
Figure 64. Stones from left to right: C3, C8-1, C8-2, before and after water absorption .....	78

<b><u>Figure</u></b>	<b><u>Page</u></b>
Figure 65. Drying rate properties of the limestones from the site (C3, C8-1, C8-2).....	78
Figure 66. Water absorption by capillarity of the limestones from the site (C3, C8) and from the historic quarry (Qave) .....	80
Figure 67. Drying rate properties of the limestones from the site (C3, C8) and from the historic quarry (Qave).....	80
Figure 68. Distribution of bacterial phyla of the samples from Alakapı (A.st.1, A.st.3), from the standing surfaces of the columns (C1.st.1-C9.st.1) and from the recently excavated surfaxes of the columns (C5.ex.1-C8.ex.1) (st: standing part, ex: excavated part, in: inner part).....	82
Figure 69. Samples from standing and recently excavated surfaces of the 5 <sup>th</sup> , 7 <sup>th</sup> , 8 <sup>th</sup> columns .....	84

# CHAPTER 1

## INTRODUCTION

### 1.1. Problem Definition

The stone monuments and findings, which are the documents of ancient civilizations, in archaeological sites are being deteriorated. In order to preserve stone monuments and archeological findings, their material characteristics, weathering processes, possible prevention and conservation measures need to be investigated.

In archaeological sites, standing, buried and excavated stones can degrade due to weathering, including repeated wetting-drying and freezing-thawing cycles, temperature and relative humidity changes, salt crystallization, atmospheric pollution, wind, rain and biological activities (Doehne and Price 2010, Camuffo 1995, Schaffer 1932, Kühnel 2002, Scherer 2006, Press and Siever 2002). Weathering processes of stone can lead to loss of material, discoloration/ deposits, detachment and fissures/ deformation (Fitzner et al. 1997).

One of the most important weathering processes affecting ancient monuments and archaeological sites, is bio-colonization by microorganisms. Those that originate from microorganisms in stone deterioration are named as biodegradation in general frame. Both the mineral structure of the stone and the environmental conditions to which they are exposed are influential in the distribution of bacterial communities, which directly determines the biodegradation process. To control microbiological deterioration, a detailed and interdisciplinary collaboration is essential for the conservation of the structures and artefacts in archaeological sites.

### 1.2. Aim and Significance of the Study

The aim of this study is the determination of the characteristics of stone materials used in Anavarza archaeological site, the weathering problems, their causes and prevention measures for the purpose of conservation. In this scope, the limestones of the columns present on the main street and of the triumphal arch (Alakapı) were investigated.

This study also aims to evaluate the effect of micro-organisms on stone surfaces related to other possible weathering agents (such as salts) by comparing the stone surface characteristics of the standing, recently excavated and sound parts of the stones. In this context, the relation between the stone weathering and the bacterial diversity on stone surfaces was investigated by using molecular based techniques.

Interdisciplinary collaboration is significant for the conservation of the structures and artefacts in archaeological sites. In this context, this study with a detailed microbiological research makes a valuable contribution to this area.

The ancient city of Anavarza (Anazarbos), chosen as the study area, was accepted in the UNESCO World Heritage Tentative List on April 15, 2014. In this respect, this research will serve as a resource for future studies in this area, and contribute to preserve an archaeological heritage that will be accepted as a World Heritage Site.

### **1.3. Content of the Study**

This study is composed of five chapters; introduction, stone weathering, methods, results and conclusion.

In the first chapter, problem definition, aim and significance of the study are presented. Then, study area is identified with its geographical and meteorological characteristics.

In the second chapter, stone weathering and possible decay reasons are explained in detail. Stone conservation and conservation measures in archaeological sites are discussed.

In the third chapter, site survey and sampling phases are discussed with reference to visual inspection and on site investigation. Then, the methods of the laboratory investigation applied on the stone and soil samples taken from the area, as well as on fresh stone samples from the historic quarry are described.

In the fourth chapter, experimental results are evaluated. First, mineralogical and chemical compositions of limestone and soil samples are identified. Then, petrographical and microstructural properties of stone samples are explained. Soluble salt content and moisture transport properties of limestones are explained. At last, bacterial colonization of stones are described in detail. In addition, overall assessment is done by using all obtained data.

In conclusion, all outputs regarding the characteristics of stones and weathering in the site are summarized.

## 1.4. Study Area

In this study, Anavarza archaeological site (Adana, Turkey) that was included in the UNESCO World Heritage Tentative List in 2014 was selected for planning the excavation works and necessary preservation measures.

### 1.4.1. Geographical and Meteorological Characteristics

The ancient city of Anavarza is the 1<sup>st</sup> Degree Archaeological Site in the vicinity of Dilekkaya Village, Kozan District, about 70 km northeast of Adana. The city is nearly 40 km distant from the Mediterranean Sea (Figure 1).



Figure 1. The map showing the location of Anavarza.  
(Source: Google Earth 2020)

It is an ancient city in the Cilicia region and surrounded by walls built on the plain at the foothills of the Anavarza Mountain lying in the north-south direction (Figure 2). The area has alluvial soils and agricultural activities have been widely carried out around the site. Carbonate-bearing rock types are common in the Cilicia region, crumbs and carbonates predominate especially in the Anavarza region (MTA 2021, Kaya and Yetiş 2020). Schist, dolomite and quartzite belonging to Paleozoic formations are in the north of the region as well as cretaceous limestones, conglomerates and granites are in the northeast (Ertunç 1991, Gök 2006). The city is in the third-degree seismic zone (seismic hazard in terms of seismic spectral acceleration values between 0.2 and 0.3 g, (g: 981 cm/s<sup>2</sup>)) according to the 1996 Turkey Seismic Hazard Map (AFAD 2021).



Figure 2. The air photo showing the ancient city of Anavarza surrounded by calcareous rocks (Source: Ergeç 2001, Adana İl Kültür ve Turizm Müdürlüğü 2021).

The average values of climatic data of the site for a long period (1991–2020) were taken from the Turkish State Meteorological Service (MGM 2021) (Figure 3). It shows monthly average temperatures and average relative humidity as well as monthly average rainfall values below (Figure 3).

The area has Mediterranean climate. Extremely high temperatures are recorded in the summer period; winter months are warm and rainy. During the winter months (December, January and February), average temperature is low and average rainfall is high. The rainfall is higher than 100 mm/m<sup>2</sup> in December and January (Figure 3). During the summer months (June, July and August) average temperature increases, average rainfall decreases (Figure 3). Average temperature values are between 9.5-29.2°C in a year and the maximum average temperature value is recorded in August. Average relative



humidity values are high almost all periods of the year, have been recorded between 45-66% (Figure 3).

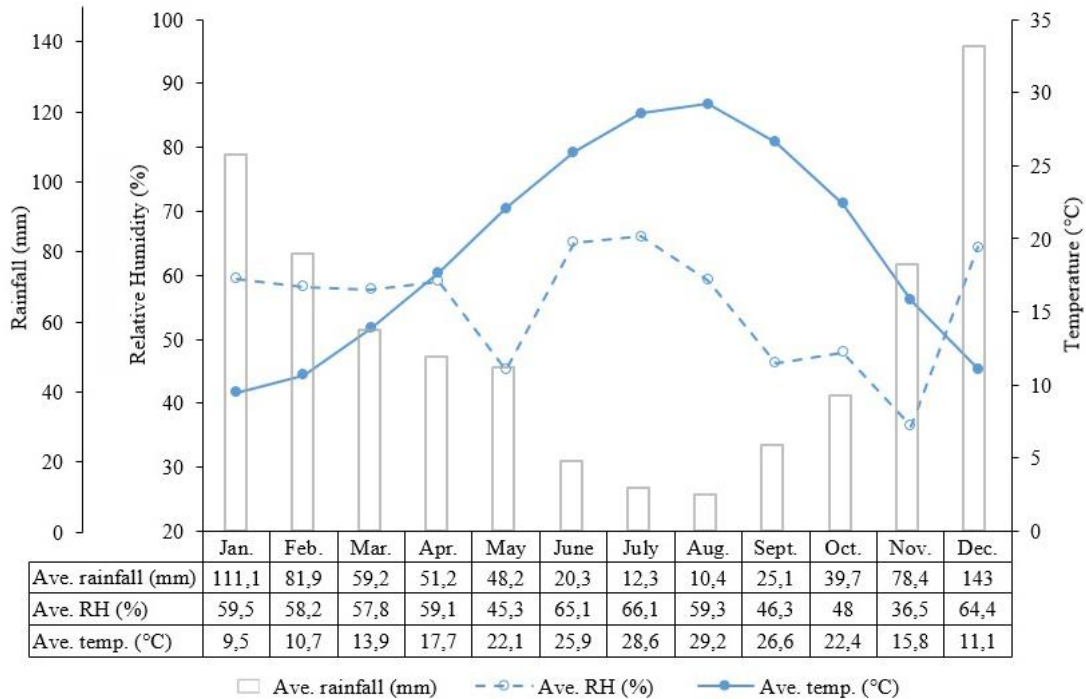


Figure 3. Average values of temperatures and maximum temperatures (°C) and average values of rainfall (mm) measured in 1991-2020 in Adana (Source: MGM 2021).

### 1.4.2. The Ancient City of Anavarza

The history of the Anavarza dates back to the 1st century BC based on the coins and inscriptions; however, recent excavations and researches revealed that its history dates back to the Hellenistic period (Gough 1952, Yüceer et al. 2021). The ancient city has been called many names such as Anazarba, Ayn Zarba, Anazarbos, Anazarbus and Anavarza (Gough 1952, Hançer 2016). The name Anazarbus is thought to come from the word "Nezarba", which means invincible in Persian (Gough 1952).

The city is divided into two parts: the lower settlement and the upper settlement. The lower settlement is located in the plains and is surrounded by walls while the upper settlement, including the castle, is located on the mountain (Gough 1952).

The lower settlement is surrounded by walls with five city gates that provide access to the city (Gough 1952). The city gates, the colonnaded road, baths, churches are some of the important structures in the lower settlement (Figure 4). The amphitheatre and the stadium are located outside of the walls. There are two aqueducts extending to the north: to Hacilar village (Sumbas stream) and to Gaziköy village (Buyruk 2016) (Figure 4).

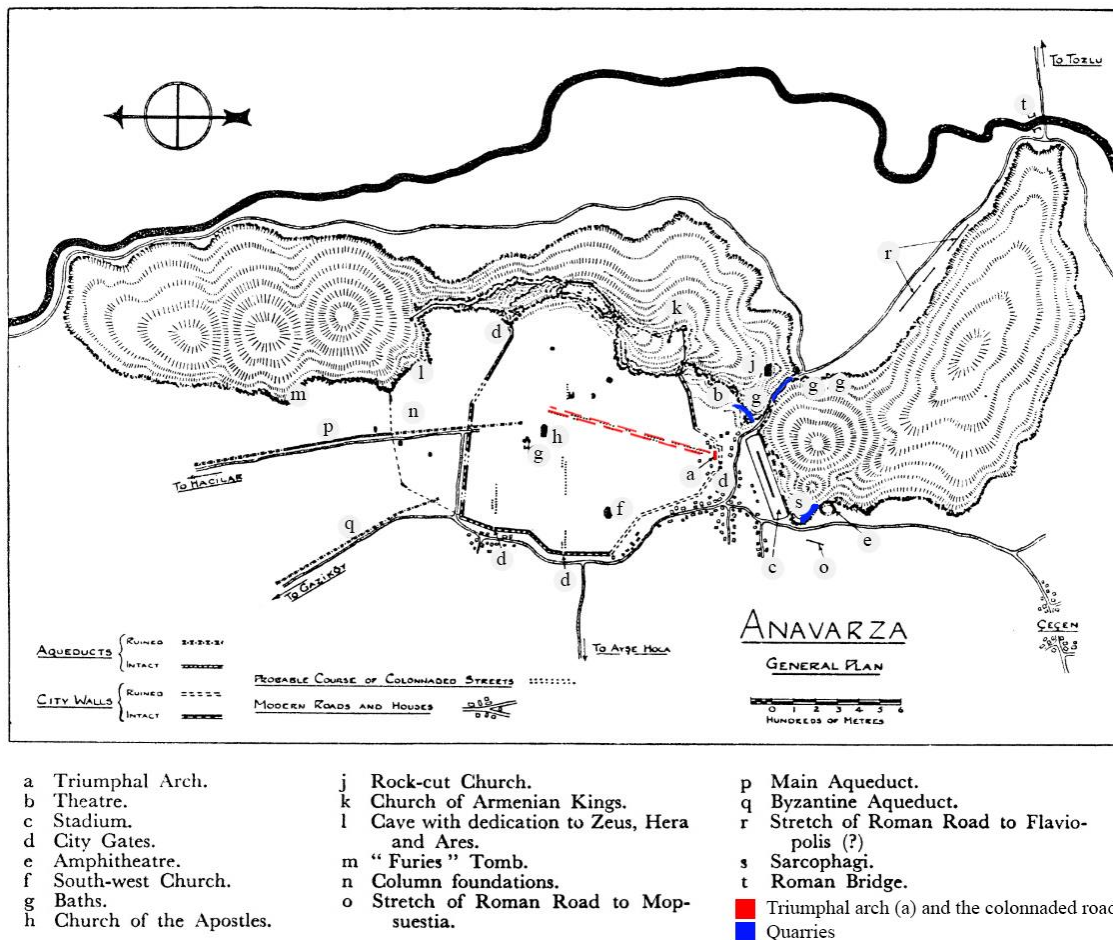


Figure 4. Plan of the ancient city of Anavarza.  
(Source: Gough 1952)

Anavarza is located in a flat area surrounded by calcareous rocks. The ancient city was built with limestones quarried from these rocks (Ergeç 2001). Three places are known to be used as quarry. These places are visible nearby the nekropol area, the amphitheatre area and the area called "Ali kesigi" (Figure 5).

The triumphal arch (Alakapı) is one of the important remaining structure of the Roman period on the site (Gough 1952) (Figure 6, 7). The colonnaded road starting from the triumphal arch is on south to north direction, approximately 1150 m. length and 30-34 m width (Buyruk 2016) (Figure 6). There are stone columns on both sides of this stone paved road (Figure 8).



Figure 5. The image showing the traces of processing in the quarry near the amphitheater area.



Figure 6. The image of the triumphal arch (Alakapı) and the colonnaded road.



Figure 7. The image of the triumphal arch (Alakapı).



Figure 8. Stone columns on the colonnaded road.

The excavations, which started in 2013 under the Directorate of the Adana Museum, are still ongoing. The excavations were especially carried out in the area around the triumphal arch (Alakapı) and the colonnaded road. Figure 9 shows the old image of the triumphal arch taken by Gertrude Bell in 1905 (Gertrude Bell Archive). Restoration works of the triumphal arch started in 2017 and completed in 2020 (Figure 10).



Figure 9. The image of the triumphal arch (Alakapı) in 1905  
(Source: Gertrude Bell Archive)



Figure 10. The images of the triumphal arch (Alakapı); in 2018 (A), during the restoration works in 2019 (B) and after restoration in 2020 (C).

The structures of the city are mostly made of limestone. Different types of deterioration can be seen on the surfaces of the stone materials. Discoloration, disintegration, cracking and biological growth were observed on the limestone walls and columns in the area, described in details in section 3.1.1. (Figure 11, 12).



Figure 11. Deterioration on limestones in the forms of black crust, yellow patina, loss of cohesion, biological colonization, cracks.



Figure 12. Biological colonization on the Stones.

## CHAPTER 2

### STONE WEATHERING

#### 2.1. Introduction

Natural stones have been widely used for many purposes from the ancient times. They are significant components of the built heritage that should be conserved as a whole with all their architectural and material characteristics.

Stone deterioration can occur in different forms and depending on different weathering conditions. It is of utmost importance to investigate the cause and source of the deterioration before any measures can be taken to prevent further stone degradation and before any conservation technique is applied. It is stated in international regulations on conservation that this is an expertise that will require interdisciplinary study among different disciplines. The need of preservation of archaeological monuments and findings was first reported on the Madrid Conference in 1904 (Locke 1904). Then, Athens Charter in 1931, emphasized the necessity of interdisciplinary collaboration and the use of modern techniques and materials in conservation works (ICOMOS 1931). The Recommendation on International Principles Applicable to Archaeological Excavation accepted in 1956 by UNESCO, strongly recommended leaving the archaeological sites partially or totally unexcavated in the case of lack of sufficient excavation methods, proper maintenance and conservation methods (UNESCO 1956). All these decisions were supported in the Venice Charter in 1964, Article 2 of the charter underlines that “The conservation and restoration of monuments must have recourse to all the sciences and techniques which can contribute to the study and safeguarding of the architectural heritage” (ICOMOS 1964). When considered in this context, it is clear that the conservation can not only be the responsibility of the architect or archaeologist, and that all necessary specialist areas should be involved.

## 2.2. Stone Weathering

Stone weathering has been an important concern for centuries as many historical buildings and artefacts have been constructed with natural stones worldwide. Thus, studies on stone weathering are quite extensive. Among all of these studies, “The Weathering of Natural Building Stones” (Schaffer 1932) is one of the first detailed resources on stone deterioration. In this book, weathering associated with chemical and physical phenomena, soluble salts and living organisms are explained. Besides, the book of Doehne and Price (2010) is another comprehensive source that makes an overview of current research on stone deterioration. Numerous international conferences have been held in this field. The “International Congress on Stone Decay and Conservation” is one of the important conferences that has been held every three or four years since 1972. The title of the last conference was “Monument future: decay and conservation of stone” was held in 2020 (Stone 2020).

Stone is one of the durable materials, however it deteriorates over time as a result of the interaction between the stone and its environment. Several factor(s) from stone itself (e.g. type, origin, mineral structure) and from the environment (e.g. temperature, RH, wind, atmospheric pollution) are affecting in stone deterioration (Scherer 2006).

The durability of stones depends on their mineralogical, chemical, physical and mechanical properties (Gauri and Bandyopadhyay 1999). Depending on temperature and relative humidity changes in the environment, drying-wetting and freezing-thawing cycles, swelling-shrinkage of clays, crystallization and dissolution of salts occur. The recurrence of these cycles cause differential stresses on stone material and accelerate deterioration process (Doehne and Price 2010, Lee and Yi 2007, Scherer 2006, Camuffo 1995). Air pollution, biological growth (by producing acids) and chemicals used in previous conservation treatments can increase acidic environment on stone surfaces and cause chemical deterioration (Doehne and Price 2010, Press and Siever 2002). Natural disasters (e.g. earthquake, fire, flood), war, vandalism and improper conservation studies can generally lead to mechanical deterioration (Doehne and Price 2010, Press and Siever 2002).

Stone monuments and findings in archaeological sites are highly susceptible to deterioration after excavation. Soluble salts and clay minerals are not effective on buried stone since there is no wetting and drying cycles under the soil. However, they cause



rapid deterioration with the formation of wetting and drying cycles after the stone is unearthed (Thorn et al. 2002). Since stones are exposed to atmospheric conditions after excavation, they are colonized by microorganisms and thus deteriorate rapidly. Besides, the exposure time to atmosphere has impact on microbial composition on stones (Gorbushina and Broughton 2009).

The diagnosis of weathering processes affecting structures and artefacts in archaeological areas is essential to preserve cultural heritage. Possible decay reasons mentioned above could be classified into three groups: the natural environment (e.g. water, wind, temperature, RH), man-made decay (e.g. vandalism, air pollution, incompetence material) and biological deterioration (plants, microorganisms). In this respect, weathering in natural environment is explained in the next section, salt deterioration, air pollution, and then biodeterioration, which is the most observed damage type in the area, are considered in detail in the following sections.

### **2.2.1. Weathering in Natural Environments**

The presence of water (e.g. rain water, moisture) as well as the pores and fractures in the stone that allow the water to enter the stone masses are effective in stone deterioration (Gauri and Bandyopadhyay 1999). Once the stone material is exposed to water, differential stresses could occur on the stone material with the effect of wetting-drying and freezing-thawing cycles, swelling-shrinking of clays, crystallization and dissolution of salts, and this causes stone deterioration (Doehne and Price 2010, Lee and Yi 2007, Scherer 2006, Camuffo 1995).

Wetting leads to water absorption on the stone. This may cause the stone to expand and/or reduce the cohesiveness between the mineral grains. In this way, wetting and drying cycles cause damage on the stone (Gauri and Bandyopadhyay 1999). Freezing and thawing cycles occur in cold climates. Water enters cracks and pores in the stone and freezes at lower temperatures. This activity, called frost action, causes stone degradation depending on behavior of water at freezing temperature, intensity, rate and duration of freezing, and characteristics of rock (Gauri and Bandyopadhyay 1999).

Carbonate rocks generally contain clays. These clay minerals are one of the possible damage agents of stone deterioration. Since clay minerals have high surface area to volume ratio, their water-absorption capacity is high as well (Gauri and

Bandyopadhyay 1999). When the stone material is exposed to water, clays expand. With the effect of drying-wetting activities, swelling and shrinking of clays repeats and damaging stresses can occur (Scherer 2006).

One of the mechanisms that cause stress on the stone is salt damage and is explained in detail in the section below.

### **2.2.2. Salt Deterioration**

Salt crystallization is one of the main causes of damage of materials in historical buildings as well as in structures and artefacts in archaeological sites (Schaffer 1932, Price 1996). Salt deterioration is affected, next to the type of salts, by the properties of the material (e.g. type, porosity) and by the environment (e.g. temperature, relative humidity, amount and intensity of precipitation) (Charola and Bläuer 2015).

Soluble salts may have multiple sources: air pollution, salts from sea or desert, soil, deicing salt, inappropriate cleaning materials or treatments. They can be carried from the soil to the building structure e.g. by rising damp of ground water or be transported by the wind from the sea shore or the desert. Another origin of salts can be the atmospheric pollution (see section 2.2.3), as polluted air can contain high amount of sulphate and nitrate (Price 1996). Besides, salts can originate from man-made materials: for example, bricks can contain sodium sulfate if these elements were present in the original clay and the bricks were not fired properly. Moreover, the use of the buildings (e.g. stable, salt storage) can be another source of salts (Price 1996, Charola 2000, Charola and Bläuer 2015).

Salts can enter and be transported in the porous building materials in the presence of water. Common moisture sources are e.g. capillary rise of groundwater, infiltration by rain water and surface condensation (Charola 2000). Salt can only move through pores and cracks of the material by dissolving in water. When the salt solution is (super) saturated, salts will crystallize.

Salt crystallization pressure is generally considered as the main damage mechanism in salt contaminated materials (however, other mechanisms such as chemical weathering, sulphation cannot be excluded) (Goudie and Viles 1997). Repeated dissolution and crystallization cycles lead to accumulation of salts and, if the pressure produced by crystallization overcomes the tensile strength of the material, damage occurs (Steiger et al. 2011, Price 1996).

Every salt can cause crystallization damage, however only salts which have one than more hydration state can cause both, crystallization and hydration damage, e.g. sodium sulfate, as either the anhydrous salt thenardite ( $\text{Na}_2\text{SO}_4$ ) or the decahydrate mirabilite ( $\text{Na}_2\text{SO}_4 \cdot 10\text{H}_2\text{O}$ ) (Charola 2000). When the salt is hydrated, its volume increases and this may cause hydration pressure.

Each salt has different solubility capacity in water. Soluble salts can be classified into two groups: slightly soluble salts (e.g. gypsum), highly soluble salts (e.g. sodium chloride, sodium nitrate). Chlorides and nitrates are the highly soluble salts while gypsum and calcite are slightly soluble salts (Charola and Bläuer 2015).

Generally, more than one salt could be found in building materials. When a salt mixture is present, the solubility of each salt is affected by the others, i.e. if the two salts with a common ion in solution, their solubilities increase, if no common ion, only the solubility of less soluble salt increase (Charola and Bläuer 2015). For example, in the case of gypsum and calcite, their solubilities increase when they present with salts such as NaCl or KCl (Charola and Bläuer 2015). Besides, when the relative humidity of equilibrium of gypsum gets lower, when this is present in a mix with other salts; as a consequence, the frequency of the crystallization-dissolution cycle increases and even a quite harmless salt such as gypsum may become damaging (Charola 2000).

Salt deterioration is affected by the properties of the material (e.g. type, porosity) and by the environment (e.g. temperature, relative humidity) (Charola and Bläuer 2015):

*Material characteristics:*

The porous structure of the materials (e.g. porosity, pore size, pore distribution) plays an important role on the water (and thus salt solution) absorption and drying rate of the material. For instance, water evaporates fast in materials with large, well connected pores, more slowly in fine porous materials. Consequently, during evaporation, salts will tend to accumulate in the smaller pores (or in the material with smaller pores in the case of combination of materials).

- *Environmental factors:*

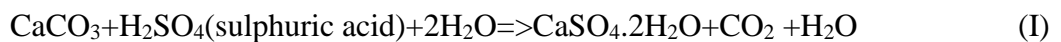
The climate of the area, air pollution, weather properties, e.g. temperature, relative humidity and their fluctuations are the main environmental factors affecting salt weathering on stone materials. Besides, shape of the building, the areas which shaded by trees or protected from rainwater, could be considered some environmental parameters (Charola 2000).

### 2.2.3. Atmospheric Pollution

Atmospheric pollution is one of the decay reasons affecting outdoor stone monuments. It's well known that global climate change and air pollution have critical impacts on heritage materials. Air pollution plays an important role on stone deterioration dependent on the climatic conditions and stone itself as well (e.g. type, shape, position on the facade).

The main gaseous pollutants which can cause damage on building materials are carbon dioxide (CO<sub>2</sub>), sulphur dioxide (SO<sub>2</sub>) and nitrogen dioxide (oxides) (NO<sub>x</sub>). These pollutants increase acidic environment on stone surfaces and lead to visual changes, the term "crust" is generally used for this weathering phenomena. The air pollution-related damage processes of stones are commonly acknowledged to be gypsum formation and carbonate dissolution (Sabbioni 2003).

Sulfur dioxide gas (SO<sub>2</sub>) is a major factor in the deterioration of calcite containing stones. SO<sub>2</sub> present in the polluted air reacts with calcite mineral of calcereous stones, in the presence of water and turns it to the gypsum based on the reaction below (Goudie and Viles 1997). Since the higher volume of gypsum than calcite crystals and the solubility of gypsum in water, damage occurs.



In addition, particulate matter such as fly ash from coal-fired power plants can accumulate on stone surfaces and contribute to the blackish appearance of the crusts (Del Monte and Sabbioni 1983, Balland-Bolou-Bi et al. 2016).

A number of studies on weathering crust formation from Budapest (Török 2002), Venice (Maravelaki-Kalaitzaki and Biscontin 1999) and Germany (Graue et al. 2013) have been carried out to determine the effect of air pollution on stone deterioration. Different types of crusts were described on limestones from a polluted atmospheric area in Budapest and categorized into four groups: thick white crust, thin white blistering crust, thick framboidal black crust and thin laminar black crust (Török 2002). In this study, gypsum (alongside calcite) was determined in all crust formations as a result of atmospheric pollution, it was highly present in thin white blistering crust (up to 70%) and thick framboidal black crust (more than 60%) (Török 2002). Similarly, another study on weathering crust formation from Istria stone in Venice carried out by Maravelaki-Kalaitzaki

and Biscontin (1999) showed gypsum presence in the dendritic black crusts (54,8%) and in the compact black crust (12,6%). In other study, weathering crust formation from three historic cathedrals located in different environments; the industrial (Cologne), rural (Altenberg) and urban (Xanten) areas in Germany was investigated (Graue et al. 2013). In comparison to gypsum formations from these three different cathedrals, the results showed that Cologne had a high accumulation of large gypsum crystals, Xanten had smaller and less abundant and Altenberg had fine grained, present in the form of salt efflorescence. It was concluded in a direct correlation between intensity of the damage in different environments and SO<sub>2</sub> concentration in the air (Graue et al. 2013).

#### **2.2.4. Biodeterioration**

One of the weathering processes affecting ancient monuments and archaeological sites, is bio-colonization by microorganisms. Those that originate from microorganisms in stone deterioration are named as biodegradation in general frame. Both the mineral structure of the stone and the environmental conditions to which they are exposed are influential in the distribution of microbiological communities, which directly determines the biodeterioration process (Scheerer et al. 2009, Warscheid and Braams 2000).

Microbial communities can heavily colonize stone materials in favorable conditions and this may result in discoloration, colored patinas, pitting, erosion, cracks and even severe damages. Microorganisms can easily multiply within the fractures and pores which are formed by the physical, chemical and other factors of the stones in their own structures and cause macro and micro cracks. These organisms accelerate physical deterioration by applying pressure on the pores of the stones as well as chemical deterioration by creating an acidic environment (Urzi and De Leo 2001). They can produce some type(s) of acids (e.g. sulfuric acid, oxalic acid) by the result of their metabolic activity and then cause chemical deterioration of the stone surface by reacting with the stone minerals (Scheerer et al. 2009, Warscheid and Braams 2000). In addition to this, some microorganisms such as bacteria, fungi can penetrate into the materials and cause severe damage due to metabolic functions, enzymatic activity and mechanical attack (Sterflinger and Piñar 2013).

Biological growth develops depending on stone substrate and environmental factors (Warscheid and Braams 2000). Bioreceptivity is the term that defines the ability

of the substrate to be colonized (Guillitte 1995). The concept mainly remarks that different types of stones could be colonized differently in the same environmental conditions. Accordingly, it is extremely important to determine stone characteristics and environmental factors that affect biodeterioration.

*Stone characteristics:*

Stone characteristics such as chemical composition, porosity, permeability and roughness play role on the development of the microorganisms (Guillitte 1995, Warscheid and Braams 2000). High porosity and rough surfaces enable the attachment and colonization of microorganisms on the substrate easily (Caneva et al. 2008). High porosity creates a suitable environment for microbial growth as it facilitates the penetration of moisture deep into the stone. Besides, stone material with a long water retention time offers appropriate conditions for biological colonization (Warscheid and Braams 2000). Additionally, the chemical composition of the stone is important in terms of the amount of degradable minerals (e.g. feldspars, iron and clay minerals) as they can be nutrients for microorganisms (Caneva et al. 2008).

*Environmental factors:*

Environmental factors are strongly associated with biological attack on stone materials. Water, light, temperature, pH, CO<sub>2</sub>, air pollution, neighbouring different material etc. have impact on microbial colonization. Water plays a primary role in biodeterioration. The amount and availability of water determines the rapidity at which a surface is colonized and therefore reducing water is important for prevention of biodeterioration (Caneva et al. 2008). Light is a limiting factor, it is the main source for photosynthesizing organisms such as algae, mosses and lichens to obtain energy. Temperature is another parameter, microorganisms can survive in a wide range of temperature due to their resistance ability (Caneva et al. 2008). Additionally, air pollution (e.g. acid rain) might provide a suitable environment for microbial growth by supplying nutrients (Scheerer et al. 2009) and airborne pollutants may deposit on stone surfaces as well and this influences biological colonization (Zanardini et al. 2000).

#### **2.2.4.1. Biodeterioration Mechanisms**

Microorganisms can cause deterioration on stone through different mechanisms such as discoloration, biocorrosion and/or biofilm formation (Warscheid and Braams 2000). Discoloration is mainly accepted as an aesthetic problem that could be seen on the

stone surface in different colors thanks to the pigmentation ability of microorganisms (Scheerer et al. 2009). Pigment production (e.g. melanin, chlorophyll) is related to both genetic factors (on species level) and environmental factors (e.g. pH, light) (Caneva et al. 2008). Chlorophyll is a green photosynthetic pigment produced by cyanobacteria and algae while melanin is another pigment which is produced by several bacteria (Urzi et al. 1992, Warscheid and Braams 2000). Carotenoid pigments appear as red, yellow, orange, brown stains on stone surfaces and produced by cyanobacteria, algae, bacteria or archaea. Especially, salt-loving, halophilic microorganisms are pink-red colored because of having high amount of carotenoid in their cell membrane (Oren 2009, Schröer et al. 2021).

Microorganisms could produce organic and inorganic acids and this enables to biocorrosion of stones. Chemolithotrophic organisms release inorganic acids (e.g. nitric acid, sulfuric acid) while chemoorganotrophic organisms release biocorrosive organic acids (e.g. oxalic acid) by the result of their metabolic processes, and besides chemoorganotrophic bacteria and fungi can oxidize metals like Fe and Mn (Warscheid and Braams 2000, Scheerer et al. 2009). Sulfuric acid is produced by sulfur-oxidizing bacteria and nitric acid is generally produced by nitrifying bacteria (Sand 1997). Oxalic acid is formed by fungi, lichen, cyanobacteria and some bacteria, and this cause whewellite and weddelite minerals (calcium oxalate) on calcereous stones by the reaction between oxalic acid and calcium carbonate (Del Monte and Sabbioni 1983, McNamara and Mitchell 2005). Since calcium oxalate is less soluble in water than calcium carbonate, this calcium oxalate formation generally considered as a protective layer (McNamara and Mitchell 2005).

Biofilm formation is another biodeterioration mechanisms on stones, is explained in detail in the following section.

#### **2.2.4.2. Biofilms**

Biofilms are complex heterogeneous microbial communities in which microbial cells are embedded in extracellular polymeric substances (EPS) (Costerton et al. 1995). The EPS provides to adhere microbial cells to each other and to substrate surface as well (Costerton et al. 1995). In this way, biofilm formation enables many advantages to the microbial community: increasing communication and genetic exchange between microorganisms (Martino 2016), and adaptation to varied environmental stresses such as

biocides, disinfectants, nutrient deficiency (Gaylarde and Morton 1999, Costerton et al. 1995, Kemmling et al. 2004). Additionally, the EPS causes contamination of the substrate easily by airborne particles, aerosols, minerals and organic compounds due to the adhesion ability (Costerton et al. 1995, Kemmling et al. 2004).

Biofilms lead to accelerating of the deterioration of the stone material due to the presence of active microorganisms and their metabolic products (e.g. acids, pigments) (Gaylarde and Morton 1999). They can develop on stone surfaces as well as fissures and cracks by forming physical forces (Figure 13) (Beimforde 2011). Additionally, biofilms may modify the water content, water permeability, the pore size and surface hardness of the stone (Warscheid and Braams 2000).

Biological processes are considered as irreversible, biodeterioration lead to structural and aesthetic damage that modifies the sustainability of the building (Ciferri et al. 2000, Balland-Bolou-Bi et al., 2016). On the other hand, biofilm formation on stone surfaces might be deteriorative and protective as well, and thus their physical and chemical interaction with the stone substrate have to be worked in detail (Dornieden et al. 2000).

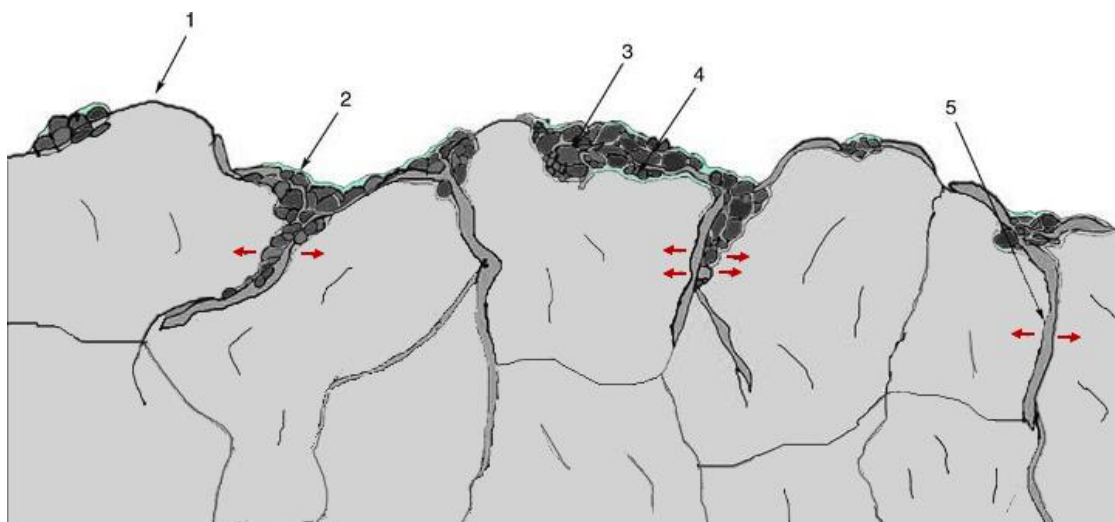


Figure 13. Interactions between stone material, environmental conditions and biofilm, 1: Atmosphere and substrate interaction, 2: Atmosphere and biofilm interaction, 3: Interaction between metabolic compounds and substrate, 4: Physicochemical interaction between biofilm and substrate, 5: Physical forces due to microbial growth (Source: Beimforde 2011)



### **2.2.4.3. Thriving Microorganisms on Stones**

Microorganisms (e.g. fungi, algae, archaea, lichen, bacteria) may use the substrate for attachment to the surface as well as having nutrient and energy source (Dornieden et al. 2000). Microorganisms can be divided into three groups that depends on the way of obtaining energy: Phototrophic, chemoorganotrophic and chemolithotrophic organisms (Scheerer et al. 2009).

Phototrophics such as cyanobacteria and algae are considered the first colonizers on historic stone buildings (Tiano 2002). These microorganisms obtain energy by using sunlight during photosynthesis. They can create biofilms and be visible as green to black stains on stone surfaces (Scheerer et al. 2009). Phototrophic microorganisms can develop on stone surface and/or penetrate into the pores and fissures of the stone, besides they can grow under a thin stone layer to provide protection against hot temperature and UV-radiation (Warscheid and Braams 2000).

Chemoorganotrophics are fungi, actinomycetes and non-filamentous bacteria, they use organic matter to obtain energy. Chemolithotrophic organisms such as sulfur oxidizers, nitrifying bacteria need specific inorganic compounds (e.g. ammonia, nitrites, sulphide) as energy sources and produce some acids (e.g. nitric acid, sulfuric acid) (Warscheid and Braams 2000).

Microorganisms can grow in different parts of the stone: epilitic organisms on stone surfaces, chasmolitic organisms in small cracks and fissures, endolithic organisms inside the stone (Tiano 2002).

### **2.2.4.4. Bacterial Colonization**

Bacterial communities (especially belonging to Cyanobacteria groups) play powerful role on biodeterioration process. The mineral structure of the stone and the environmental conditions to which they are attached are also influential in the distribution of bacterial communities. The pH of the substrate, substratum, water, temperature, light and CO<sub>2</sub> play role on the development of the microorganisms (Stewart 2012, Warscheid and Braams 2000, McNamara and Mitchell 2005). A significant correlation between pH of the stones and damage was determined in the bacterial colonization on historic limestones in United Kingdom by Skipper and Skipper (2014). The increased acidity on stone surfaces was concluded likely related to the impact of air pollution in the area, as

well as bacterial colonization that could produce acid (Skipper and Skipper 2014). Another study on bacterial distribution on stones from three different environments in the West Lake Cultural Landscape in Hangzhou of China indicated the dominant Cyanobacteria colonization in the area were correlated with the light intensity and air humidity (Li et al. 2016).

Bacteria are categorized as autotrophic and heterotrophic bacteria based on their energy requirements. Autotrophic bacteria are found inside the stone whereas heterotrophic bacteria are found on surface of the stone. As autotrophic bacteria, sulphur bacteria obtain their energy from oxidation of organic sulphur compounds like sulphides and nitrifying bacteria obtain their energy from inorganic compound of nitrogen like ammonia and nitrous acid (Mishra 1995, McNamara and Mitchell 2005). Sulfuric acid is formed mainly by bacteria belonging to the genus *Thiobacillus* while nitric acid is generally produced by nitrifying bacteria of the genera *Nitrosomonas* (or *Nitrosovibrio*) and *Nitrobacter* (Sand 1997). Heterotrophic bacteria is related to organic substances found on stone surfaces (Mishra 1995, McNamara and Mitchell 2005).

Recent studies carried out on bacterial colonization on limestones (summarized in detail below) have shown that bacterial species belonging to the phylum Cyanobacteria, Actinobacteria, Proteobacteria and Archaea are frequently detected on cultural heritage monuments, and other phyla such as Bacteroidetes, Firmicutes, Phodothermaeota, Acidobacteria, etc. have also been found (McNamara et al. 2006, Gaylarde et al. 2012, Mihajlovski et al. 2017, Pinheiro et al. 2019, Schröer et al. 2020, Coelho et al. 2021).

Cyanobacteria (and algae) is pioneer organisms on stone surfaces with their high colonization capability and has been detected in many cultural heritage sites in different climates (Caneva et al. 2008). Cyanobacteria can adapt to survive in extreme habitats thanks to their thick outer envelope and protective pigments (Crispim and Gaylarde 2005). The presence of cyanobacteria on stone surfaces in tropical climates, for example in the monuments of the Angkor Wat Complex, Cambodia, is associated with their resistance to desiccation and high solar radiation (Gaylarde et al. 2012).

Actinobacteria and Proteobacteria have been predominantly detected in bacterial communities on limestones at different sites. The bacterial distribution of the limestones from the ruins of the Chaalis Abbey, France showed that Alphaproteobacteria (40.2%) and Actinobacteria (38.7%) were the dominant phyla (Mihajlovski et al. 2017). Bacterial distribution on Lede stone from the urban (Ghent) and rural (Berlare) area in Belgium showed that Actinobacteria (33%) and Proteobacteria phyla (32%) were mainly found in

Ghent while Actinobacteria phylum were dominant in Berlare (71%) (Schröder et al. 2020). Bacterial distribution on limestone walls of the Old Cathedral in Coimbra, Portugal indicated that the major bacterial populations belonged to Actinobacteria, Proteobacteria, Bacteroidetes and Cyanobacteria in all samples (Coelho et al. 2021). Bacterial distribution on limestones from the Maya Archaeological Site Ek'Balam in southern Mexico indicated that Proteobacteria (the Alphaproteobacteria) was the dominant group and a large number of Actinobacteria and a number of photosynthetic microorganisms were detected in the epilithic community while Actinobacteria was the dominant, and a large number of Acidobacteria and low Firmicutes were identified in the endolithic community as well (McNamara et al. 2006).

Actinobacteria (e.g. the genera *Rubrobacter*, *Arthrobacter*, *Crossiella*) may frequently develop on the stone material due to their filamentous growth and effective use of various nitrogen and carbon sources (Saarela et al. 2004). Proteobacteria phylum have Alphaproteobacteria (e.g. the genus *Sphingomonas*) which is phototrophic, Betaproteobacteria and Deltaproteobacteria that are chemolithotrophic including nitrifying bacteria (e.g. the genus *Nitrosomonas*) and sulfur/iron reducing bacteria (e.g. the genus *Thiobacillus*) (Pinheiro et al. 2019). Metabolic remains of these nitrifying bacteria and sulfur/iron reducing bacteria (inorganic acids) have an important impact on deterioration of stone structures (Zurita et al. 2005).

In addition to bacterial community, archaea play a critical role on stone deterioration. They develop slowly in extreme ecosystems such as salinity, high acidity or high temperature (Caneva et al. 2008). The genus *Halococcus* is one of the halophilic (salt-loving) archaea that commonly found in salt attacked monuments and thus salt crusts, salt efflorescences provide an appropriate environment for development (Steiger et al. 2011, Ethenauer et al. 2014, Piñar et al. 2009). *Halococcus* have been detected in many salt attacked monuments, for example on sandstones of the Portchester Castle, UK (Zanardini et al. 2016), on the limestone walls of the Old Cathedral in Coimbra, Portugal (Coelho et al. 2021) and in chapel of St. Virgil in Vienna, Austria (Piñar et al. 2009).

### **2.3. Stone Conservation**

Stone conservation is an interdisciplinary and multi-stage work that plays a critical role in the preservation of our built cultural heritage. The systematic approach for

effective and sustainable monument conservation includes three steps: anamnesis, diagnosis and therapeutical steps described in Table 1 (Fitzner 2002).

Table 1. Anamnesis, diagnosis and therapeutical steps  
(Source: Fitzner 2002)

Anamnesis	Monument identification, historical background, location, environmental parameters, etc.
Diagnosis	Building materials, material characteristics, state of deterioration, deterioration processes and factors, intensity of damages and need of preservation measures, etc.
Therapeutical Steps	Conception, calculation, test application and implementation of preservation measures, long-term observation, maintenance, etc.

Identification of the building(s) including its historical background and environmental parameters is the first step of stone conservation works (see section 1.4). In the diagnosis part, conservation studies have been carried out by visual observation in situ and by using mapping method (see section 3.1). The mapping provides a detailed documentation of the stone weathering including type, extent and distribution of weathering forms (e.g. loss of stone material, detachment). Based on mapping results, sampling is performed for experimental investigations (see section 3.2). To make a comprehensive diagnosis, samples should be taken from unweathered, weathered and treated stones (Fitzner 2002). In experimental study (see section 3.3.), various techniques can be used to determine characteristics of stones, both sound and weathered parts (e.g. mineralogical, chemical, textural) and to understand weathering processes and causes. Based on all of these studies, conservation strategies should be determined.

The European standard titled “EN 17652, Cultural heritage - Investigation and monitoring of archaeological deposits for preservation in situ” explains the necessary investigations for in-situ preservation and monitoring of archaeological sites (CEN 2021). Based on this standard (CEN 2021), assessment of the state of preservation of archaeological materials, evaluation of the preservation conditions of archaeological deposits and risk classification could be determined to make an overall assessment of the archaeological site (see section 4.7.).

In the European standard above-mentioned, the state of preservation is classified into four groups (Table 2). The classification should be specific for the site, not comparable between different sites. Different materials in the site and their significance should be considered and then their state of preservation should be determined (CEN 2021).

Table 2. State of preservation of assets classification (SP)  
(Source: CEN 2021)

State of preservation of assets class (SP)	Description
SP 4	Excellent state of preservation
SP 3	Good state of preservation
SP 2	Poor state of preservation
SP 1	Very poor state of preservation

Preservation conditions could be different in some part of the site than the others. The condition classes are described in the Table 3 below.

Table 3. Preservation condition class (PC)  
(Source: CEN 2021)

Preservation conditions class (PC)	Description
PC 4	Excellent preservation condition
PC 3	Good preservation condition
PC 2	Poor preservation condition
PC 1	Very poor preservation condition

For risk assessment, the scores determined on the tables above (Table 2, 3) are used, and thus risk classes are determined (Table 4).

Table 4. Risk class (RC) with description of risk of loss  
(Source: CEN 2021)

	SP 4 Excellent	SP 3 Good	SP 2 Poor	SP 1 Very poor		Risk class (RC)	Description of risk
PC 4 Excellent						RC A	Low risk of loss of significant heritage material
PC 3 Good						RC B	Medium risk of loss of significant heritage material
PC 2 Poor						RC C	High risk of loss of significant heritage material
PC 1 Very poor						RC D	Immediate risk of loss of significant heritage material

### 2.3.1. Conservation Measures in Archaeological Sites

Stone monuments in archaeological sites are at risk from multiple factors: natural (e.g. wind, rain, flood, earthquake) and human-related hazards (e.g. pollution, vandalism, mass tourism, inadequate conservation measures) (Palumbo 2000). In addition, climate change, globalization and sustainability have been serious challenges for the stone conservation in the 21<sup>st</sup> century and have affected appropriate conservation strategies (Viles 2013). By considering all these factors, conservation strategies should be designed for archaeological sites.

Stone conservation measures could be classified into two groups: active and preventive conservation (Doehne and Price 2010). Active conservation includes interventions applied to stones such as surface cleaning (e.g. laser cleaning, biocides, nanoparticles), desalination and consolidation (e.g. lime based elements, organic polymers, epoxies) (Doehne and Price 2010).

Preventive conservation measures include interventions to address the causes of deterioration, such as controlling water, temperature or relative humidity to prevent further deterioration of the stones (Doehne and Price 2010). Preventive conservation presents a comprehensive approach for the archaeological sites. This approach covers many preventive measures: conservation legislation, maintenance, pollution control, traffic control, visitor management, disaster planning, monument monitoring, protective shelters, control of groundwater, wind fences and reburial (Palumbo 2000, Demas 2004, Doehne and Price 2010).

Considering today's conservation principles, preventive strategies to avoid deterioration should be developed in archaeological areas. The purpose of preventive stone conservation is to minimize the deterioration rate by reducing aggressive forces (modifying local environmental factors) and/or increasing resistance to these forces (applying consolidants or other treatments) (Viles 2013). After these interventions, their results should be monitored and managed in the long term.

Stone findings in archaeological sites are highly susceptible to deterioration after excavation. In this context, it is necessary to develop preventive conservation measures to prevent further weathering on stones. Biocolonization is one of the most important weathering processes affecting stone monuments in archaeological sites. Nowadays, environmentally friendly methods or low impact procedures to control microbiological deterioration are strongly encouraged to reduce risks on human health and the environment. Before any intervention, a detailed work has to be done to understand biological formation on stones and their physical and chemical interaction with the stone substrate. Their bioprotective or biodegradative effects on stones should be considered as well.

## CHAPTER 3

### METHODS

This research focuses on the investigation of the weathering forms observed on limestones used in Anavarza archaeological site, their characteristics and causes for the purpose of their conservation. In this chapter, site survey and sampling phases of the study are discussed. Then, the laboratory investigation to determine limestone characteristics, their weathering forms and causes are reported in detail.

#### 3.1. Site Survey

The first step of the study is the site survey held in June 2018. Visual analysis and sampling were carried out during the site survey. Then, the site surveys were performed in November 2018, July and November 2019.

##### 3.1.1. Visual Observation

The study started with a visual analysis and mapping of the weathering forms of limestones in the site. The weathering forms of the limestones used in the archaeological site were investigated by visual observation and then documented by using mapping method and photos.

Photographical documentation was performed during the site surveys. The mapping technique was carried out on these photos. Based on the visual analysis and mapping, the weathering types of the limestones were determined considering the MDCS (the Monument Diagnosis and Conservation System) (MDCS homepage).

The weathering forms observed on the limestones of the arch and of the columnate are surface change, disintegration, cracking and biological growth. These weathering types are classified considering MDCS damage atlas as below:

- Surface change: Deposit in the forms of *soiling*; transformation in the forms of *patina* and *crust (black)* (Figure 14, 15),



- Disintegration: Layering in the forms of *exfoliation*, *spalling* and *scaling*; loss of cohesion in the forms of *crumbling* and *erosion (selective weathering)* (Figure 16, 17, 18),
- Cracking: Crack and hair crack (Figure 17),
- Mechanical damage: Scratch (Figure 19),
- Biological growth: Higher plants and thriving micro-organisms in the forms of *lichens*, *algae* (Figure 20).



Figure 14. Soiling on the excavated and black crust on the standing parts of stone surfaces.



Figure 15. Yellow patina and black crust observed on the stone surfaces.



Figure 16. Exfoliation and spalling observed on stone surfaces.



Figure 17. Scaling and hair cracks observed on stone surfaces.



Figure 18. Crumbling and erosion observed on stone surfaces.



Figure 19. Stretch observed on stone surfaces.

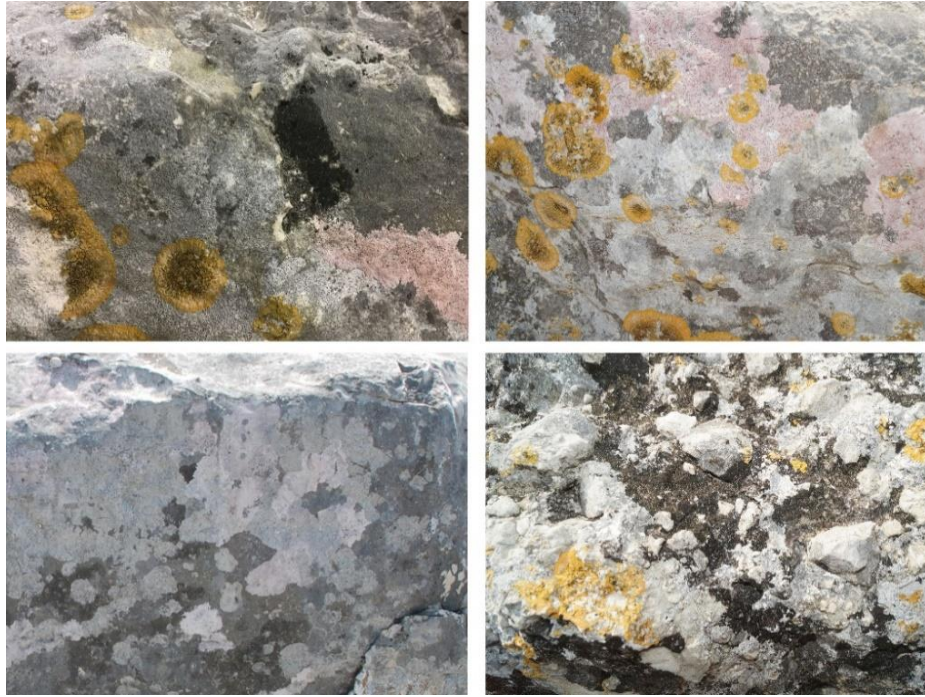


Figure 20. Thriving micro-organisms (lichens, algae, bacteria etc.) observed on stone surfaces.

Different damage types are observed on limestones of the triumphal arch (Alakapı) at different heights from the ground level. Three main zones can be distinguished: zone 1, up to 75 cm from the ground; zone 2, including the triumphal arch; zone 3, at the top of the arch (Figure 21). In the zone 1, layering in the form of scaling is observed on that surface of the stone. Besides, biological growth and soiling are seen on some parts, as well. In the zone 2, a yellow patina can be observed on part of the surface. Black crust is clearly observed on the right corner of the structure. Erosion can be observed on many parts of the stones as well, possibly due to rain water, action of wind or cleaning methods. In the zone 3 of the structure, the stone is severely damaged and has lost its cohesion in the form of crumbling (Figure 21).

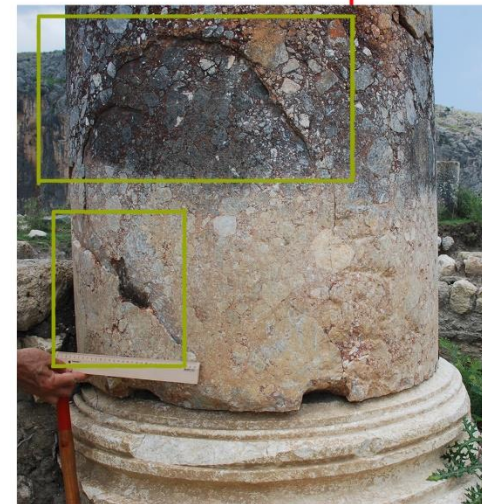
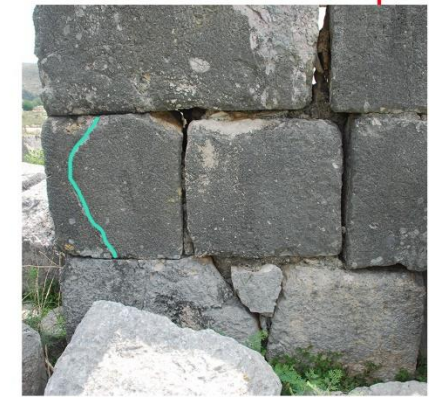
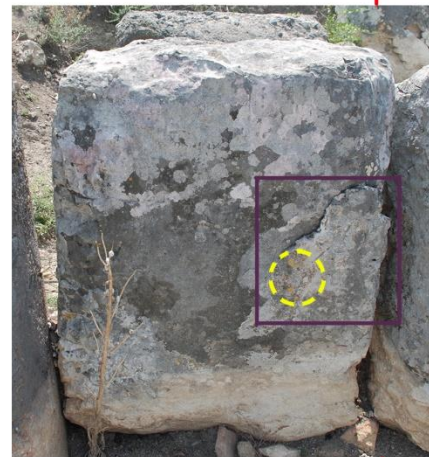
The limestones of the columns present on the main street leading to the triumphal arch (Alakapı) show biological growth in the form of algae, lichens, bacteria (Figure 22). The severity of the biological growth can be distinguished in two part: severe damage in the standing parts of the columns and less damage in the recently excavated parts of the columns. In addition, layering in the form of exfoliation and spalling can be observed on both parts of limestone surfaces (Figure 22).



- |                                                 |                                                 |                                     |
|-------------------------------------------------|-------------------------------------------------|-------------------------------------|
| — Disintegration » Layering (Scaling)           | — Surface change » Transformation (Patina)      | — Biological growth (higher plants) |
| — Disintegration » Loss of cohesion (Crumbling) | — Surface change » Transformation (black crust) | — Mechanical damage (scratch)       |
| — Disintegration » Loss of cohesion (Erosion)   | — Surface change » Deposit (Soiling)            | — Cracking (crack-hair crack)       |



Figure 21. Mapping of the weathering forms of stones used in the triumphal arch (Alakapı)



✓ Surface change » Deposit (thriving micro-organisms/biological growth)

— Biological growth (higher plants)

- - - Biological growth (lichens)

- - - Biological growth (algae)

— Disintegration » Loss of cohesion (Erosion)

— Disintegration » Layering (Exfoliation)

— Disintegration » Layering (Spalling)

— Cracking (crack-hair crack)

Figure 22. Mapping of the weathering forms of stones used in the colonnaded road.

### 3.1.2. On site investigation

As mentioned before, the severity of the damage is different between the standing part and the recently excavated part of the limestone columns. The standing parts of the stone surfaces are blackish, whereas the more recently excavated part are lighter in colour (Figure 23). This color change on the standing parts of the stone surfaces is probably related to microbiological colonization (e.g. cyanobacteria and algae). The standing parts of the stone surfaces have been exposed to atmospheric conditions longer than the recently excavated parts, and thus, these parts have been heavily colonized by microorganisms, in the presence of water.

Surface temperatures can be different between dark colored and light colored areas on stone surfaces. Darker stone surfaces might absorb more sunlight; this can cause more stress within the stone by temperature changes (e.g. heating/cooling and wetting/drying cycles) (Warscheid and Braams 2000).

In order to get insight into the surface temperatures, thermal images of both the triumphal arch and of the colonnade were taken. (Figure 23). Thermal camera used in this study, Testo 868 has a spectral range from 7.5 to 14  $\mu\text{m}$ , temperature range -30 to 650  $^{\circ}\text{C}$ . The surface temperatures of the standing parts were higher than the recently excavated ones; thus can be due to the absorption of larger amounts of solar radiation. To support this, further studies including monitoring of the surface temperature in time is required.

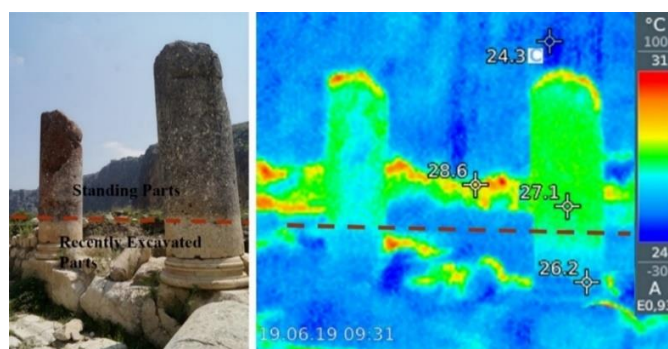


Figure 23. Photo and thermal image of the standing parts and the excavated parts of the stone surfaces

The visual analysis and mapping indicates that biological growth (higher plants/ thriving micro-organisms) are a common decay type in the limestones of the arch and of

the colonnade. The biological weathering occurs as a result of micro-organisms (e.g. algae, lichen, bacteria) that can grow on stone surfaces, in fractures and pores of the stones within the suitable environmental conditions. These micro-organisms can easily multiply and cause macro/micro cracks by applying pressure on the pores of the stones. Furthermore, they can produce some type(s) of acids (e.g. sulfuric acid, oxalic acid) by the result of their metabolic activity and then cause chemical deterioration of the stone surface by reacting with the stone minerals (Scheerer et al. 2009, Warscheid and Braams 2000).

In this study, the effect of micro-organisms on stone surfaces related to other possible damage agents (such as salts) has been evaluated by comparing the stone surface characteristics of the standing, colonized parts and the sound, recently excavated part of the columns. By assessing the cause(s) of the deterioration and understanding the damage process, preventive conservation strategies can be developed for archaeological sites. To this scope, the research aims to provide useful preservation measures after the excavation.

### **3.2. Sampling**

Taking into consideration the above-mentioned research aims, sampling (Figure 24) was performed from stone surfaces showing severe deterioration (yellow patina, black crust, thriving microorganisms in the form of algae, lichens, bacteria) in the standing part of the columns as well as from locations in the recently excavated part of the limestones, where less severe damage (patina) was present. By comparing more and less decayed samples and relating decay to the presence and type of bacteria and other possible weathering agents (such as salts), a sound diagnosis on the cause(s) of the damage can be made.

Besides, stone samples were taken from the inner part of the columns, in order to have sound material, which can be used for the identification of the stone type(s). In addition, large size limestone materials were taken from the old quarry near the area for investigation of the stone properties.

Next to stone samples, soil samples (excavated soil) were collected from where the stone columns were excavated (at 5-10 cm. depth) in order to determine subsoil environment (e.g. soil type, clay and soluble salt content).

Limestone samples were taken from the standing and recently excavated surfaces by scrubbing stone surfaces and chipping stone pieces. In Figure 24, an overview of the locations and the criteria used for collecting the samples is given.

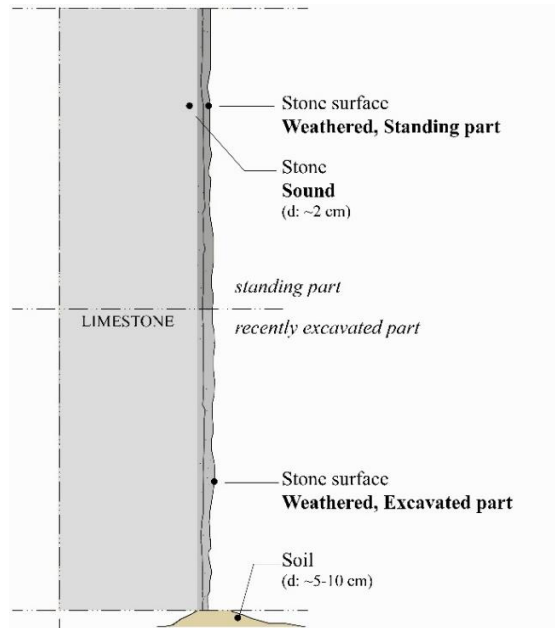


Figure 24. Figure showing where the samples were collected.

Samples were labelled with letters and numbers (Figure 25). In the sample code, the first letter indicates where the sample was collected (A: sample on the Alakapı (the triumphal arch), C1: sample from the 1<sup>st</sup> column on the main road). The second letter indicates the part of the stone where the sample was collected (St: Standing part, Ex: Excavated part, In: Inner part). If the sample is soil, the second letter indicates it (So: Soil). If more than one sample was collected, an increasing number is used (Figure 25).

1 <sup>st</sup>	2 <sup>nd</sup>	3 <sup>rd</sup>	
A	st.	1/2/3.	A.ex.1 : Alakapı excavated part sample 1
C1	ex.		C4.st.3 : Column 4 standing part sample 3
C2	in.		
	so.		C2.so.1 : Column 2 soil sample 1

Figure 25. Figure showing the sample code













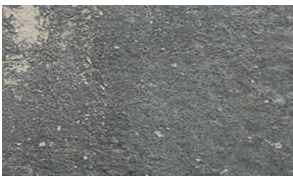
In total 12 limestone samples were collected; 4 samples from Alakapı and 9 samples from the colonnaded road. Nine soil samples were collected; 2 samples nearby Alakapı and 7 samples nearby the colonnaded road (Table 5, 6).



Table 5. Sample codes with indication of sampling location and damage

<b>Code of sample</b>	<b>Height (~cm)</b>	<b>Depth (~cm)</b>	<b>Damage</b>
A.st.1	150	0-1	severe (yellow patina)
A.in.1	150	1-3	-
A.so.1	0	5-10	-
A.st.2	120	0-1	severe (biological growth)
A.in.2	120	1-3	-
A.so.2	0	5-10	-
A.st.3	120	0-1	severe (black crust)
A.in.3	120	1-3	-
A.st.4	120	0-1	severe (yellow patina)
A.in.4	120	1-3	-
C1.st.1	60	0-1	severe (biological growth)
C1.in.1	60	1-3	-
C2.st.1	75	0-1	severe (biological growth)
C2.in.1	75	1-3	-
C2.so.1	0	5-10	-
C3.st.1	120	0-1	severe (biological growth)
C3.st.2	120	0-1	severe (biological growth)
C3.st.3	120	0-1	severe (biological growth)
C3.in.1	120	1-3	-
C4.st.1	120	0-1	severe (biological growth)
C4.st.2	120	0-1	severe (biological growth)
C4.st.3	120	0-1	severe (biological growth)
C4.st.4	120	0-1	severe (biological growth)
C4.in.1	120	1-3	-
C4.so.1	0	5-10	-
C5.st.1	100	0-1	severe (biological growth)
C5.ex.1	25	0-1	less severe (patina)
C5.in.1	100	1-3	-
C5.so.1	0	5-10	-
C6.st.1	100	0-1	severe (biological growth)
C6.in.1	100	1-3	-
C6.so.1	0	5-10	-
C7.st.1	100	0-1	severe (biological growth)
C7.ex.1	50	0-1	less severe (scaling, patina)
C7.in.1	100	1-3	-
C7.so.1	0	5-10	-
C8.st.1	100	0-1	severe (biological growth)
C8.ex.1	50	0-1	less severe (scaling, patina)
C8.in.1	100	1-3	-
C8.so.1	0	5-10	-
C9.st.1	50	0-1	severe (biological growth)
C9.in.1	50	1-3	-
C9.so.1	0	5-10	-
Q.1	75	2-10	-
Q.2	75	2-10	-
Q.3	75	2-10	-
Q.4	75	2-10	-
Q.5	75	2-10	-

Table 6. Table showing the places where the scraped/chipped stone samples collected

Sample code	Sample image	Sample code	Sample image
Alakapı: A.st.1, A.in.1		Alakapı: A.st.2, A.in.2	
Alakapı: A.st.3, A.in.3		Alakapı: A.st.4, A.in.4	
1st column: C1.st.1, C1.in.1		2nd column: C2.st.1, C2.in.1	
3rd column: C3.st.1 (grey) C3.st.2 (yellow) C3.st.3 (pink) C3.in.1		4th column: C4.st.1 (white) C4.st.2 (l.grey) C4.st.3 (yellow) C4.st.4 (d.grey) C4.in.1	
5th column: C5.st.1, C5.ex.1, C5.in.1		6th column: C6.st.1, C6.in.1	
7th column: C7.st.1, C7.ex.1, C7.in.1		8th column: C8.st.1, C8.ex.1, C8.in.1	
9th column: C9.st.1, C9.in.1			

### 3.3. Laboratory Investigation

In this section, the methods of the laboratory investigation applied on the stone and soil samples taken from the area, as well as on fresh stone samples from the historic quarry are described.

First of all, three types of samples were collected from the area with the aim as below:

*Stone samples (samples codes Ax-x-x and Cx-x-x):*

- Sound inner parts of stone (samples codes Ax-in-x and Cx-in-x): to determine the chemical, mineralogical, microstructural and petrographical properties of the stone. Additionally, the soluble salt content has been assessed as well, by ion chromatography (IC) and hygroscopic moisture content (HMC), mainly for comparison with the outer, decayed part of the stone. Determination of bacterial communities.

- Weathered surfaces, both standing and excavated parts (samples codes Ax-st-x, Cx-st-x and Ax-ex-x, Cx-ex-x): to determine the effect of weathering on chemical, mineralogical, microstructural properties of the stone. The content and distribution of soluble salts have been assessed by ion chromatography (IC) and hygroscopic moisture content (HMC). On these samples, the presence and type of bacterial communities have been assessed.

*Soil samples (samples codes Ax-so-x and Cx-so-x):*

- Sample from soil: to determine the chemical and mineralogical properties of the soil and the soluble salt content

*Fresh stone samples from the historic quarry (sample code Q-x):*

- Sample from quarry: As it is not possible to collect enough large sized material from the archeological site for the assessment of the moisture transport properties of the stone, it has been decided to use the fresh stones from the nearby historic quarry. In this scope, the following properties have been measured: porosity, water absorption by capillarity and drying rate.

All measurements and tests carried out are summarized in Table 7. To determine all properties of the stones and soils summarized above, different methods were used and described in the sections 3.3.1-3.3.6.

Table 7. Analysis methods used in the research

Research	Methods
Site survey	Visual analysis, mapping, thermal imaging, sampling
Determination of mineralogical compositions	X-ray Diffraction (XRD), Fourier Transformed Infrared Spectroscopy (FT-IR)
Determination of chemical compositions	Scanning Electron Microscope-Energy Dispersive X-ray Spectrometry (SEM-EDS), thermal analysis (TG/DTA)
Determination of petrographic and microstructural properties	Polarizing microscope, SEM-EDS
Determination of hygroscopic moisture content and soluble salts	Hygroscopic moisture content (HMC), conductivity, ion chromatography (IC)
Determination of moisture transport properties	Standard test methods, gravimetric methods
Determination of causal agent of microbiological deterioration	Culture-dependent/culture-independent advanced molecular techniques

### 3.3.1. Determination of Mineralogical Composition of Stone and Soil Samples

The mineralogical composition of samples taken from weathered surfaces and sound inner cores of the limestones were investigated by X-ray Diffraction (XRD) and Fourier Transformed Infrared Spectroscopy (FT-IR) analyses.

Besides, in order to determine the mineralogical composition of the soils, X-ray Diffraction (XRD) analysis was carried out.

For the XRD analysis; stone samples and soil samples were ground to particles less than 53 $\mu$ m grain diameter. The XRD analysis were applied on these powdered samples by using a Rigaku Miniflex 600 with CuK $\alpha$  radiation in the range of 5-70 $^{\circ}$ .

FT-IR analysis is another method used to determine the mineralogical characteristics of the stone samples. For the FT-IR analysis, the powdered samples were mixed with KBr (1 sample/10 KBr) and pressed into pellets under approximately 10 tons/cm $^2$  pressure. The analysis were performed on these pellets by using a Perkin Elmer-FT-IR System Spectrum BX spectrometer by scanning each of the samples four times.

### **3.3.2. Determination of Chemical Composition of Stone and Soil Samples**

The chemical composition of samples taken from weathered surfaces and sound inner cores of the limestones were determined by Scanning Electron Microscope-Energy Dispersive X-ray Spectrometry (SEM-EDS). The analysis were also performed on soil samples to determine their chemical composition.

For the chemical analysis, stone samples and soil samples were ground to particles less than 53 $\mu$ m grain diameter and pressed into pellets under about 10 tons/cm<sup>2</sup> pressure. The EDS analysis were performed on these pellets in three different zones of each sample by using a FEI Quanta 250 FEG.

Additionally, as support to the chemical analysis, thermal analysis (TG/DTA) were carried out on stone samples. The contents of hygroscopic (adsorbed) water, organic materials and carbonates of the weathered surfaces and sound inner parts of the stones were determined by TG/DTA based on the weight losses of the materials.

The thermogravimetric analysis was carried out by using Hitachi STA7300 TG/DTA in nitrogen atmosphere at a temperature range of 25-1000°C with a controlled heating rate of 10°C/min. In this analysis, fine ground sample was placed inside the analysis equipment and heated in the furnace at 25°C to 1000°C for 3 hours. During this heating, weight losses at these temperatures were precisely measured.

TGA instrument recorded loss of hygroscopic (adsorbed) water (< 200°C), loss of structural water bounded to hydraulic components and loss of organic components (200°C-500°C), and loss of carbon dioxide gas due to decomposition of calcium carbonates (> 900°C) (Wang et al. 2000).

### **3.3.3. Determination of Petrographic and Microstructural Properties of Stones**

The petrographic analysis by means of observations on thin sections were carried out on sound parts of some limestone samples in order to determine the microstructural properties and mineralogical characteristics of the sound limestone.

The samples used in the petrographic analysis were first cut to 8-10 mm thick pieces. Then, the sample surfaces were polished and fixed to the glass slide using an

epoxy resin. These samples on the glass slide were then placed under pressure for 24 hours. After that, the samples were cut to approximately 2 mm thick slices and ground up to 30  $\mu\text{m}$  thickness (Figure 26). Then, the samples were cleaned in an ultrasonic cleaner to ensure all contamination had been removed. The thin sections were studied by the use of polarized light microscope (OLYMPUS BX51-P).

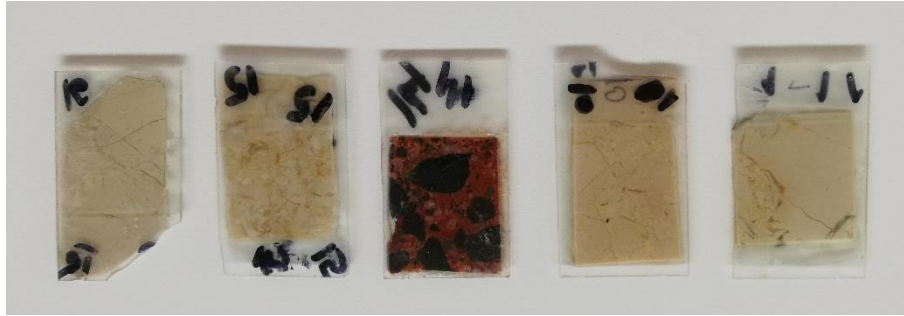


Figure 26. Thin section samples.

Additionally the microstructural properties of stones were determined by Scanning Electron Microscope-Energy Dispersive X-ray Spectrometry (SEM-EDS). SEM investigations were performed on the unpolished stone surfaces and on the cross section of the samples. The aim of these SEM investigations was the determination of the morphological properties and the assessment of the difference in deterioration between the surface and the inner part of the stone. In addition, EDS mappings were performed on the section samples to compare the chemical characteristics from the surfaces through to the interior of the stone.

Different types of samples were prepared. Samples from the surface of the stone, were cut in pieces with dimensions of 2x2x2 cm, dried in an oven at 40 °C for 24 hours and then the originally exposed surface of the stone was investigated by SEM. Other samples were covered with epoxy resin for 24 hours (Figure 27) and cross sections (from surface to depth) were obtained by cutting the stone cut into slices of about 2-3 mm thickness with Buehler low speed saw using water (Figure 27). After that, the cross sections were coated with gold, dried in an oven at 40 °C for 24 hours.

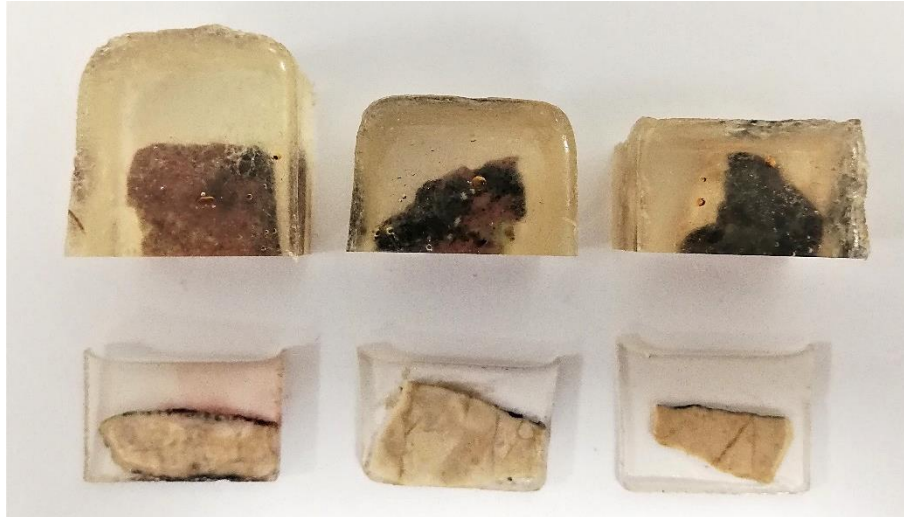


Figure 27. Samples covered with epoxy resin and cut cross section samples.

SEM observations were carried out using a FEI Quanta 250 FEG type instrument. This instrument has a SE/BSE (Secondary Electrons/Backscattered Electrons) detector with three modes (high vacuum, low vacuum and ESEM), equipped with energy dispersive spectrometer (EDS) by Oxford Aztec. For this study, the BSE detector with high and low vacuum, as well as the EDS detector were used.

### 3.3.4. Determination of Soluble Salts

For the determination of the presence of soluble salts of stone and soil samples from the site, different methods were used: hygroscopic moisture content (HMC), conductivity of the solutions and ion chromatography.

#### *Hygroscopic moisture content (HMC) on stone samples*

The HMC gives an indication of the presence of soluble, hygroscopic salts (Lubelli et al. 2004).

The stone samples were cut in pieces with thickness of about 1 cm (from the surface up to 5 cm in depth) and powdered (Figure 28). The samples were reduced to powder in a mortar, dried and then placed in a climatic cabinet (Weiss) at 20°C / 95% RH. After 4 weeks, the samples are weighed again. The hygroscopic moisture content (HMC) was calculated as follows:

$$\text{HMC} = [100 \times (\text{weight}_{95\% \text{ RH}} - \text{weight}_{\text{dry}})] / \text{weight}_{\text{dry}}$$



Figure 28. Powder samples for HMC measurements.

#### *Ion chromatography (IC) on stone samples*

Stone samples and samples from the soil nearby the excavated area were analyzed by ion chromatography (IC), to determine the type and concentration of soluble salts (ions) in the samples.

For this analysis, 1.00 gr of finely-ground samples (grain size smaller than 53  $\mu\text{m}$ ) was mixed with 50 ml deionised water. After stirring thirty minutes, the mixtures were stored two weeks for the precipitation of the particles. Then, these mixtures were filtered with a filter of size 0.20  $\mu\text{m}$ . The obtained solutions were analyzed to quantify the ions: both anions (e.g. sulphate, chloride, nitrite, nitrate, phosphate, fluoride) and cations (e.g. sodium, ammonium, potassium, calcium, magnesium) were measured by using a Thermo Scientific Dionex ICS-5000 +.

#### *Conductivity on soil samples*

Percent soluble salts in soil samples were indicavately determined by an electrical conductivity meter (Black 1965). For percent soluble salt analysis, 1.00 gr of finely-ground samples less than 53  $\mu\text{m}$  were mixed with 50 ml distilled water. After stirring, the mixtures were filtered. The conductivity of the filtered solutions was measured by an electrical conductivity meter (WTW MultiLine P3 pH/LF) and then percent soluble salt contents were calculated as follows (Black 1965):

$$\text{Soluble Salts (\%)} = [(A \times V_{\text{sol}}) / 1000] \times [100 / M_{\text{sam}}]$$

where;



$A = \text{Salt concentration (mg/lit)} = 640 \times EC$

$EC = \text{Electrical conductivity measured by electrical conductivity meter}$

$(\text{mS/cm} = \text{mmho/cm})$

$640 = \text{Constant}$

$V_{\text{sol}} = \text{Volume of the solution (ml)}$

$M_{\text{sam}} = \text{Weight of the sample (mg)}$

### **3.3.5. Determination of Moisture Transport Properties of Stones from the Historic Quarry**

The moisture transport properties of the stones from the historic quarry were assessed by measuring density and porosity, the water absorption by capillarity and drying rate of the limestones.

First of all, the values of bulk density ( $\text{g/cm}^3$ ) and porosity (%) of the limestone samples were determined by immersion at atmospheric pressure (Van der Klugt and Koek 1994). Stone samples were dried in an oven at  $40^\circ\text{C}$  for 24 hours and then they were weighed by a precision balance (Mettler Toledo XS4002S DeltaRange) to determine their dry weights ( $M_{\text{dry}}$ ). Then, the samples were saturated with distilled water at atmospheric pressure. After being saturated with water, their saturated ( $M_{\text{sat}}$ ) and the hydrostatic weights ( $M_{\text{arch}}$ ) in distilled water were measured by using the precision balance.

The bulk densities (D) and porosities (P) of the samples were calculated as follows:

$$D (\text{kg/m}^3) = (1000 \times M_{\text{dry}}) / (M_{\text{sat}} - M_{\text{arch}})$$

$$P (\%) = [1 - D/2650] \times 100$$

Where  $2650 \text{ Kg/m}^3$  is the density of a building material without pores (Van der Klugt and Koek 1994).

Water absorption by capillarity and drying rate of the stones are other methods used for the determination of the moisture transport behavior (CEN 2009, CEN 2014).

For water absorption measurements, stones from the historic quarry were cut in cubes of 5 cm side. The specimens were dried in an oven at  $40^\circ\text{C}$  until constant weight and were weighed ( $m_d$ ) before beginning the test. Then, the sample was placed into a vessel with a grid at the bottom, in such a way that the water level was 2 mm above the bottom surface of the specimens and the chronometer was started (Figure 29). For

measuring water absorption, each sample was taken off the water and then its weight ( $m_i$ ) was measured at different time intervals ( $t_i$ ). The time intervals between the weightings were determined related to the speed of water absorption of the samples. To maintain the water level constant, water was added as necessary throughout the test.

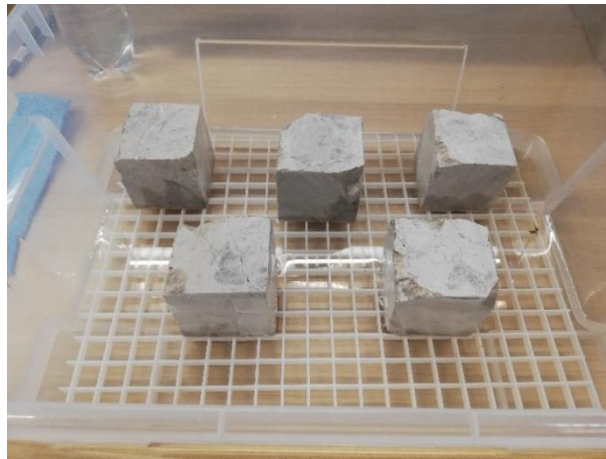


Figure 29. Specimens for water absorption measurement.

The amount of water absorbed by the samples per unit area ( $Q_i$ ) at time ( $t_i$ ) were calculated as follows:

$$Q_i = [(m_i - m_d)/A]$$

where;

$Q_i$  : water absorbed per unit area ( $\text{kg}/\text{m}^2$ )

$m_d$  : mass of the dry specimen (kg)

$m_i$  : mass of the specimen at time  $t_i$  (kg)

$A$  : area of the specimen in contact with water ( $\text{m}^2$ )

$t_i$  : time elapsed from the beginning of the test (s)

Then, all of the calculated values of  $Q_i$  are reported in a graph as a function of the square root of time ( $t_i^{1/2}$ ), to determine the capillary water absorption curve. The capillary water absorption coefficient (WAC) is calculated: this is the slope of the linear section (at least 5 successive aligned points) of the curve.

The drying rate was assessed on the same cubic samples (5x5x5 cm) used for the capillary absorption. First of all, the samples were saturated with water by capillary rising absorption and then total immersed into the water to reach their constant mass. After that,

all faces of the samples (except the top surface) were sealed by using a water impermeable material (e.g. tape) and weighed at time  $t=0$  (Figure 30).



Figure 30. Sealed specimens for drying rate measurements.

Then, the samples were placed at  $22 \pm 2$  °C and drying occurs through the top surface. The samples were weighed periodically to measure their drying behaviour. The measurements were performed until the specimens reached the constant weight. The temperature and RH in the laboratory were monitored and varied between 20.5-29.5 °C and 40-74.5 % RH.

The amount of water present in the sample per unit area ( $\text{kg}/\text{m}^2$ ) at time ( $t_i$ ) were calculated as follows:

$$M_i = [(m_i - m_f)/A]$$

where;

$m_i$  : mass of the sealed specimen at time  $t_i$  (kg),

$m_f$  : final mass of the sealed specimen at time  $t_f$  (kg)

$t_i$  : time elapsed from the beginning of the test (h),

$t_f$  : final time of the test (h),

A : area of the drying face ( $\text{m}^2$ )

Then, all of the calculated values of  $M_i$  were reported in a graph as a function of the time ( $t_i$ ) to determine the drying curve.

### 3.3.6. Determination of Bacterial Communities

To determine the bacterial communities that play an important role in the microbiological deterioration on stone surfaces, culture-dependent and culture-independent advanced molecular techniques were used.

#### *Storing of samples:*

The samples were taken from stone surfaces by using sterile swabs and put into sterile tubes. Some of the samples were stored in the refrigerator at +4°C for cultivation studies, and some were stored at -20 and -80°C for advanced molecular studies.

#### *Processing of samples:*

In cultivation studies of microorganisms in laboratory environments, all species could not be obtained since the environmental conditions present in the field can not always be reproduced in a good way (Bloomfield et al. 1998, Bogosian et al. 2000). To solve this problem, R2A and VL55 medium, and different cultivation methods such as prolongation of incubation time, incubation of samples at relatively high and low temperatures were performed (Figure 31, 32, 33). During cultivation period for three months, their development was monitored daily.



Figure 31. Cultivation of samples in R2A liquid medium.



Figure 32. Growth of samples in R2A liquid medium

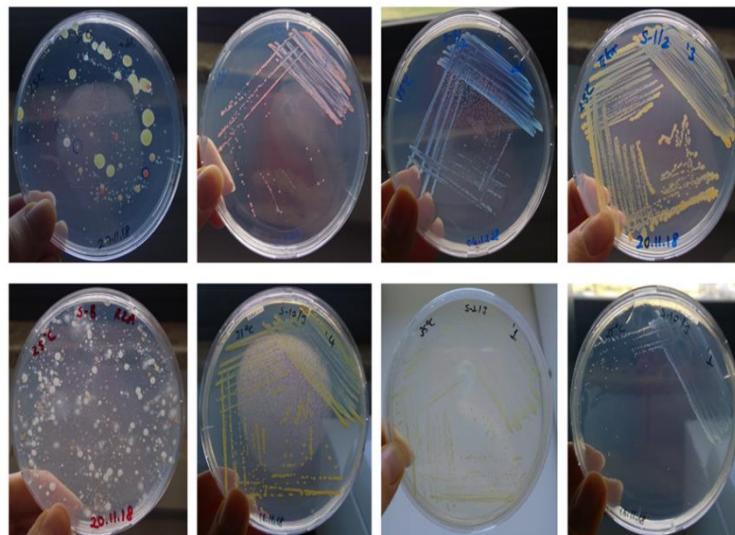


Figure 33. Growth of samples in R2A solid medium

*Isolation, characterization and identification of bacterial communities:*

After incubation, cultures were serially diluted three times to obtain pure colonies. For the phylogenetic characterization of the strains, DNA of the samples were extracted with the fast-DNA® Soil Kit according to the manufacturer's instructions (Ettenauer et al. 2012).

27 F (forward 5'- AGA GTT TGA TCC TGG CTC AG -3') and 1492 R (reverse 5'- GGT TAC CTT GTT ACG ACT T -3') primers and GoTaq® DNA Polimerase Kit

(Promega, Leiden, the Netherlands) were used for amplification of bacterial 16S rRNA gene regions by classical PCR. After that, they were purified using a purification kit in accordance with the manufacturer's instructions. These prepared samples were sent to the company for the sequencing process and then the results were received. Next generation sequencing (NGS, pyrosequencing) method, which has been frequently preferred in advanced molecular techniques in recent years, has been applied on the samples in order to determine the diversity on the basis of species.

## CHAPTER 4

### RESULTS AND DISCUSSION

In this part, the results of the mineralogical and chemical compositions, microstructural properties and soluble salt content of the samples taken from the standing surfaces, recently excavated surfaces and sound inner cores of the limestones are determined and compared. Mineralogical, chemical compositions and soluble salt content of soils (excavated soil) are determined as well. Additionally, petrographic observations of sound inner cores of the stones and moisture transport properties of the sound stones from the site and the historic quarry are investigated. Lastly, bacterial distribution analysis of stones from the standing surfaces, recently excavated surfaces and sound inner cores of the limestones are investigated and compared.

#### 4.1. Mineralogical Composition of Stone and Soil Samples

The results of mineralogical composition analysis carried out by XRD and FT-IR show that weathered surfaces of limestones have different mineralogical composition than those of sound inner cores due to the effect of weathering on the surface. In the following sections, the mineralogical compositions of sound inner cores and weathered surfaces (standing and recently excavated) of stones, and soils are described.

##### 4.1.1. Sound Inner Cores of Stone Samples

XRD patterns and FT-IR spectrums indicate that the sound inner cores of limestones are mainly composed of calcite (C:  $\text{CaCO}_3$ ) and quartz (Q:  $\text{SiO}_2$ ) minerals (Figure 34).

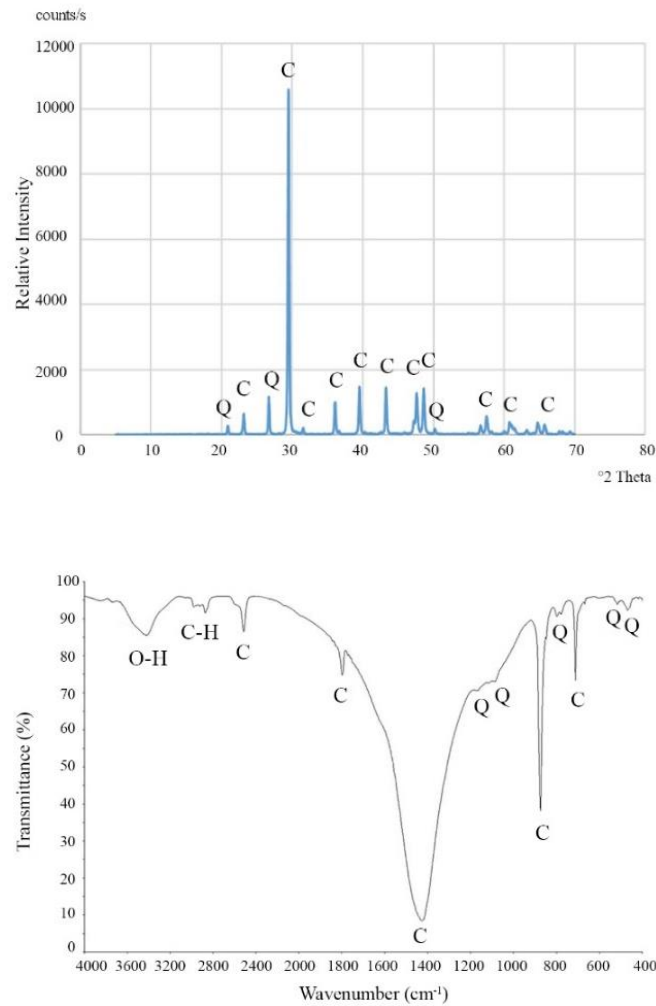


Figure 34. X-ray diffraction (XRD) pattern and FT-IR spectra of sound limestone (A.in.2, A.in.3) (C: calcite, Q: quartz).

#### 4.1.2. Weathered Surfaces of Stone Samples

The results of XRD and FT-IR analysis show that weathered surfaces of limestones both standing parts and recently excavated parts consist of calcite (C:  $\text{CaCO}_3$ ) and quartz (Q:  $\text{SiO}_2$ ) minerals. Apart from these minerals, which are components of the stone, calcium oxalate mono hydrate [Whewellite ( $\text{CaC}_2\text{O}_4 \cdot \text{H}_2\text{O}$ )], calcium oxalate dihydrate [Weddelite ( $\text{CaC}_2\text{O}_4 \cdot 2\text{H}_2\text{O}$ )], calcium sulfate dihydrate [Gypsum ( $\text{CaSO}_4 \cdot 2\text{H}_2\text{O}$ )] and amorphous phase which are largely aluminosilicates peaks were identified on the standing surfaces of limestones by XRD (Figure 35).

The presence of these minerals and of biological formations were clearly determined by FT-IR analyses too (Figure 35). On the FT-IR spectrums of stone surfaces,



calcite ( $\text{CaCO}_3$ ) with the bands at  $\sim 2513, 1797, 1430, 876, 712 \text{ cm}^{-1}$ , quartz ( $\text{SiO}_2$ ) at  $\sim 1031 \text{ cm}^{-1}$ , whewellite ( $\text{CaC}_2\text{O}_4 \cdot \text{H}_2\text{O}$ ) and weddellite ( $\text{CaC}_2\text{O}_4 \cdot 2\text{H}_2\text{O}$ ) at  $\sim 1635, 1323, 783 \text{ cm}^{-1}$ , gypsum ( $\text{CaSO}_4 \cdot 2\text{H}_2\text{O}$ ) at  $\sim 3546, 3409, 1146, 1119, 671, 470 \text{ cm}^{-1}$  and O-H bands at  $\sim 3420$  are observed. C-H stretching bands at around  $2918$  and  $2850 \text{ cm}^{-1}$  show the sign of biological tissues on the stone surfaces (Figure 35).

Whewellite and weddellite occurs on stone surfaces as result of the reaction between oxalic acids, produced by microbiological formations, with calcium carbonate which is the major mineral of calcareous stones (Reaction I) (Gadd 2007).

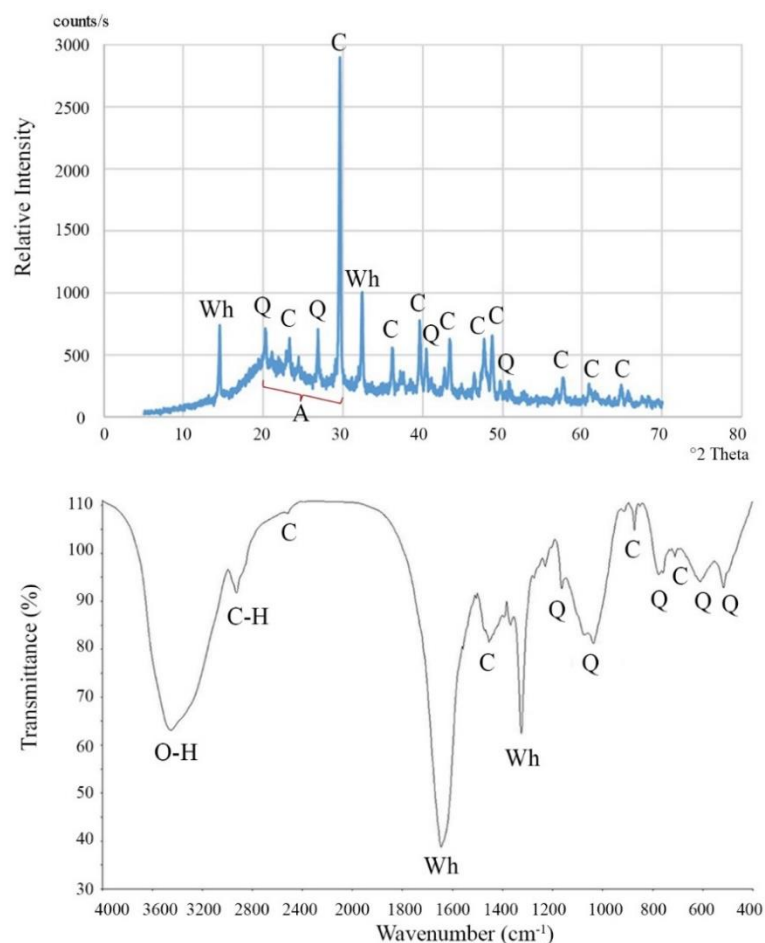
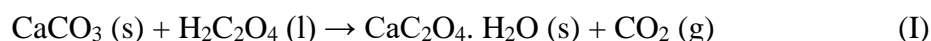


Figure 35. X-ray diffraction (XRD) pattern and FT-IR spectra of standing part of the column 3, sample C3.st.2 (C: calcite, Q: quartz, Wh: Whewellite, A: Amorphous substances (Aluminosilicates), O-H: Oxygen-Hydrogen bands, C-H: Carbon-Hydrogen bands).

Figure 36 shows XRD patterns and FT-IR spectrums of the recently excavated stone surfaces. This indicates that they are mainly composed of calcite and quartz minerals (Figure 36). Unlike the standing parts (Figure 35), recently excavated surfaces do not yet have whewellite minerals (Figure 36).

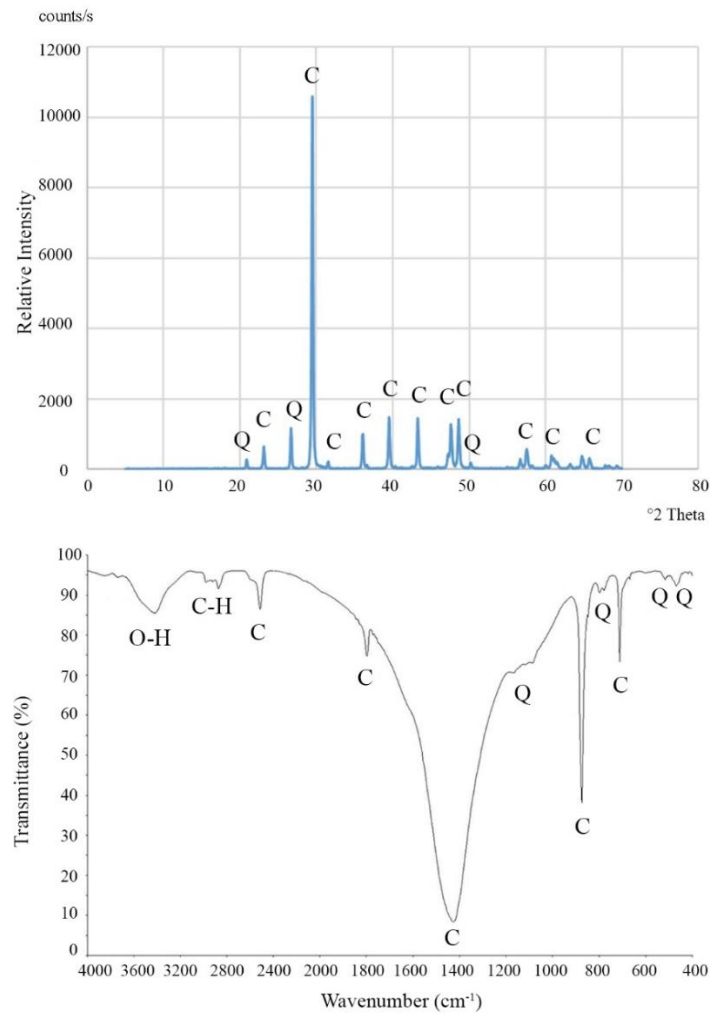
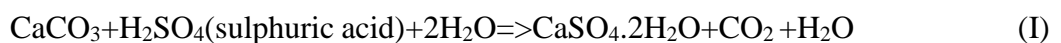


Figure 36. X-ray diffraction (XRD) pattern and FT-IR spectra of recently excavated part of the column 7, sample C7.ex.1 (C: calcite, Q: quartz, O-H: Oxygen-Hydrogen bands, C-H: Carbon-Hydrogen bands).

In addition, the observed gypsum formation (Figure 37) is most probably the result of the reaction between SO<sub>2</sub> gases present in the polluted air and the calcite in the limestone, in the presence of moisture. This reaction occurs at the surface of the stone and results in the formation of gypsum crust (Reaction I) (Goudie and Viles 1997).



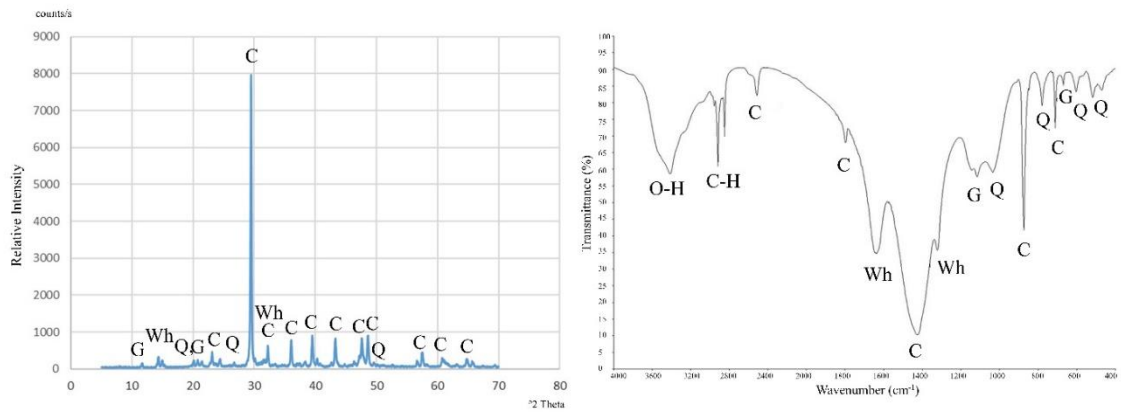


Figure 37. X-ray diffraction (XRD) pattern and FT-IR spectra of the standing surfaces (sample A.st.3) of limestones (C: calcite, Q: quartz, Wh: Whewellite, G: Gypsum, O-H: Oxygen-Hydrogen bands, C-H: Carbon-Hydrogen bands).

### 4.1.3. Soil Samples

XRD patterns indicate that soils are composed of calcite and quartz along with some feldspars such as anorthite and muscovite (Figure 38).

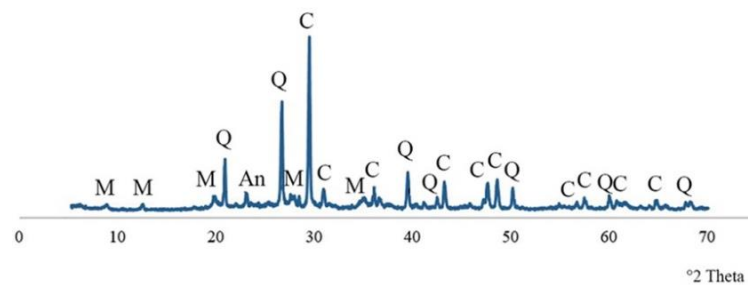


Figure 38. XRD graphic of the soil (C7.so.1) (C: Calcite, Q: Quartz, An: Anorthite, M: Muscovite).

## 4.2. Chemical Composition of Stone and Soil Samples

The results of chemical composition analysis carried out by SEM-EDS confirm the results of XRD and FT-IR analyses. The results of the chemical composition analysis indicate that limestones are mainly composed of a high amount of CaO, low amounts of SiO<sub>2</sub>, Al<sub>2</sub>O<sub>3</sub>, FeO and other oxides. Besides, the chemical composition and the thermal

analysis (TG/DTA) of stone samples show differences between inner cores and stone surfaces. The results are described in detail in the following sections.

#### **4.2.1. Sound Inner Cores of Stone Samples**

EDS analysis shows that sound inner cores of limestones are composed of a high amount of CaO (~92.5 %), low amounts of SiO<sub>2</sub>, Al<sub>2</sub>O<sub>3</sub>, MgO (~6.5 %) and trace amounts of P<sub>2</sub>O<sub>5</sub>, K<sub>2</sub>O, SO<sub>3</sub> and Na<sub>2</sub>O (Table 8).

The results of the SEM-EDS analysis results confirm those of the thermal analysis (Table 8). In the TG/DTA analysis of the stone samples, weight losses are observed in the range of 30°C–200°C, 200°C–600°C and 600°C–900°C, which are mainly due to absorbed water, decomposition of organic matter and carbon dioxide, respectively (Wang et al. 2000, Rodriguez et al. 2011). The thermographs of the inner cores of the stones show that the weight loss between 600°C–900°C is nearly 43%. The weight losses correspond to calcium carbonate content nearly 95% in the limestone samples (Table 8).

#### **4.2.2. Weathered Surfaces of Stone Samples**

The SEM-EDS results indicate that the amount of CaO decreases from sound inner cores to weathered surfaces of limestones both standing parts and recently excavated parts, whereas the amount of SiO<sub>2</sub>, Al<sub>2</sub>O<sub>3</sub> and FeO increases (Figure 39). The high amounts of SiO<sub>2</sub>, Al<sub>2</sub>O<sub>3</sub> and FeO on stone surfaces are due to the effect of degradation of the surface and more specifically to the accumulation of fine silt and clay minerals from the nearby surroundings.

In addition to clays, high amounts of SO<sub>3</sub> on some limestone surfaces, especially sample A3.st.1 (Table 8), support the presence of gypsum formation and confirm the results of XRD and FT-IR described in section 4.1.2. As earlier mentioned, high SO<sub>3</sub> concentration of the stone surfaces could indicate the effects of air pollution due to SO<sub>2</sub> gases. It might be formed as a result of the straw and stubble burning around the archaeological area. Besides, high content of the P<sub>2</sub>O<sub>5</sub>, especially samples C7.ex.1 and C8.st.1 (Table 8), could show the activities such as preparation, storage and disposal of food and the fertilization of soil in the archaeological site (Herz and Garrison 1997).

Table 8. Weight losses (TG/DTA) and oxide composition (SEM/EDS) of stones

Sample	Weight losses (%)		Oxide composition (%)								
	200-600°C	600-800°C	Na <sub>2</sub> O	MgO	Al <sub>2</sub> O <sub>3</sub>	SiO <sub>2</sub>	P <sub>2</sub> O <sub>5</sub>	SO <sub>3</sub>	K <sub>2</sub> O	FeO	CaO
A1.st.1	3.5	38.8	0.48	2.76	11.21	48.77	6.89	3.14	2.01	4.97	18.79
A1.in.1	1.1	42.3	0.06	1.46	1.00	2.89	0.35	0.42	0.36	0.35	93.13
A2.st.1	10.7	36.7	0.17	1.11	3.12	10.79	1.03	1.05	0.73	1.13	80.87
A2.in.1	0.5	40.2	0.04	0.88	0.63	9.77	0.07	0.41	0.22	0.33	87.63
A3.st.1	9.2	31.1	0.85	1.52	2.96	9.42	3.04	5.62	1.88	1.17	73.54
A3.in.1	0.1	65.7	0.10	0.87	0.63	6.75	0.14	0.96	0.24	0.19	90.12
A4.st.1	0.6	43.9	0.07	0.94	0.81	2.00	0.13	0.75	0.22	0.08	94.99
A4.in.1	0.5	43.2	0.10	1.31	0.66	1.69	0.37	0.37	0.07	0.30	95.14
C1.st.1	8.8	67	0.04	0.89	1.77	6.08	0.31	0.33	0.32	0.71	89.55
C1.in.1	0.5	41.9	0.19	0.80	1.79	6.50	0.03	0.11	0.30	0.38	89.91
C2.st.1	18.06	33.1	0.37	0.88	2.53	9.26	0.95	1.01	0.73	0.69	83.57
C2.in.1	0.7	43.7	0.19	0.80	0.40	1.33	0.07	0.04	0.15	0.18	96.74
C3.st.1	18.2	33.6	0.07	0.69	1.65	4.31	0.29	0.55	0.34	0.46	91.65
C3.in.1	1.8	41.9	0.05	0.71	1.48	3.33	0.06	0.11	0.20	0.38	93.68
C3.st.2	49.3	14.2	-	-	-	-	-	-	-	-	-
C3.st.3	-	-	0.30	0.90	2.01	5.32	0.92	0.98	0.45	0.54	88.60
C4.st.1	11.1	38	0.18	1.02	2.09	5.83	0.53	0.97	0.26	0.19	87.27
C4.in.1	0.8	43	0.14	0.56	0.65	2.15	0.06	0.10	0.10	0.19	96.04
C4.st.2	17.9	34.4	0.39	1.06	1.31	5.55	0.82	1.29	0.46	0.16	88.69
C4.st.3	36.6	22	1.51	3.48	9.71	21.68	1.20	3.02	0.69	0.00	57.38
C4.st.4	11.9	36.3	0.07	1.05	2.05	5.44	0.38	0.63	0.48	0.77	89.14
C5.st.1	1.2	36.8	0.23	1.28	3.06	9.13	3.82	0.18	0.60	1.36	80.34
C5.in.1	0.6	65.4	0.14	0.79	1.22	3.45	0.09	0.23	0.29	0.17	93.61
C5.ex.1	3.2	53.3	0.40	2.03	13.62	27.84	0.27	0.21	3.21	4.63	47.77
C6.st.1	28.1	26.8	0.68	2.52	6.66	16.52	0.92	1.28	0.76	0.33	69.52
C6.in.1	0.9	43	0.07	1.15	1.02	2.56	0.19	0.10	0.29	0.36	93.85
C7.st.1	1.5	34.3	0.22	0.96	2.91	11.20	0.90	1.15	0.99	0.97	80.69
C7.ex.1	13.7	38.7	0.32	1.17	3.86	7.74	13.25	0.28	0.61	1.18	71.60
C8.st.1	2.8	21.8	0.34	5.34	4.44	12.83	14.80	0.57	0.75	1.69	58.55
C8.in.1	0.5	44.3	0.06	9.96	2.23	3.62	0.18	0.04	0.19	0.51	83.22
C9.st.1	21.2	30.7	0.20	1.01	3.68	7.50	1.06	1.15	0.77	1.12	83.52
C9.in.1	1	43.6	0.01	0.73	1.03	0.62	0.20	0.19	0.10	0.11	96.99

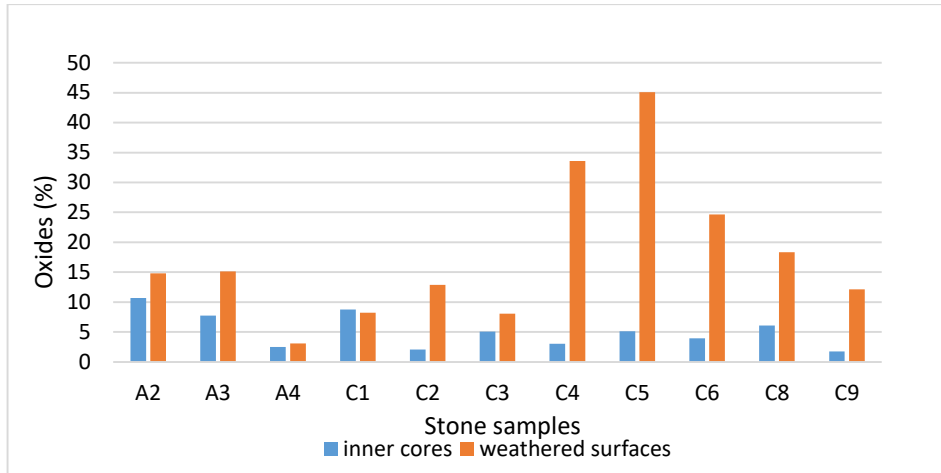


Figure 39. Total % amounts of clays ( $\text{Al}_2\text{O}_3$ ,  $\text{SiO}_2$  and  $\text{FeO}$ ) of samples from inner cores and weathered surfaces.

Thermal analysis supports the SEM-EDS analysis results. In the thermographs of the standing surface of the limestone, weight losses are observed in the range of 30–200 °C, 200–600 °C and 600–900 °C, which are mainly due to absorbed water, decomposition of organic matter and carbon dioxide, respectively. The high percentage weight loss at 200–600 °C and 600–900 °C for standing surfaces shows the presence of higher amount of organic matter due to biological colonization (Figure 40). Figure 41 reports all TGA curves of the stone samples from both the inner cores and the surfaces together. As mentioned before, the inner cores of the stones show that the intense weight loss between 600°C–900°C, as a result of the deterioration of calcite crystals (Figure 41).

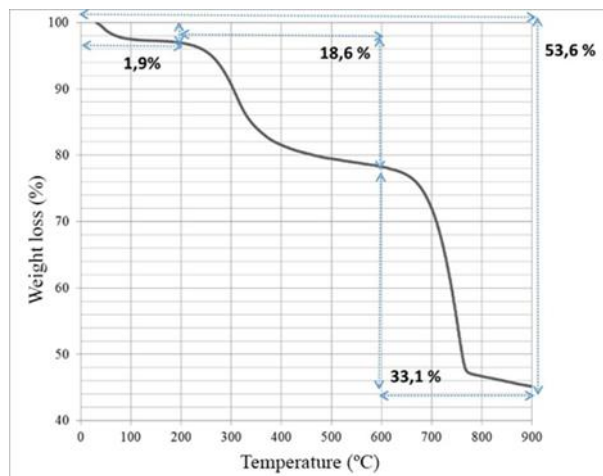


Figure 40. TGA curve of the standing surface of stone sample (C2.st.1).

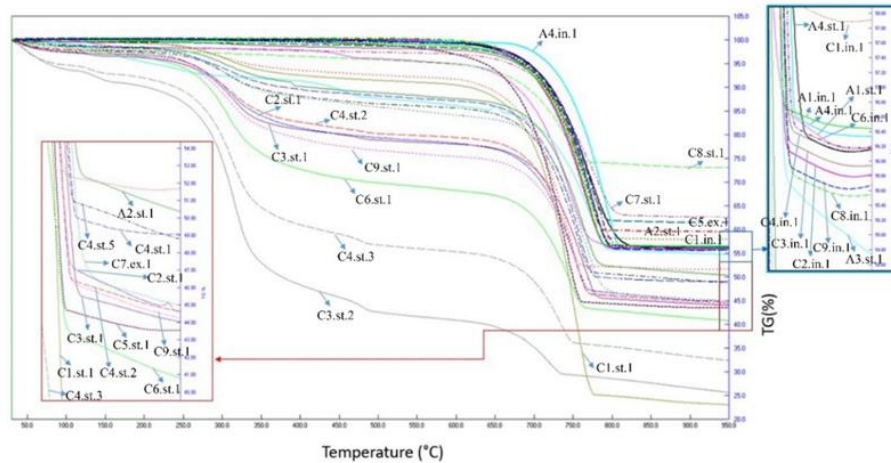


Figure 41. TGA curves of all stone samples.

### 4.2.3. Soil Samples

SEM-EDS analyses indicate that the soils are composed primarily of  $\text{SiO}_2$ ,  $\text{CaO}$ ,  $\text{Al}_2\text{O}_3$  and  $\text{FeO}$ . Other elements are present in minor amounts:  $\text{Na}_2\text{O}$ ,  $\text{K}_2\text{O}$ ,  $\text{MgO}$  and  $\text{P}_2\text{O}_5$  (Table 9). The results of both XRD (described in section 4.1.3) and EDS show that they are calcareous and siliceous soils.

Table 9. Mean values and standard deviation (in parentheses) of major oxide compositions of soils (9 samples) (%)

	$\text{Na}_2\text{O}$	$\text{MgO}$	$\text{Al}_2\text{O}_3$	$\text{SiO}_2$	$\text{P}_2\text{O}_5$	$\text{SO}_3$	$\text{K}_2\text{O}$	$\text{FeO}$	$\text{CaO}$
<b>Soil</b>	0.51 (0.07)	3.53 (0.19)	13.54 (1.47)	44.61 (5.07)	1.77 (0.42)	0.25 (0.11)	2.84 (0.26)	5.75 (0.69)	27.19 (7.58)

### 4.3. Petrographic and Microstructural Properties of Stone Samples

The petrographic observations have been carried out on thin sections of the core of the stone samples (C2.in.1, C3.in.1, C4.in.1, C5.in.1, C9.in.1) (Figure 42). SEM analysis was performed on the surface and cross section of the stone samples collected from the 3<sup>rd</sup> column (C3), the 6<sup>th</sup> column (C6) and the 7<sup>th</sup> column (C7). The results of both studies are described in the following sections 4.3.1 and 4.3.2.

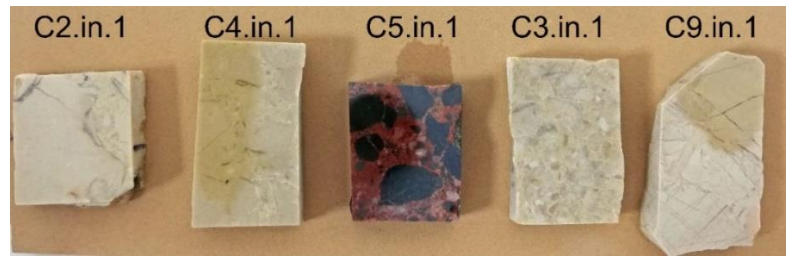


Figure 42. The stone samples for petrographic analysis.

### 4.3.1. Sound Inner Cores of Stone Samples

The petrographic observations of the stone sample C2.in.1 show that the limestone is consisted of micritic, coarse crystalline calcite (micritic limestone) (Figure 43). The results show that the stone sample C3.in.1 is microcrystalline calcite and contains abundant well-calcitized fossils (biosparitic limestone) (Figure 44).

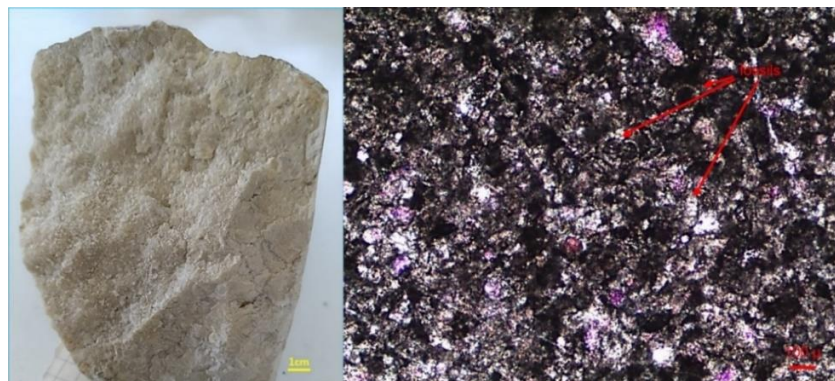


Figure 43. Macroscopic and microscopic images of sample C2.in.1.

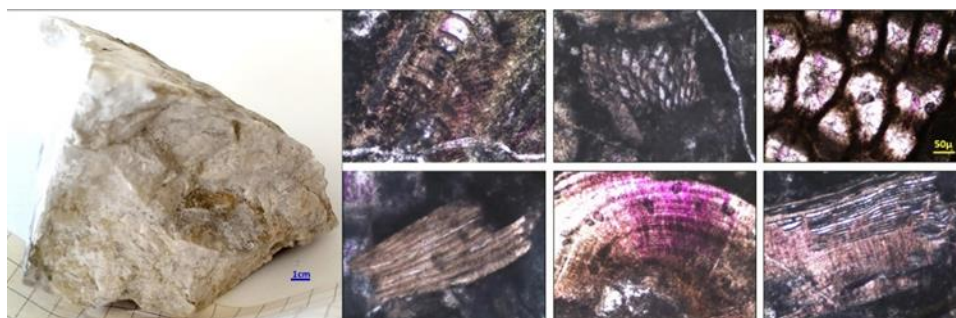


Figure 44. Macroscopic and microscopic images of sample C3.in.1.



Stone sample C4.in.1 has a homogeneous micritic calcite structure and contains sparsely crystallized dolomite grains (limestone with low dolomite content) (Figure 45).

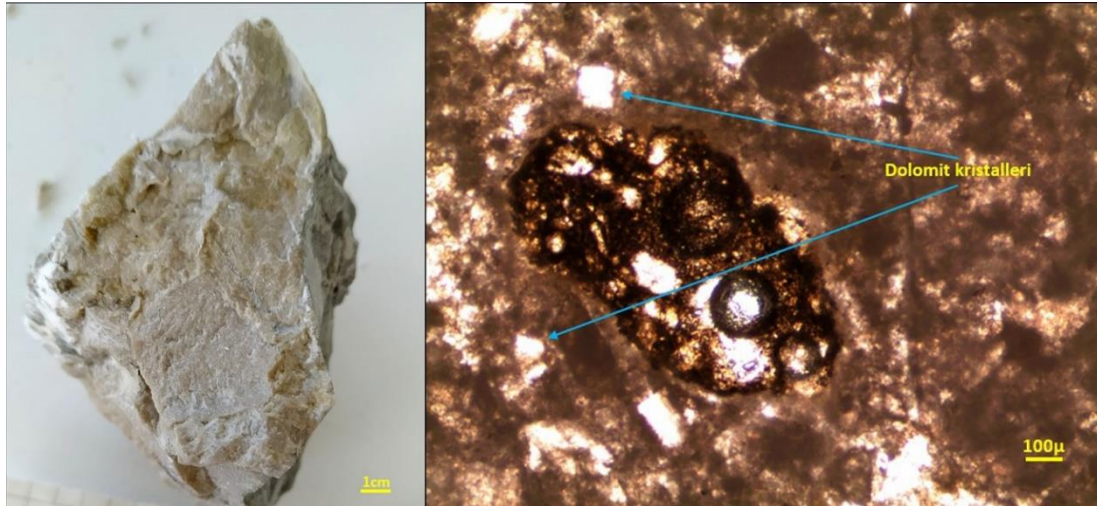


Figure 45. Macroscopic and microscopic images of sample C4.in.1

Stone sample C9.in.1 shows highly micritic calcite and tightly developed dolomite crystals (dolomitic limestone) (Figure 46).

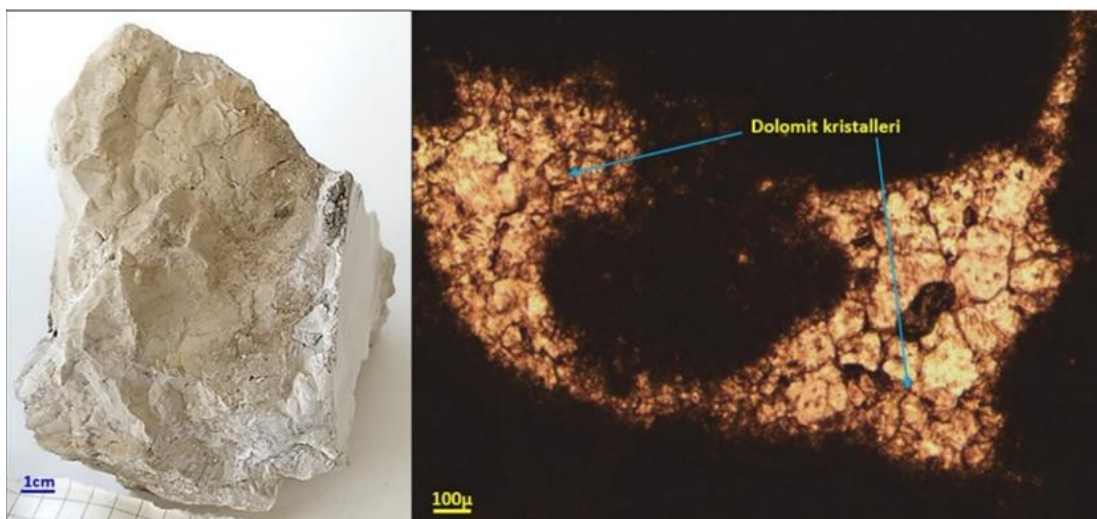


Figure 46. Macroscopic and microscopic images of sample C9.in.1

Stone sample C5.in.1 is an iron-rich brecciated limestone with microcrystalline calcite crystals in large grains (Figure 47). The opaque materials are observed, which are likely to be micritic calcite and hematite with high iron content, holding the angular grains together (Figure 47).

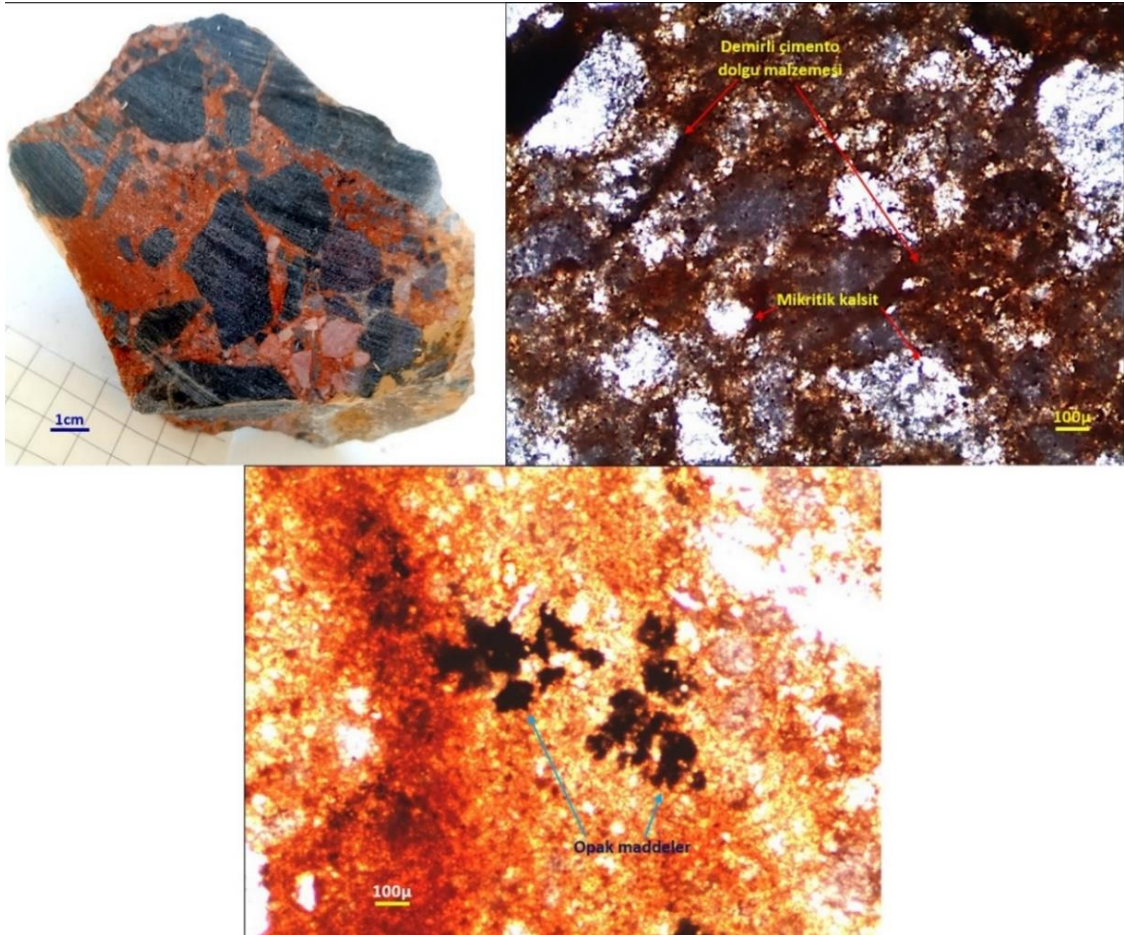


Figure 47. Macroscopic and microscopic images of sample C5.in.1.

Based on the above petrographic observations, it can be concluded that stone samples C2.in.1, C3.in.1, C4.in.1 and C9.in.1 have similar properties. These stones are micritic, dolomitic and biosparitic limestones. On the other hand, stone sample C5.in.1 shows different properties. This is an iron-rich brecciated limestone with microcrystalline calcite.

Almost all of the columns in the area have similar appearance and petrographic properties as well. Differently, the column C5 (with column C8) has a rare limestone type

used in that area. These stones may have been brought into the city from another area (different from the historic quarry used in that area), and/or in different period.

### **4.3.2. Weathered Surfaces of Stone Samples**

As earlier reported, common type of deterioration present on the limestones in the site is biological growth (thriving micro-organisms). Microorganisms generally play an effective and powerful role in the degradation of stones. They can proliferate in the cracks, fractures or pores of the stones and develop the deterioration. The degree of interaction between these organisms can lead to a slower or accelerated degradation of the stone material (Warscheid and Braams 2000).

In this section, SEM observations performed by scanning electron microscope to investigate the biodegradation of limestones are reported. SEM observations were carried out on the stone sample taken from the 3<sup>rd</sup> column (C3), the 6<sup>th</sup> column (C6) and the 7<sup>th</sup> column (C7) and both the surface and the section of these samples were investigated in detail.

Microbiological colonization on the surface of the 3<sup>rd</sup> column is seen in different colors such as black, grey, yellow or pink thanks to the pigmentation ability of microorganisms (Figure 48). The sample C3.st.1 was taken from greyish stains on the surface. The sample C3.st.2 was taken from a yellow spot from this pigmented biofilm where lichens were observed and the sample C3.st.3 was taken from pink stains where biopitting is visible on the surface (Figure 48).

The 3<sup>rd</sup> column (C3) is covered by a very developed microbiological colonization throughout to the inner cores of the stone (Figure 49). This is probably due to the distribution of bacterial communities, also the environmental conditions and the mineral structure of the stone, as described before. Some microorganisms such as bacteria, fungi might penetrate into the materials and cause severe damage (Sterflinger and Piñar 2013). Endolithic microorganisms (fungi, green algae, cyanobacteria) are responsible for biopitting on stone surfaces (Caneva et al. 2008). Presence of biopitting on this stone surface and microbial development throughout to the inside of the stone may show fungi and bacteria formation in this biofilm.

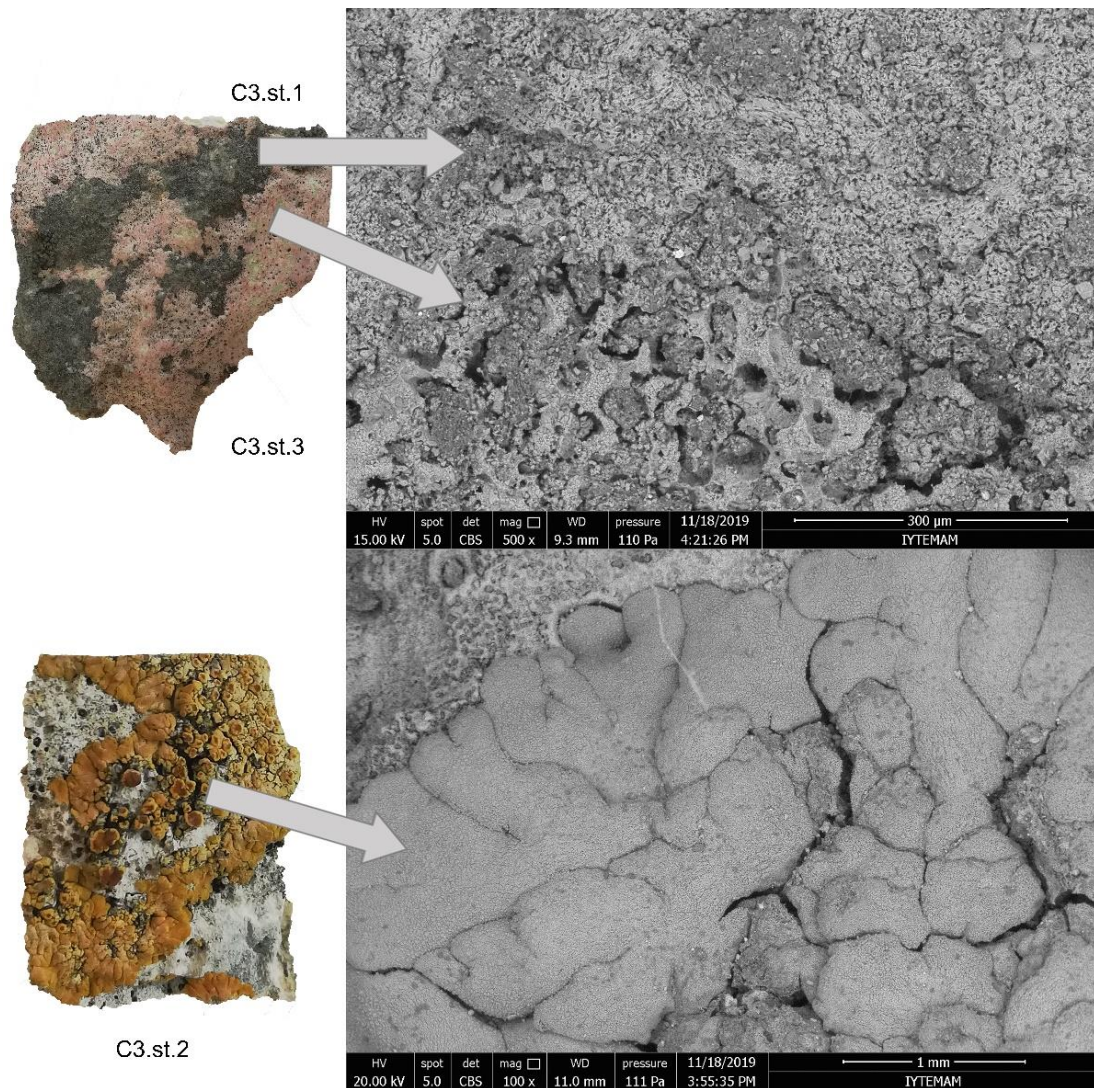


Figure 48. SEM images of the sample C3.st.1, C3.st.2 and C3.st.3.

This stone has two different microbiological colonization layers (1,2) under a thin stone layer (3) (Figure 49, 50). The presence of microorganisms under a few millimeters thick stone layer provides protection against high temperature and UV-radiation (Warscheid and Braams 2000).

Figure 49 also indicates that the sound limestone is mainly composed of CaO (98.37%). In the first and second microbiological colonization layers, the amount of CaO decreases and SiO<sub>2</sub> and other oxides increases (Figure 49). Third layer is a few millimeters thick stone layer and has high amount of CaO (96.44%). First and second layers have higher CO<sub>2</sub> due to the organic matter. Besides, the EDS mapping show that the amount C increases from the inside of the stone to the surface because of the organic matter (Figure 51).

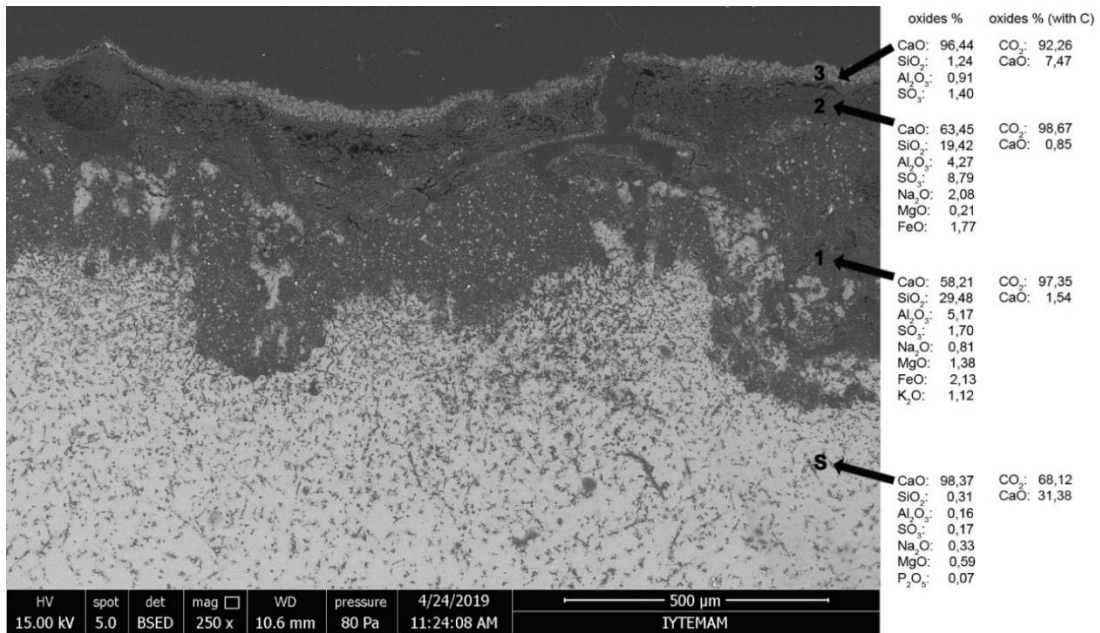


Figure 49. SEM image and EDS results of the intersection of the standing stone sample from the 3<sup>rd</sup> column.

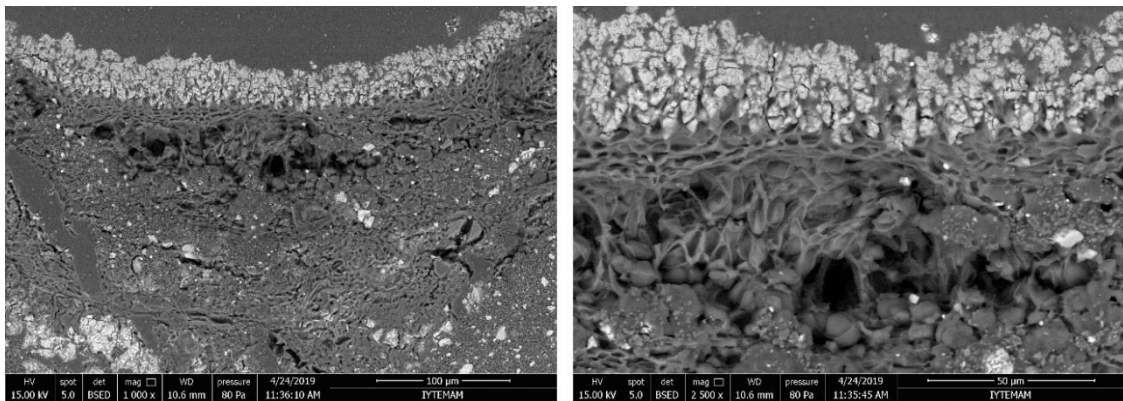


Figure 50. SEM images of the deterioration layers on standing stone sample from the 3<sup>rd</sup> column.

The thickness of microbiological colonization on this limestone varies between 130 and 170 μm for the second layer of microbiological colonization (Figure 51). The first layer of microbiological colonization developed throughout to the inner cores more as seen in the figure 49, probably because of bacteria and fungi as mentioned above.

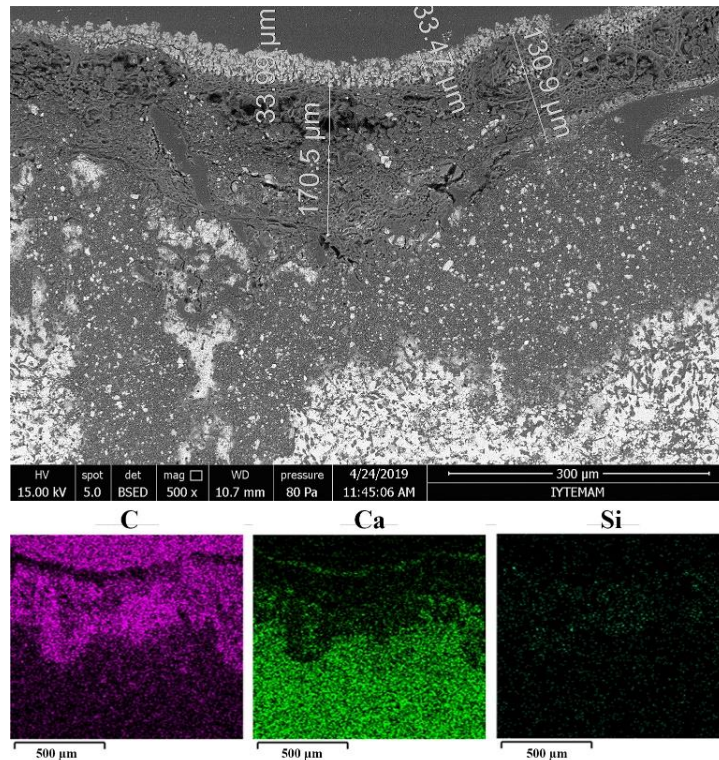


Figure 51. SEM image and EDS mapping of the intersection of the standing stone sample from the 3<sup>rd</sup> column.

The 6<sup>th</sup> column (C6) is covered by biological formations as black, dark and light grey color stains. The thickness of microbiological colonization on this limestone is nearly 680  $\mu\text{m}$  thickness on the stone surface (Figure 52).

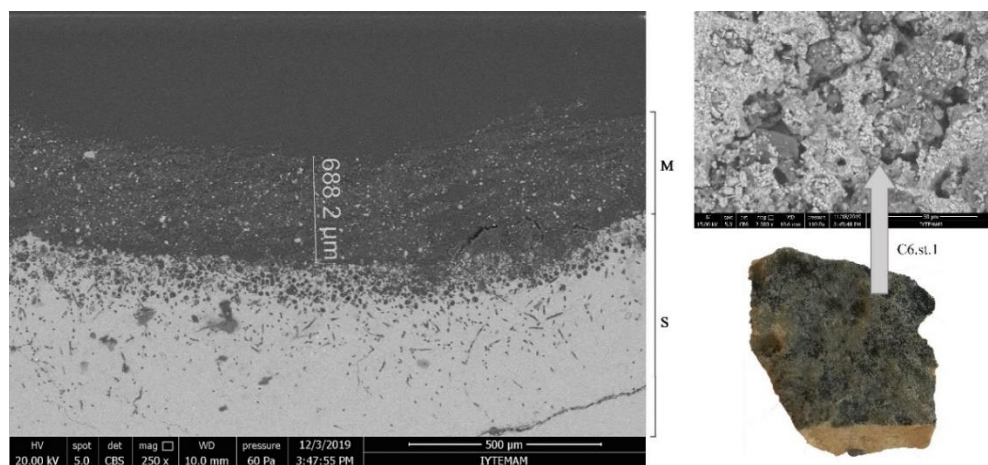


Figure 52. SEM image of the intersection of the standing stone sample from the 6<sup>th</sup> column (C6.st.1), (M: microbiological formation, S: stone inside).

Figure 53 shows the development of biodeterioration between the standing surface and the recently excavated surface of the 7<sup>th</sup> column (C7). It reveals that microbiological colonization is more developed on the standing surface of stone sample (C7.st.1) than the recently excavated surface (C7.ex.1) (Figure 53).

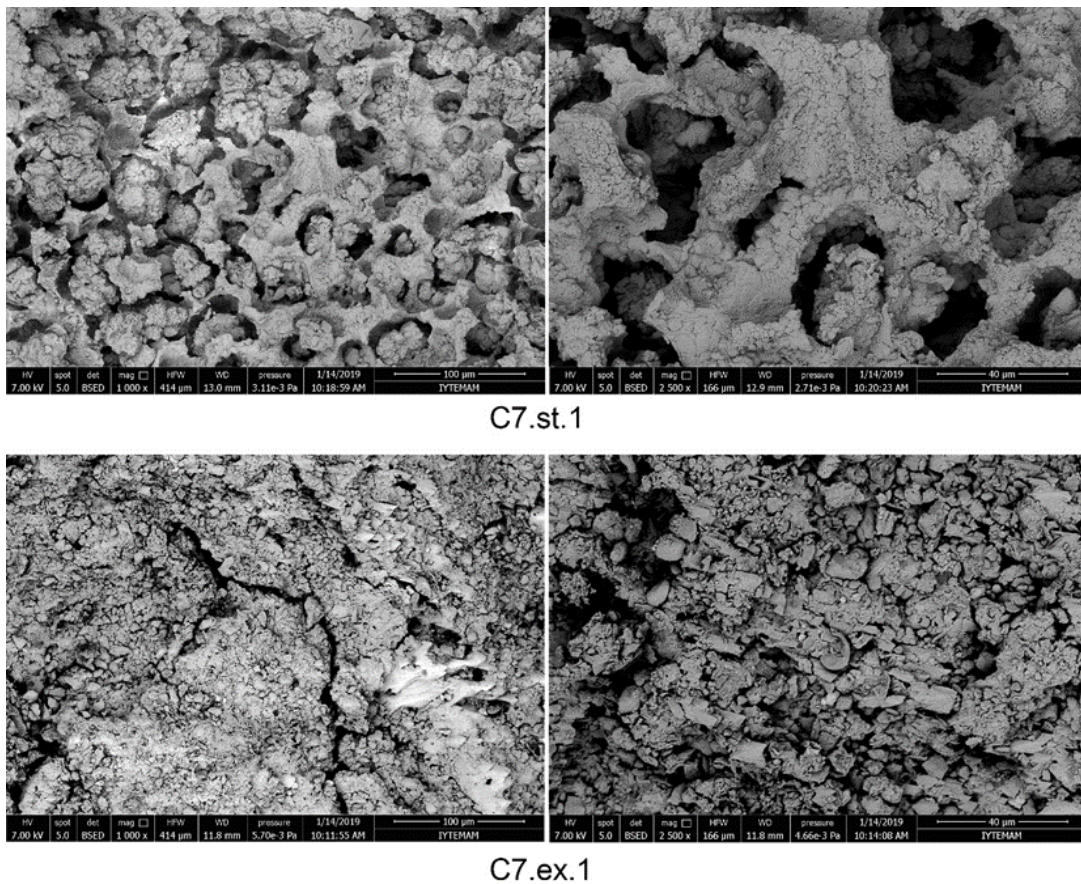


Figure 53. SEM images of the standing surface (C7.st.1) and the recently excavated surface (C7.ex.1) of the 7<sup>th</sup> column.

Figure 54 shows SEM image and EDS mapping of the sample from the recently excavated surface of the the 7<sup>th</sup> column (C7.ex.1). It indicates a thick clay accumulation that varies between 50 and 200  $\mu\text{m}$  on the recently excavated parts of the limestone surface (Figure 54). That supports the presence of high amounts of  $\text{SiO}_2$ ,  $\text{Al}_2\text{O}_3$  and  $\text{FeO}$  on stone surfaces described in chemical composition analysis before. It is mainly due to the accumulation of fine silt and clay minerals from the nearby surroundings. Clay minerals are not effective in stone deterioration before excavation since there is no wetting and drying cycles under the soil. However, they cause rapid deterioration with

the formation of wetting and drying cycles after the stone is unearthed (Thorn et al. 2002). In addition, clay minerals on stone surface provide an appropriate environment for microbiological growth. Since stones are exposed to atmospheric conditions after excavation, they are colonized by microorganisms and thus deteriorate rapidly. Besides, the exposure time to atmosphere has impact on microbial composition on stones (Gorbushina and Broughton 2009).

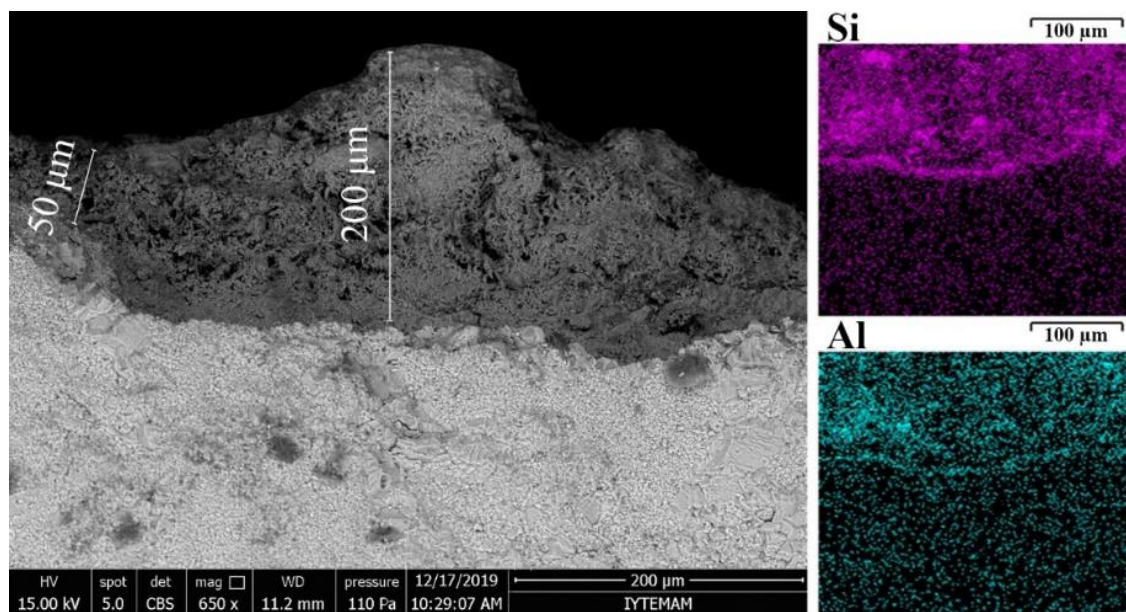


Figure 54. SEM image and EDS mapping of the intersection of the recently excavated part of the 7<sup>th</sup> column (C7.ex.1).

#### 4.4. Soluble Salts of Stone and Soil Samples

For the determination of the presence of soluble salts in the stone and soil samples from the site, different methods were used: hygroscopic moisture content (HMC), conductivity and ion chromatography (IC).

The hygroscopic moisture content (HMC) gives an indication of the presence of soluble, hygroscopic salts (Lubelli et al. 2004). Therefore, HMC at 20°C / 95% RH of powder samples taken from different depths (0-1cm, 1-2cm, 2-5cm) of the stones was assessed. The results show that the most stone samples have generally low HMC values (0.10 -1.49) (Appendix D), indicating that no significant amount of soluble, hygroscopic



salts are present in the stone. In addition, the results of the electrical conductivity measurements indicated that soil samples contain less than one percent of soluble salts (Appendix E).

On a selection of 3 samples (A.st.1, A.st.2 and A.st.3), the ion content has been determined by IC. The salt content in two of the samples (A.st.1, A.st.2) taken from Alakapı (the triumphal arch) (Table 10), can be classified as “low”, according to Snethlage (Snethlage 2005). Differently, sample A.st.3, has a somewhat higher content of chloride and nitrate ions, which according to Snethlage, can be classified as “moderate”; a very high content of sulfates is measured in sample A.st.3. The differences between the salt content among samples A.st.1, 2 and 3 taken from the triumphal arch, might be related to their different locations; A.st.3 was taken from a sheltered area of the pilaster on the south-west façade of the triumphal arch, where a black crust is visible (Figure 55). A.st.1 and A.st.2 were collected from the pilaster on the south corner of the triumphal arch; A.st.1 from the south-east part where a yellow patina was observed, A.st.2 from the north-west part of the pilaster where a black discoloration was observed on a nonsheltered area probably because of biological growth (Figure 55).

Table 10. HMC and IC results of the samples from Alakapı.

code	height/ depth (cm)	HMC (%)	Anions (micromol/g)			Cations (micromol/g)			
			chlorine (Cl)	nitrate (NO <sub>3</sub> <sup>-</sup> )	sulphate (SO <sub>4</sub> <sup>2-</sup> )	sodium (Na)	potassium (K)	magnesium (Mg)	calcium (Ca)
A.st.1	150/0-1	0.31	0.65	n.a.	1.71	2.59	4.03	1.77	12.16
A.st.1	150/1-2	0.16	-	-	-	-	-	-	-
A.st.2	120/0-1	0.46	3.62	3.11	23.44	2.04	2.79	2.89	28.21
A.st.2	120/1-2	0.46	-	-	-	-	-	-	-
A.st.3	120/0-1	1.45	15.27	19.57	32.49	7.62	13.93	n.a.	61.44
A.st.3	120/1-2	0.89	-	-	-	-	-	-	-

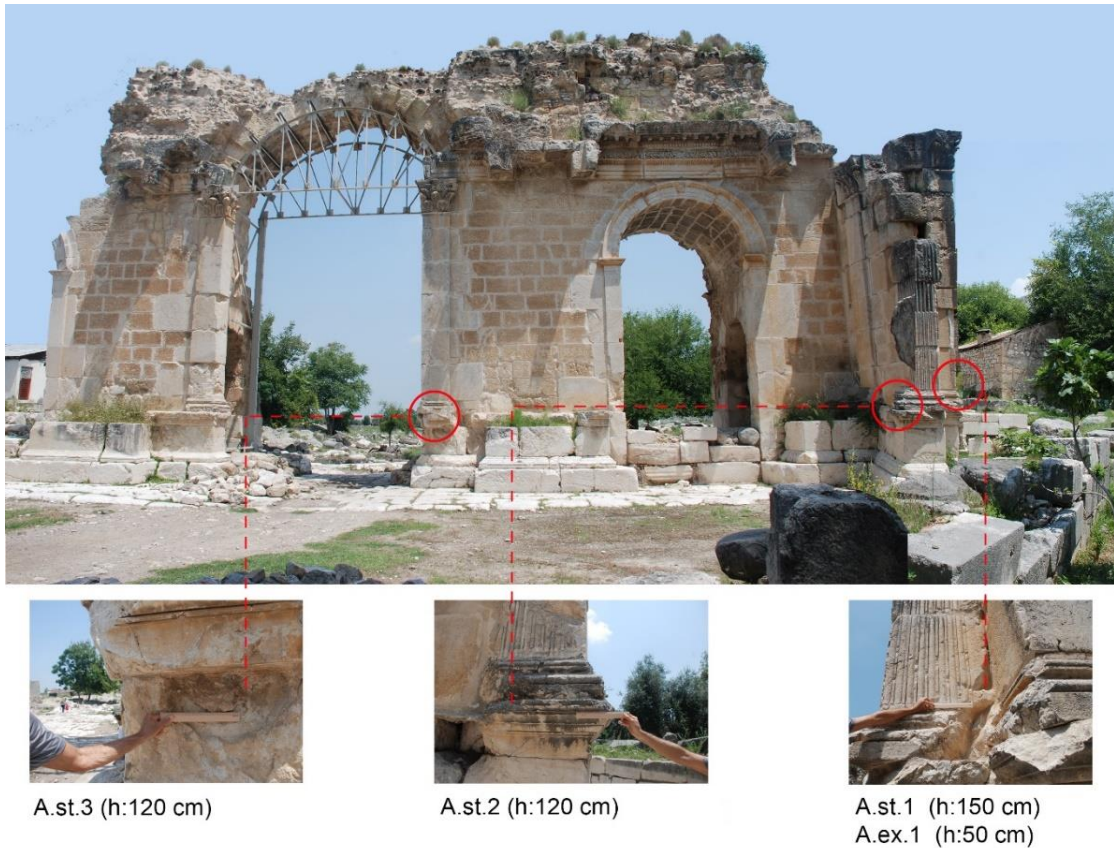


Figure 55. Sample locations on the Alakapı.

High amounts of sulphate ( $\text{SO}_4^{2-}$ ) are present in sample A.st.3 (Figure 56); this, in combination with the presence of Ca ions, suggests the presence of gypsum in this sample. This conclusion is in agreement with the results of XRD and FT-IR described in section 4.1.2. As earlier mentioned, a main source of sulphate (leading then to the formation of gypsum crust on lime-containing materials) is air pollution. Sulfur dioxide gas ( $\text{SO}_2$ ) present in the polluted air reacts, in the presence of water, with calcite mineral, present in the calcareous stones, and turns it to the gypsum (see section 2.2.3).

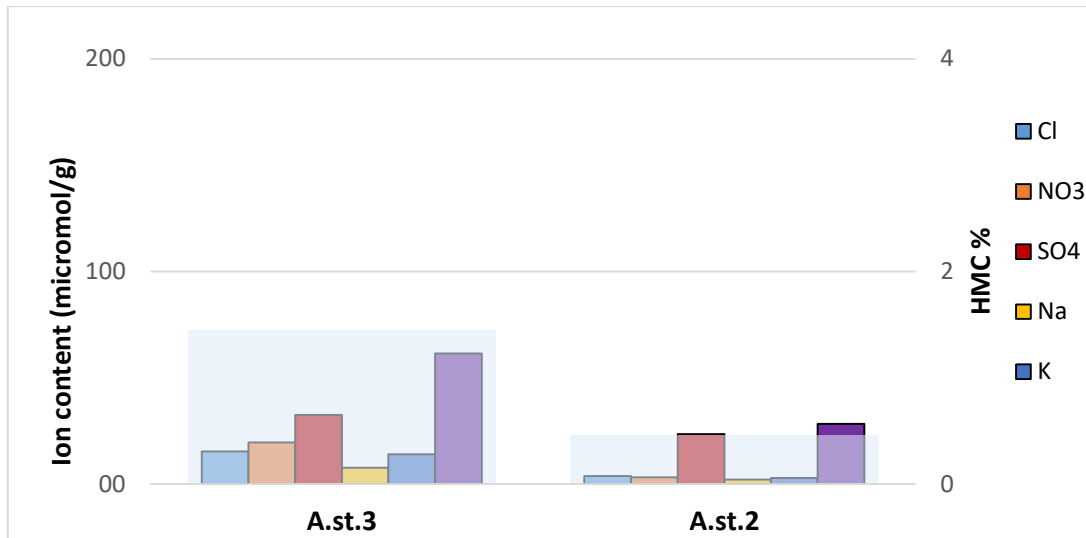


Figure 56. Ion content and HMC graphics of the sample A.st.3 and A.st.2.

The IC results show that samples A.st.3 and A.st.2 have different amount of ions. These mixed ions can precipitate as various salts, depending on the environmental conditions (temperature and relative humidity). One of the model which can be used to make a prediction of the crystallization process of salt mixtures at a specific temperature and RH range is ECOS model (Price 2000), supported by the user interface software RUNSALT (Bionda 2005). By using RUNSALT, the salt crystallization diagrams of the samples A.st.3 and A.st.2 were calculated (Figure 57, 58). Beside the ionic composition of samples resulting from the IC analyses, the environmental conditions at the site in 2019 (average 20.42 °C temperature and 55.46 % RH) were used (MGM 2020) as input for the calculation.

Figure 57 and 58 show the crystallization behavior of the salts in the samples A.st.3 and A.st.2. At about 55% RH (average RH at the site), calcium sulphate is the major phase; this is mostly present as anhydrite ( $\text{CaSO}_4$ ); for temperature lower than 12°C, it is present in the form of gypsum ( $\text{CaSO}_4 \cdot 2\text{H}_2\text{O}$ ). At the temperature of about 20°C (average temperature at the site), calcium sulfate crystallizes in the form of gypsum ( $\text{CaSO}_4 \cdot 2\text{H}_2\text{O}$ ) in the range of 60-90% RH, and as anhydrite ( $\text{CaSO}_4$ ) below 60% RH. The diagrams indicate that the sample A.st.3 has higher amounts of salts (calcium sulphate) than the sample A.st.2, as determined by the higher content of sulphate ions ( $\text{SO}_4^{2-}$ ) (see IC results). Besides, as shown by the diagram of the sample A.st.3, next to these slightly soluble salts, also soluble salts such as NaCl (halite),  $\text{KNO}_3$  (niter), KCl (sylvite) can crystallize at RH in the range between 50 and 35% RH.

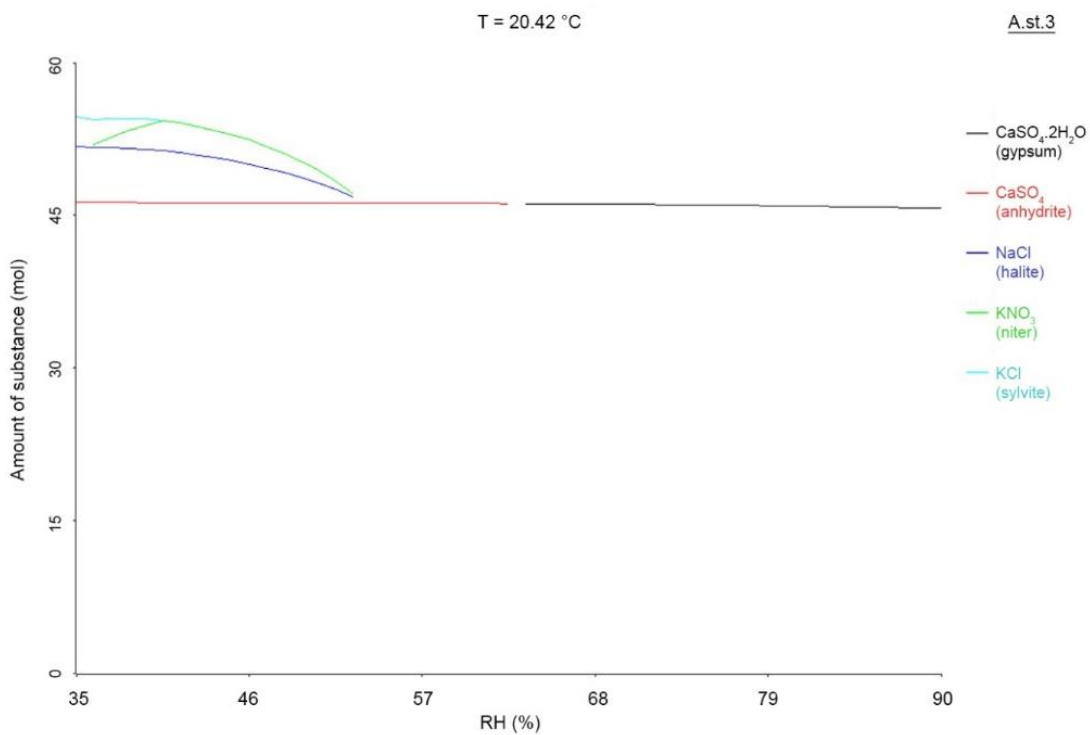
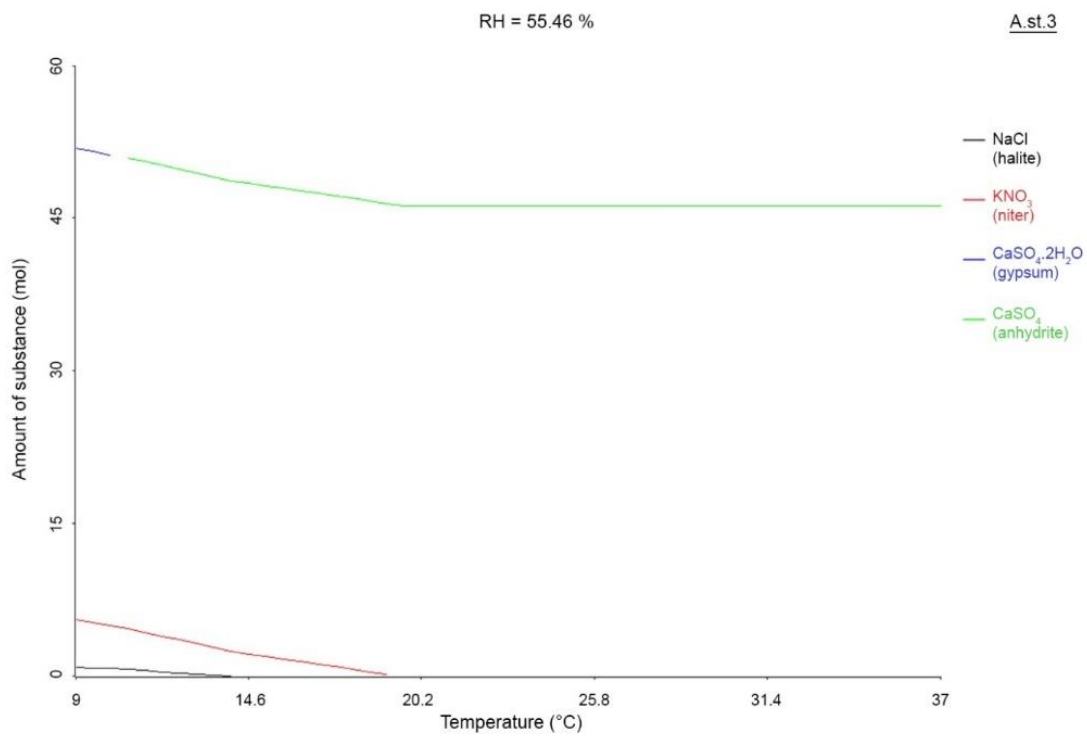


Figure 57. Salt diagram of the sample A.st.3

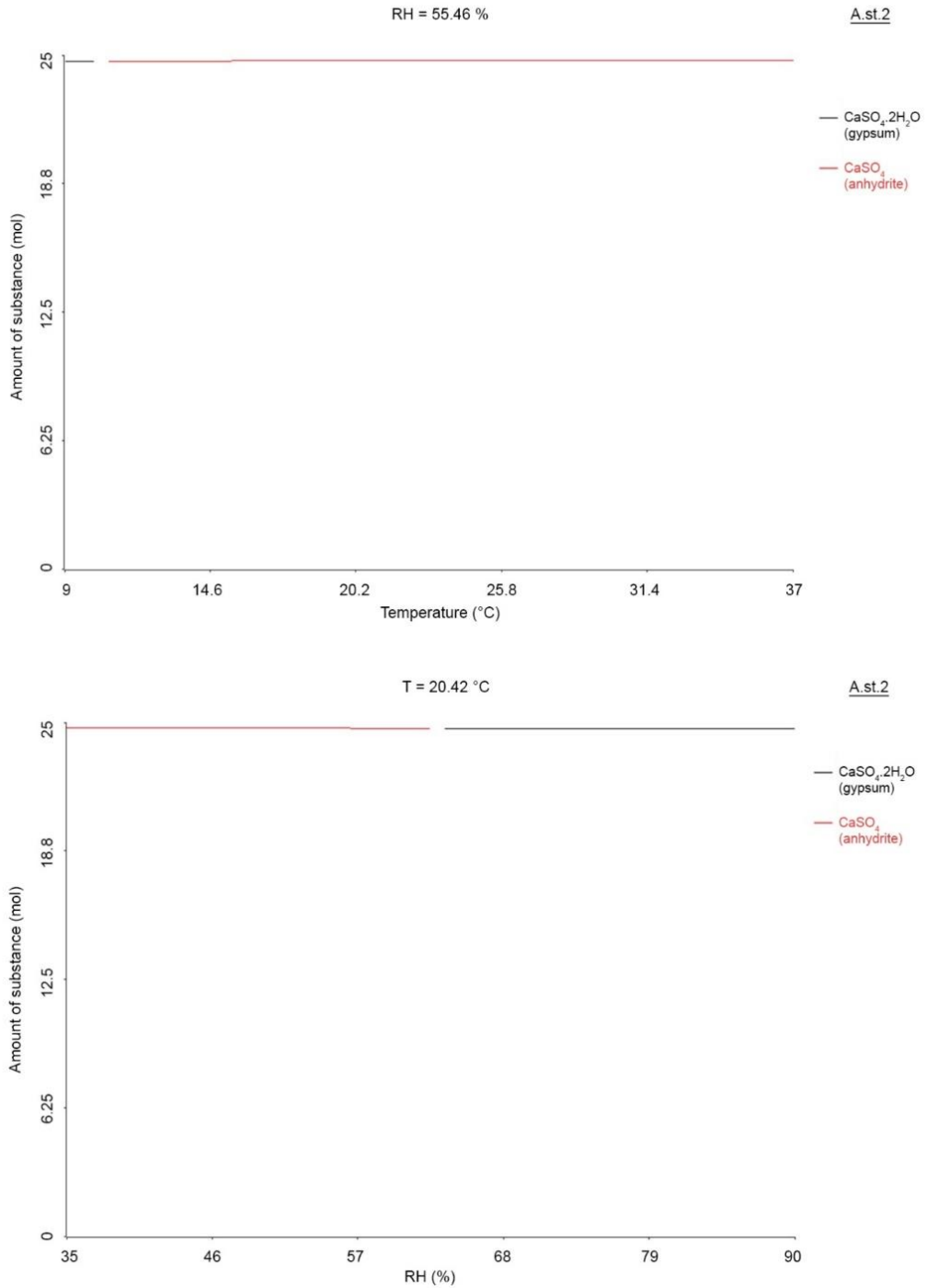


Figure 58. Salt diagram of the sample A.st.2

#### 4.5. Moisture Transport Properties of Stones

In the following sections (4.5.1. and 4.5.2.), the results of the the moisture transport properties of the stones from the site and the historic quarry are reported. Then,

in section 4.5.3, the results of the moisture transport properties of stones from the historic quarry and from the site were compared, in terms of the compatibility for further conservation works.

#### **4.5.1. Moisture Transport Properties of Stones from the Historic Quarry**

Figure 59 shows the water absorption curves of stones from the historic quarry. The limestone samples have a slow absorption behavior, due to their low porosity (see next paragraph) and probably to the presence of fine pores (this would need to be confirmed by measurements by Mercury Intrusion Porosimetry (MIP)). The average capillary water absorption coefficient (WAC) of these limestone is  $50.16 \pm 11.95$  gr/(m<sup>2</sup>sec<sup>0.5</sup>) (CEN 2009). Stone samples Q1 and Q3 show a slightly faster and higher water absorption than other samples. As shown by the standard deviation, there are significant differences between the specimens.

The observed large standard deviation is most probably due to lack of homogeneity in the stone: cracks and parts with different density can be distinguished with the naked eye (Figure 60).

The wetting front (i.e. the height of the capillary rise in the specimen) was monitored visually during the water absorption test. This increased fast during the first 8 hours, similarly to the water absorption curve; after, it moved up slow until full wetting of upper side of the specimen was achieved. The average capillary water penetration coefficient of these limestone is  $0.85 \pm 0.28$  cm/sec<sup>0.5</sup> (CEN 2009).

The total porosity of the stones was measured by immersion at atmospheric pressure. The results are reported in Figure 61. The measurements confirm the low porosity values and the significant variation between specimens: the average porosity is  $1.26 \pm 0.51$  vol %. It should be mentioned that the method used for measuring water absorption consider 2650 kg/m<sup>2</sup> as reference density value of a material without pores. For stones with very low porosity, the calculated results might not be very precise. In the future, it might be useful to measure the porosity under vacuum, e.g. according to the RILEM CPC11.3 recommendations (RILEM 1984).

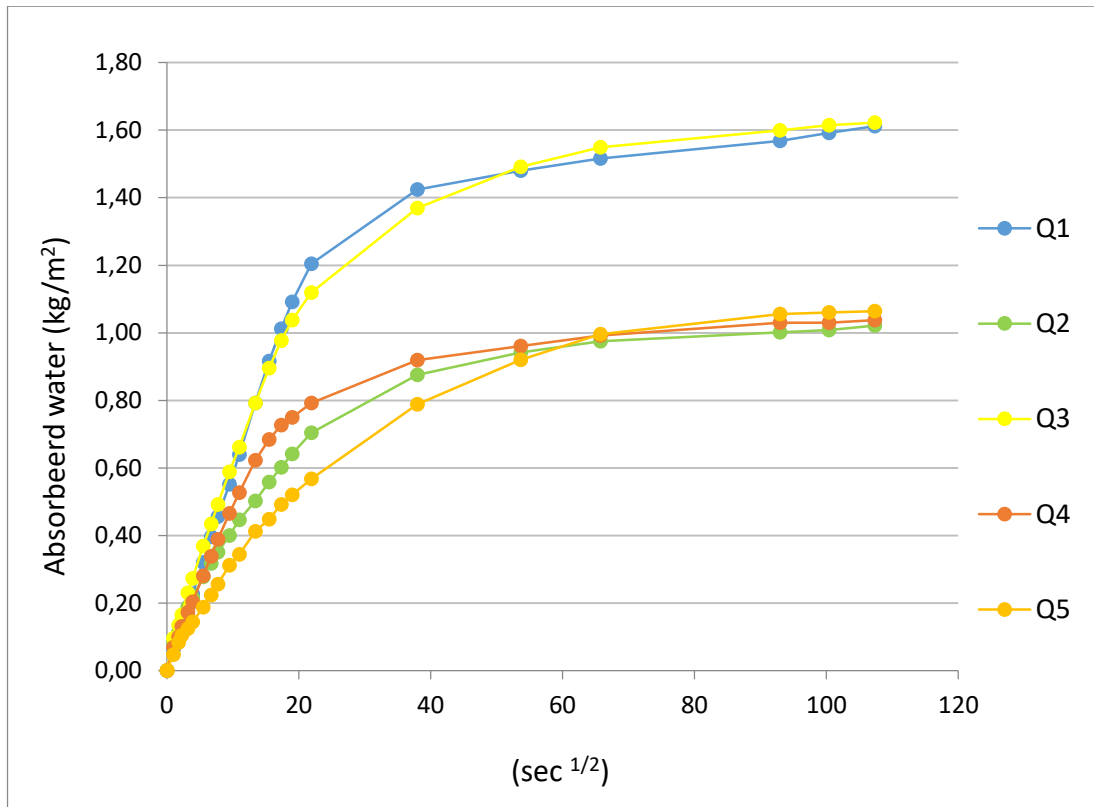


Figure 59. Water absorption by capillarity of the limestones from the historic quarry



Figure 60. Stone samples after water absorption test, Q1 and Q3

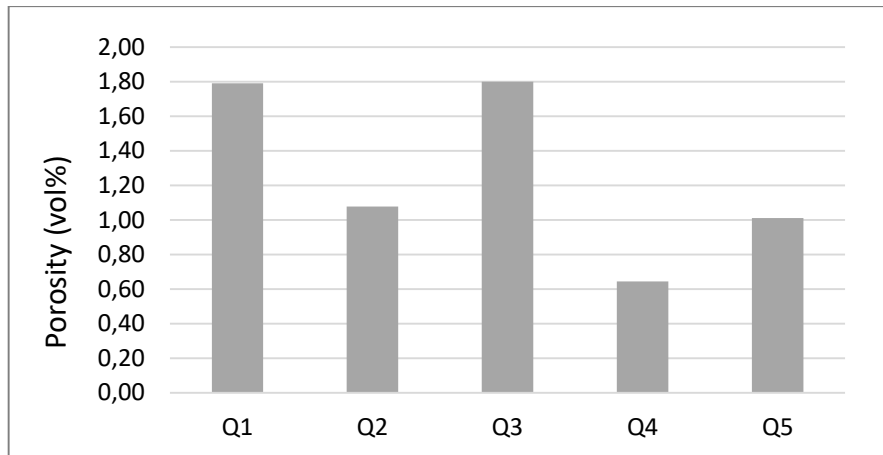


Figure 61. Porosity of stone samples from the historic quarry.

Figure 62 shows the drying rate of stones from the historic quarry. Samples Q1 and Q3 show the fastest drying behavior, most probably due to their higher porosity (1.80%) and to the presence of cracks. Sample Q4 has the slowest drying rate, most probably due to its lower porosity (0.64%) (Figure 62). These results are in line with those of the water absorption test.

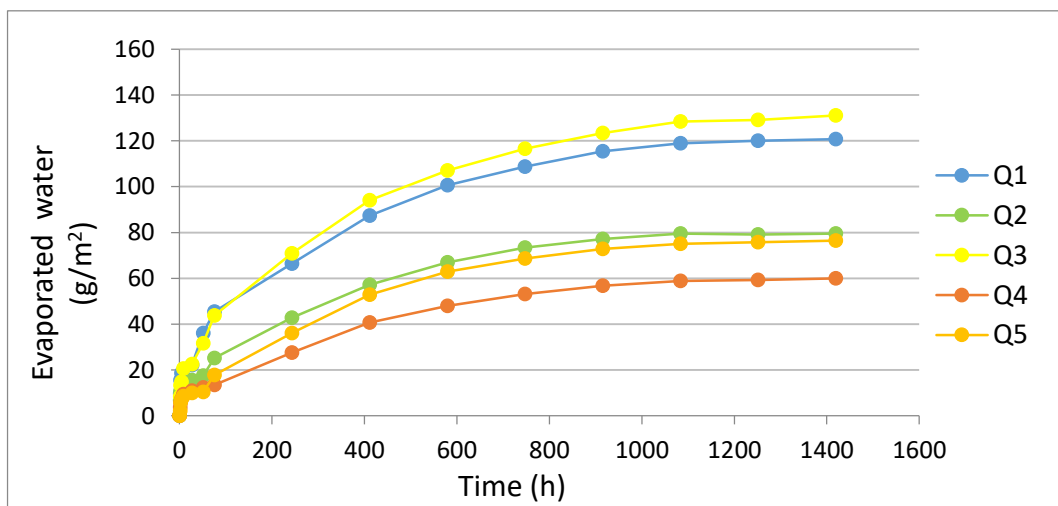


Figure 62. Drying rate properties of the limestones from the historic quarry.

Summarizing, it can be concluded that three stone specimens (Q2, Q4, Q5) from the historic quarry show similar moisture transport properties. Differently, specimens Q1, Q3 show diverging results, which are most probably related to presence of cracks in the



specimens. Therefore, in order to compare the properties of the stone from the quarry to those of the stone from the archeological site, the average moisture transport result ( $Q_{ave}$ ) of the specimens is calculated and compared to the stones from the site in the following section.

#### 4.5.2. Moisture Transport Properties of Stones from the Site

The moisture transport properties of stone samples collected from the sound, inner parts of the columns of the archaeological site (C3: Stone sample from the column 3, C8-1, C8-2: two stone samples from the column 8) are determined in this section.

Figure 63 shows the water absorption curves of stones from the site. The limestone samples show a slow absorption behavior (Figure 63). The capillary water absorption coefficient (WAC) of the stone sample C3 is  $11.41 \text{ gr}/(\text{m}^2\text{sec}^{0.5})$  and the stone sample C8 is  $19.64 \pm 6.09 \text{ gr}/(\text{m}^2\text{sec}^{0.5})$  (CEN 2009).

During the water absorption test, the wetting front (i.e. the height of the capillary rise on the lateral sides of the specimen) was monitored. This increased fast during the first hour, especially for sample C8, similarly to the water absorption curve; it increased slower for sample C3, after, it continued very slow until wetting of upper side.

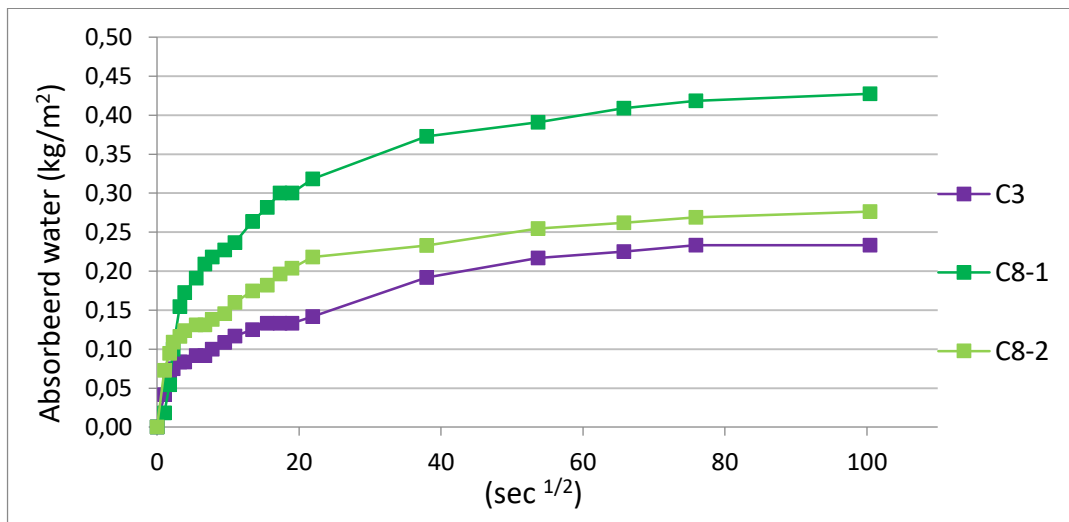


Figure 63. Water absorption by capillarity of the limestones from the site (C3, C8-1, C8-2).

Stone samples C3 and C8 have slightly different water absorption behavior and drying properties (see in next paragraph). Their difference could be distinguished with

the naked eye (Figure 64), and was confirmed also by their microstructures are assessed in the petrographic analysis section.

Figure 65 shows the drying rate of stones from the archaeological site. The drying behaviour of the samples is similar. The water evaporated fast during first 75 h, and then it continued slowly until the samples reached a constant weight.



Figure 64. Stones from left to right: C3, C8-1, C8-2, before and after water absorption.

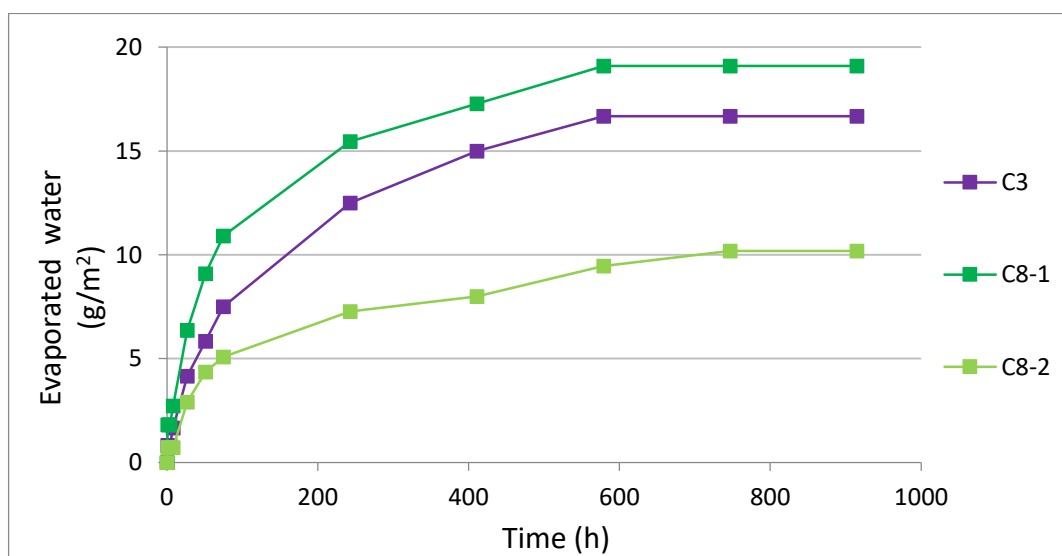


Figure 65. Drying rate properties of the limestones from the site (C3, C8-1, C8-2).

### **4.5.3. Comparison of the Moisture Transport Properties of Stones from the Historic Quarry and the Site**

In this section, the moisture transport properties of stones from the historic quarry (Qave) are compared to those from the archaeological site (C3, C8), to attempt an assessment of their compatibility with respect to moisture transport properties.

Figure 66 shows the water absorption curves of stones from the historic quarry and from the site. As described in the previous sections, the limestone samples from the quarry have a slow absorption behavior, however, the limestone samples from the site (C3, C8) show an even slower absorption behavior (Figure 66).

The capillary water absorption coefficient (WAC) of the stone sample C3 is  $11.41 \text{ gr}/(\text{m}^2\text{sec}^{0.5})$  and the stone sample C8 is  $19.64 \pm 6.09 \text{ gr}/(\text{m}^2\text{sec}^{0.5})$  while the average WAC of the limestones from the old quarry is  $50.16 \pm 11.95 \text{ gr}/(\text{m}^2\text{sec}^{0.5})$  (CEN 2009). The obtained results show the significant difference between stone samples from the site and from the historic quarry.

Figure 67 shows the drying rate properties of stones from the site and the historic quarry. The stone samples from the old quarry (Qave) show a faster drying rate than the stones from the site.

In addition to all above results, in order to understand compatibility of stones from the historic quarry and from the site, determination/comparison of their chemical, petrographical and mechanical properties have to be done.

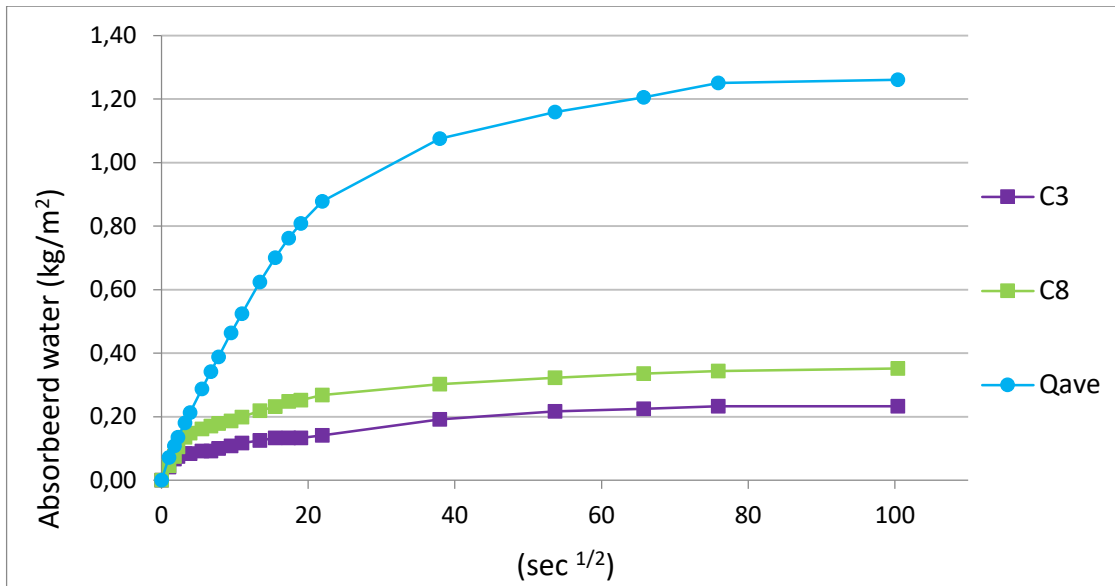


Figure 66. Water absorption by capillarity of the limestones from the site (C3, C8) and from the historic quarry (Qave).

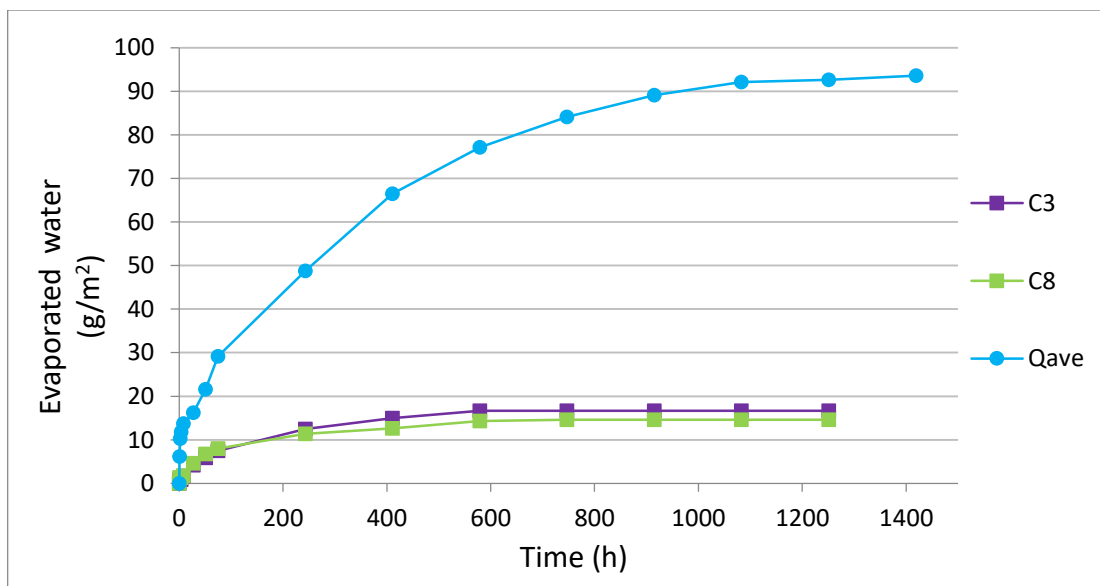


Figure 67. Drying rate properties of the limestones from the site (C3, C8) and from the historic quarry (Qave).

#### 4.6. Bacterial Colonization of Stones

Bacterial communities colonizing limestones in Anavarza were isolated and identified by using cultivation techniques and next generation sequencing (NGS, pyrosequencing) method.

A total of 15 stone samples were analyzed from weathered surfaces and sound parts of limestones: 2 weathered samples from the standing parts of Alakapı (A.st.1, A.st.3), 8 weathered samples from the standing parts of the columns (C1.st.1, C2.st.1, C3.st.2, C3.st.3, C5.st.1, C6.st.1, C7.st.1, C9.st.1), 3 weathered samples from the excavated parts of the columns (C5.ex.1, C7.ex.1, C8.ex.1) and 2 sound samples from the inner parts of the columns (C2.in.1, C6.in.1).

The distribution of the bacterial community was clarified on: the phylum level, the class level and the genus level, in the following sections. In this way, bacterial distribution of stones from the Alakapı and the columns; the weathered surfaces and the sound inner cores; the standing surfaces and the recently excavated surfaces are evaluated.

#### **4.6.1. Distribution on the Phylum Level**

Bacteria is detected in all samples taken from Alakapı and the columns; additionally, archaea is observed in one sample taken from Alakapı (A.st.3). The distribution of the bacterial community on the phylum level is shown in Figure 68. It shows that total 8 bacterial phyla and 1 archaea are determined in stone samples. Bacterial phyla are Actinobacteria, Proteobacteria, Bacteroidetes, Firmicutes, Phodothermaeota, Acidobacteria, Cyanobacteria, Deinococcus-Thermus respectively, and archaea phylum is Euryarchaeota (Figure 68).

Bacteria species belonging to the Cyanobacteria, Actinobacteria and Archaea phylum play an important role in the biodegradation of historical stones (Caneva et al. 2008, McNamara et al. 2006, Gaylarde et al. 2012).

Actinobacteria is the most frequent bacterial phylum in all stone samples (Figure 68). Actinobacteria phylum may develop on the stone material more than others, due to their filamentous growth and effective use of various nitrogen and carbon sources (Saarela et al. 2004).

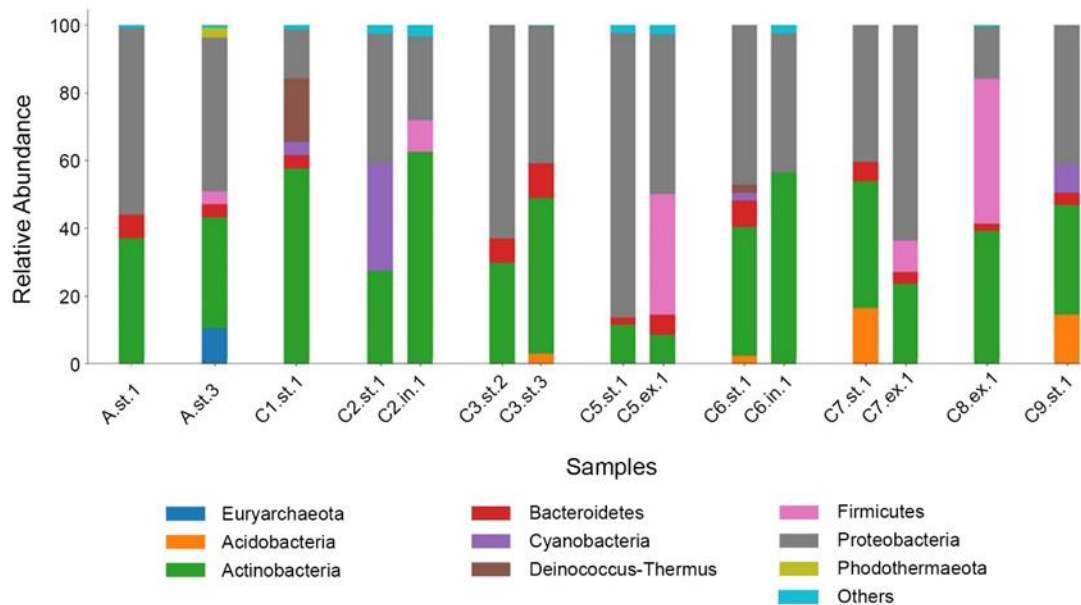


Figure 68. Distribution of bacterial phyla of the samples from Alakapı (A.st.1, A.st.3), from the standing surfaces of the columns (C1.st.1-C9.st.1) and from the recently excavated surfaxes of the columns (C5.ex.1-C8.ex.1) (st: standing part, ex: excavated part, in: inner part)

Figure 68 indicates that Actinobacteria and Proteobacteria are dominant in stone samples taken from Alakapı (A.st.1, A.st.3). Other phyla are Bacteroidetes, present in both samples and Firmicutes and Phodothermaeota present in the sample A.st.3 and Euryarchaeota is only detected in the sample A.st.3.

The sample A.st.1 is covered by a yellow patina that is also dominated by Actinobacteria (37.13%) and Proteobacteria (55.12%) as the major bacterial population (Figure 68). The sample A.st.1 is mainly composed of whewellite, calcite and quartz minerals (Section 4.1.2). Presence of whewellite shows calcium oxalate precipitation on limestone surfaces as a result of the reaction between oxalic acids, produced by microbiological formations, with calcium carbonate which is the major mineral of calcareous stones.

The sample A.st.3 is covered by a black crust that is colonized by bacteria and archae as well. Actinobacteria (32.71%), Proteobacteria (45.48%) and also Euryarchaeota (10.51%) are detected (Figure 68). The sample A.st.3 is mainly composed of whewellite, gypsum, calcite and quartz minerals. The sample A.st.3 is the only stone sample with gypsum formation, as shown by the IC (Section 4.4), XRD and FT-IR results (Section 4.1.2).

The Actinobacteria is dominant together with the Proteobacteria in the stones taken from the columns (Figure 68), except the samples taken from the recently excavated parts of the columns that will be discussed in the last paragraphs of this section.

The 1<sup>st</sup> and 9<sup>th</sup> columns (C1 and C9) are covered by a black, greyish microbial formation. The sample C1.st.1 is mainly colonized by Actinobacteria (57.76%), Proteobacteria (14.42%) and Deinococcus-Thermus (18.8) (Figure 68). The sample C9.st.1 is colonized by Actinobacteria (32.43%), Proteobacteria (41.05%), Acidobacteria (14.53%) and Cyanobacteria (8.45%) (Figure 68). As seen in these results, the bacterial population is specific for every stone in the area.

The 3<sup>rd</sup> column (C3) is covered by a well-developed microbiological colonization throughout to the inner cores of the stone. It is mainly due to the distribution of bacterial communities, the environmental conditions, and the mineral structure of the stone as well (see next paragraphs).

The stone sample C3.in.1 taken from inner cores of the 3<sup>rd</sup> column that indicated a slow absorption behavior and low porosity (Section 4.5.2). From the weathered surface of this stone, samples C3.st.2 and C3.st.3 are mainly composed of whewellite, calcite and quartz minerals. As mentioned above, presence of whewellite possibly indicates biological tissues on these standing surfaces of limestones.

Microbiological colonization on this surface of the of the 3<sup>rd</sup> column is seen in different colors such as black, grey, yellow or pink thanks to the pigmentation ability of microorganisms. The sample C3.st.2 was taken from a yellow spot from this pigmented biofilm where lichens are observed and the sample C3.st.3 was taken from a pink stain where biopitting is visible on the surface (see details in the section 4.3.2). Endolithic microorganisms (fungi, green algae, cyanobacteria) are responsible for biopitting on stone surfaces (Caneva et al. 2008). On the other hand, some microorganisms such as bacteria, fungi might penetrate into the materials and cause severe damage (Sterflinger and Piñar 2013). Presence of biopitting on this stone surface and microbial development throughout to the inside of the stone may show bacteria and fungi formation in this biofilm. As major bacterial population, the sample C3.st.2 is mainly colonized by Proteobacteria (62.98%), Actinobacteria (29.96%), Bacteroidetes (7.6%) while the sample C3.st.3 is colonized by Actinobacteria (46.02%), Proteobacteria (40.63%), Bacteroidetes (10.2%) (Figure 68).

Actinobacteria and Proteobacteria have mainly detected in the sound inner core samples (C2.in.1, C6.in.1), however high amounts of Cyanobacteria have found in the weathered surface sample C2.st.1, Bacteroidetes and low amount of other phyla were

found in the weathered surface sample C6.st.1 (Figure 68). It shows that Cyanobacteria is developed on some of the weathered surfaces of the columns, especially the sample C2.st.1 (Figure 68).

The 2<sup>nd</sup> and 6<sup>th</sup> columns (C2 and C6) are covered by biological formations as black, dark and light grey color stains. The standing surface of the 2<sup>nd</sup> column (C2.st.1) is dominated by Proteobacteria (38.02%), Actinobacteria (27.62%) and Cyanobacteria (31.63%) while the sound inner cores of this column (C2.in.1) is dominated by Actinobacteria (62.59%), Proteobacteria (24.65%), Firmicutes (9.29%) (Figure 65). The standing surface of the 6<sup>th</sup> column (C6.st.1) is dominated by Proteobacteria (47.13%), Actinobacteria (38.10%) and Bacteroidetes (7.8%) while the sound inner cores of this column (C6.in.1) is dominated by Actinobacteria (56.42%) and Proteobacteria (41.17%) (Figure 68). These results show that bacterial communities on the deteriorated surfaces and the sound inner parts of the limestones are slightly different.

As mentioned above, the Actinobacteria is dominant together with the Proteobacteria in the stones taken from the columns, except the samples taken from the recently excavated parts of the columns (C5.ex.1, C7.ex.1, C8.ex.1) (Figure 69). Firmicutes are seen highly in the samples C5.ex.1 and C8.ex.1 and it is found somewhat lower in the sample C7.ex.1 (Figure 68).



Figure 69. Samples from standing and recently excavated surfaces of the 5<sup>th</sup>, 7<sup>th</sup>, 8<sup>th</sup> columns.



The standing surface of the 5<sup>th</sup> column (C5.st.1) is dominated by Proteobacteria (84.04%) and Actinobacteria (11.64%) whereas the recently excavated surface (C5.ex.1) is dominated by Proteobacteria (47.18%), Firmicutes (35.57%) and Actinobacteria (8.63%) (Figure 68). The standing surface of the 7<sup>th</sup> column (C7.st.1) is colonized by Proteobacteria (40.37%), Actinobacteria (37.33%), Acidobacteria (16.55%) and the recently excavated surface (C7.ex.1) is colonized by Proteobacteria (63.57%), Actinobacteria (23.65%), Firmicutes (9.25%) (Figure 68). Besides, the recently excavated surface (C8.ex.1) is colonized by Firmicutes (42.75%), Actinobacteria (39.31%) and Proteobacteria (15.47%) (Figure 68). The results show that the bacterial members of the Firmicutes phylum are only detected on the recently excavated surfaces. The bacterial communities on the standing surfaces and recently excavated surfaces of the limestone columns are quite different.

#### **4.6.2. Distribution on the Class Level**

As mentioned in the previous section, the Actinobacteria and Proteobacteria is the most common bacterial phyla in these stones. Also, some other bacterial phyla are found such as Bacteroidetes and Firmicutes.

At the class level, total 18 bacteria and 1 archae classes were determined. Microbial communities on these limestones are dominated by some bacterial classes such as Actinobacteria, Rubrobacteria, Chitinophagia, Alphaproteobacteria, Bacilli and the others (Table 11). Among them, the classes Actinobacteria and Rubrobacteria represent Actinobacteria phylum while the class Alphaproteobacteria represent Proteobacteria phylum. Chitinophagia class is one of the Bacteroidetes phylum and Bacilli is one of the Firmicutes phylum (Table 11).

The bacterial classes Actinobacteria and Chitinophagia were detected in all stone samples. Actinobacteria class causes deterioration by decreasing pH in stones (Pineiro et al. 2019). Chitinophagia is the member of Bacteroidetes phylum that is a comprehensive bacteria group. It is a common colonizer and found in all samples with low amounts.

The members of the Proteobacteria Phylum; Alphaproteobacteria are mainly phototrophic while Betaproteobacteria and Deltaproteobacteria are chemolithotrophic (Pineiro et al. 2019). That is, Betaproteobacteria and Deltaproteobacteria are generally

composed of nitrifying bacteria or sulfur/iron reducing bacteria and inorganic acids produced by the result of their metabolic activity have important impact on deterioration of stone structures (Zurita et al. 2005). Alphaproteobacteria is the dominant class (the Proteobacteria Phylum), the others have not been detected in these samples, except only the sample C7.ex.1. This indicates that there is no nitrifying or sulphur/iron reducing bacteria in these stones (Table 11).

### **4.6.3. Distribution on the Genus Level**

At the genus level, total 79 bacteria and 1 archae genera were determined (see details in the Appendix F). Among them, 3 bacteria genera are most abundant in these stones: the genus *Rubrobacter*, the genus *Sphingomonas* and the genus *Bartonella*. The archae genus *Halococcaceae* were detected as well (Table 11).

As mentioned before, the majority of bacteria members identified on limestones belonged to the Actinobacteria and Alphaproteobacteria. Actinobacteria is mostly represented by the genus *Rubrobacter* and Alphaproteobacteria is mostly represented by the genera *Sphingomonas* and *Bartonella* in this area.

The genus *Rubrobacter* is found in almost all stone samples (Table 11). The presence of the genus *Rubrobacter* could be associated with discoloration phenomena, especially related to reddish discoloration of monuments (Imperi et al. 2007). Additionally, *Rubrobacter* strains have a major role in both efflorescence formation and mineral precipitation, and affects biological degradation by leading to detachment of mineral grains on biofilms (Laiz et al. 2009).

The genus *Sphingomonas* is found in almost all stone samples, similar to the genus *Rubrobacter* (Table 11). *Sphingomonas* species can be detected in a wide variety of environments due to their ability to grow in low nutrient and water conditions (Pinhassi and Berman, 2003). Besides, *Sphingomonas* are capable to produce yellow pigments on stone surfaces, which enables them to survive under high UV radiation (Mihajlovski et al. 2017).

The genus *Bartonella*, another member of Alphaproteobacteria, is found in some stones in the area (Table 11). The genera *Rubrobacter* and *Sphingomonas* have been detected in connection with stone damage phenomena in different studies, as described above. However, the genus *Bartonella* (species *Bartonella Japonica*) were not detected on

stone monuments yet. This species use some mammals as reservoir hosts (Dehio et al. 2001). They may be transferred from animals to some of the stones in the area due to animal livestock farming nearby the stones. The presence of high amount of *Bartonella Japonica* may be related to insecticide used due to intensive agricultural activities in the region. *Bartonella Japonica* can use these insecticides accumulated on stone surfaces by breaking them down and thus they can survive on stone surfaces.

In addition to bacteria, the archae genus *Halococcaceae* (phylum *Euryarchaeota*) is only detected in the sample A.st.3 (Table 11). Among all the stone samples taken from the area, A.st.3 is the only stone sample colonized by archaea as well as gypsum formation was detected. Sulphation process and the formation of gypsum crust is described in the section 4.4. For the formation of gypsum crust, a main source of sulphate is sulfur dioxide gas ( $\text{SO}_2$ ) present in the polluted air. On the other hand, sulfuric acid could be produced by some bacteria belonging to the genus *Thiobacillus* (Sand 1997). However, this genus was not found in this sample. Archaea colonization is dominated by the species *Halococcus* in this sample and this supports presence of soluble salts (e.g. gypsum). Because, *Halococcus* is one of the halophilic (salt-loving) archaea that adapt to survive in extreme environmental conditions and commonly found in salt attacked monuments (Steiger et al. 2011, Etnenauer et al. 2014, Piñar et al. 2009). Salt crusts, salt efflorescences provide an appropriate environment for *Halococcus* (Steiger et al. 2011). This indicates that the archaea colonization by the species *Halococcus* on the sample A.st.3 is possibly related to the gypsum presence.

As mentioned in the previous section, the bacterial population is different between the standing and the recently excavated surfaces. The members of *Proteobacteria* and *Actinobacteria* phyla are mainly found in the standing surface samples. Unlike this, the members of *Firmicutes* are dominantly found in the recently excavated surface samples, together with *Proteobacteria* and *Actinobacteria* members. The genus *Bacillus* belonging to the phylum *Firmicutes* (Table 11) is identified frequently on these excavated surface samples in the area. The members of the genus *Bacillus* are common inhabitant of soil, besides they can survive in other environments (such as water) as well as they frequently found on stone monuments because of their resistance to extreme environmental conditions such as high temperature (Scheerer et al. 2009, Daffonchio et al. 2000). Presence of organisms of the genus *Bacillus* on the recently excavated stones may be generated from the accumulation of fine silt and clay minerals on their surfaces. High amounts of  $\text{SiO}_2$ ,  $\text{Al}_2\text{O}_3$  and  $\text{FeO}$  on stone surfaces as a clay layer were identified by the

results of chemical composition analysis and SEM observations as well (Sections 4.2.2 and 4.3.2). The presence of the clay minerals could be supported by the surrounding soil.

Table 11. Distribution of the bacteria phylum and classes

<b>Bacteria Phylum</b>	<b>Bacteria Classes</b>	<b>Bacteria Genus</b>	<b>Stone Samples</b>
Actinobacteria	Actinobacteria	Arthrobacter	C2.in.1, C7.ex.1
		Crossiella, Kineococcus, others	All samples
	Rubrobacteria	Rubrobacter	A.st.1, A.st.3, C1.st.1, C2.in.1, C2.st.1, C3.st.3, C5.st.1, C6.in.1, C7.st.1, C7.ex.1, C9.st.1
	Thermoleophilia	*	C3.st.3, C6.in.1
	Acidimicrobia	*	C2.in.1, C9.st.1
Proteobacteria	Alphaproteobacteria	Sphingomonas	A.st.1, C2.st.1, C2.in.1, C3.st.2, C3.st.3, C6.in.1, C6.st.1, C7.st.1, C8.ex.1, C9.st.1
		Bartonella	A.st.3, C1.st.1, C2.st.1, C2.in.1, C5.st.1, C5.ex.1, C7.ex.1
		Acidisoma, others	All samples
	Betaproteobacteria	*	C7.ex.1
	Gammaproteobacteria	*	C5.ex.1, C8.ex.1
Bacteroidetes	Chitinophagia	*	All samples
	Cytophagia	*	A.st.1, C1.st.1, C3.st.2, C3.st.3, C5.ex.1, C6.st.1, C9.st.1
	Flavobacteria	*	A.st.3, C5.ex.1
	Rhodothermia	*	A.st.3
Firmicutes	Bacilli	Lactobacillus	C8.ex.1, C2.in.1, C7.ex.1, C5.ex.1
		Bacillus	C2.in.1, C7.ex.1
	Nostocales	*	C2.st.1
	Clostridia	*	C5.ex.1
Acidobacteria	Blastocatellia	*	C3.st.3, C6.st.1, C7.st.1, C9.st.1
Deinococcus-Thermus	Deinococci	*	C1.st.1, C6.st.1
Cyanobacteria	Chroococciopsidales	*	C1.st.1, C2.st.1, C6.st.1
	Oscillatoriophyceae	*	C2.st.1, C9.st.1
Euryarchaeota	Stenosarchaea group	Halococcaceae	A.st.3
<i>*the other genera</i>			

## 4.7. General Evaluation of Deterioration of the Limestones in Anavarza

The overall assessment of the study showed that:

- The most common type of deterioration on the limestones of the Anavarza archaeological site is biological growth, and different microbial communities have developed at different densities on the stone surfaces due to environmental conditions (e.g. temperature, RH, air pollution) and exposure time to open air conditions.

- The standing and recently excavated surfaces and sound inner parts of the limestones have significant differences in their mineralogical and chemical compositions, microstructural properties and bacterial communities due to the difference in biocolonization and damages related to other agents (such as salts).

- The standing surfaces and recently excavated surfaces of the limestone columns are covered by biological growth with different severity. The standing parts of the stone surfaces have been heavily colonized by microorganisms because those have been exposed to atmospheric conditions longer than the recently excavated parts. Unlike the standing parts, recently excavated surfaces do not yet have whewellite minerals as a result of biological activities.

- The bacterial communities on the standing surfaces and the recently excavated surfaces of the limestone columns are quite different. As bacterial population, the Proteobacteria and Actinobacteria phyla are mainly found in the standing surface samples. However, the Firmicutes are dominantly found in the recently excavated surface samples, together with Proteobacteria and Actinobacteria members. The most frequent genus on these excavated surface samples is *Bacillus* belonging to the phylum Firmicutes that are common inhabitant of soil (Scheerer et al. 2009, Daffonchio et al. 2000). It is probably generated from the clays that come from surroundings as well as from soil before excavation.

- The bacterial communities on the deteriorated surfaces (epilithic) and the sound inner parts (endolithic) of the limestones are slightly different. Actinobacteria phylum is predominant in the sound inner parts while Proteobacteria phylum is more frequent in weathered stone surfaces. The presence of the members of Actinobacteria phylum might be associated with their filamentous growth and effective use of various nitrogen and carbon sources (Saarela et al. 2004) and that may enable them to develop inside of the stone. The results show the presence of an endolithic bacterial community

in the inner cores of the limestones, somewhat different from the epilithic bacterial community on the limestone surfaces.

- The majority of bacterial community identified on limestones is represented by the genus *Rubrobacter* and the genus *Crossiella* (belong to the Actinobacteria phylum) and represented by the genus *Sphingomonas* and the genus *Bartonella* (belong to the Alphaproteobacteria phylum). Many of these bacterial genera have been detected in stone damage studies, however, the genus *Bartonella* has not yet been identified in stone monuments.

- The archaeal community is represented by *Halococcus* species, one of the halophilic (salt-loving) archaea, and this species has been found in the sample having gypsum on the triumphal arch.

- Taking into consideration the European standard titled “EN 17652, Cultural heritage - Investigation and monitoring of archaeological deposits for preservation in situ” (CEN 2021) described in the section 2.3., the state of preservation of the columns, preservation conditions at site and risk classification are determined below:

- Based on the all results from the investigation, the state of preservation is between poor and good state (SP 2-SP 3) for the standing stones. Because, they have been highly colonized by microflora. The recently excavated stones are between good and excellent state (SP 3-SP 4), which is a better state than the standing stones.

- For preservation conditions at site, burial environment before excavation and the environment after excavation is affecting deterioration. The characteristics of the top soil burial environment show that soils are calcereous and siliceous and no soluble salts. There is 1-2 meters single layer top soil without ground water effect. As a result, burial environment in this area for stone materials are not much deteriorative. However, other type of burial materials such as metal, wood are needed to be investigated by different parameters. After excavation, there is no extreme climate conditions at site. Therefore, the standing stones have a good preservation condition (PC 3). On the other hand, unexcavated stones under the soil before excavation in archaeological sites has a better preservation condition. For that reason, the recently excavated stones have between excellent and good preservation condition (PC 4-PC 3), because they have been exposed to atmospheric conditions less than the standing stones.

- According to these scores determined above, their risk classification shows that the standing stones have a medium risk of loss of significant stone material (RC B) while

the recently excavated stones have a between low and medium risk of significant stone material (RC A-RC B).

Based on the overall assessment of this study, the excavations should be carried out with preventive conservation measures to prevent further weathering of limestones in open atmospheric conditions. For this scope, any accumulation of clays or dust on limestone surfaces should be removed after the excavations to prevent biological growth, however the calcium oxalate layer should be protected. Biological phenomena should be controlled by changing of the environmental conditions at the site (e.g. installing drainage systems, environmentally friendly methods). After conservation interventions, their outcomes should be monitored and a regular maintenance plan should be developed. Besides, long-term monitoring of the site in terms of their environmental conditions and deterioration patterns should be performed and evaluated.

## CHAPTER 5

### CONCLUSIONS

This research has focused on the investigation of limestone deterioration problems in Anavarza archaeological site in Adana, Turkey. In this scope, the characteristics of stone materials used in the site, the weathering problems, their causes and prevention measures were determined for the purpose of conservation. One of the aims of this study was to evaluate the effect of micro-organisms on stone surfaces related to other possible weathering agents (such as salts) by comparing the characteristics of the standing and recently excavated surfaces and sound inner parts of the limestones. The study also aimed to investigate the relation between the stone weathering and the bacterial diversity on limestones.

The ancient city of Anavarza (Anazarbos), which was included in the UNESCO World Heritage Tentative List in 2014, was selected to form a basis for planning the excavation works and necessary preservation measures. Most of the structures in the area were constructed with limestones. The triumphal arch (Alakapı) is one of the important remaining structure on the site. There is a colonnaded road starting from the triumphal arch in the south-north direction. The excavations have especially been carried out around the triumphal arch and the colonnaded road. The conservation work of the triumphal arch was completed in 2020, and the excavations are still ongoing.

The study started with a visual analysis and mapping of the weathering forms on limestones of the triumphal arch (before restoration) and of the colonnaded road. The main weathering type on the limestones is biological growth. The severity of the biological growth is different between the standing and the recently excavated surfaces of the limestones. The standing parts of the stone surfaces are blackish due to microorganisms and air pollution, whereas the recently excavated parts are lighter in colour.

The sound limestones are mainly composed of calcite and quartz minerals. They consist of micritic and sparitic calcite fabrics with less fossil materials. The standing and the recently excavated parts of the limestone surfaces contain high amount of fine silt and clay minerals. These clay minerals accelerate the weathering of the limestones in the area



by swelling and shrinkage in the presence of water and provide suitable conditions for the biological growth as well. The standing parts of the stone surfaces have been heavily colonized by microorganisms because they have been exposed to atmospheric conditions longer than the recently excavated parts of the stone surfaces. In addition, the standing surfaces contain whewellite minerals. Whewellite is possibly formed by the reaction of oxalic acid produced by microorganisms and calcite on stone surfaces, its presence indicated biological tissues on the standing surfaces of limestones.

High amounts of sulphur on some of the standing limestone surface samples could indicate the effects of air pollution due to SO<sub>2</sub> gases. It might be formed as a result of the straw and stubble burning around the archaeological area.

Limestones and excavated soils contain no significant amount of soluble salts. This showed that soluble salts are not effective in the deterioration of limestones in this area. However, a somewhat higher content of chloride and nitrate ions and a high amount of sulphate were detected on the corner of the triumphal arch where a black crust is visible. This indicated the presence of gypsum due to air pollution in the area.

The colonized limestones in Anavarza had diverse bacterial and archaeal communities. Majority of the bacterial members identified on limestones belonged to the Actinobacteria and Proteobacteria phyla. Actinobacteria was dominated by the genera *Rubrobacter* and *Crossiella*, Proteobacteria was dominated by the genera *Sphingomonas* and *Bartonella*. Most of these bacteria genera have been frequently detected in the studies related to stone deterioration, however the genus *Bartonella* (*Bartonella Japonica* species) have not been found on stone monuments yet. *Bartonella Japonica* species were frequently identified on the stone samples in the area. This might be transferred from animals to the stone due to livestock farming nearby the stones or be related to insecticide used in the region due to intensive agricultural activities. In addition, the archaeal community was represented by *Halococcus* species, one of the halophilic (salt-loving) archaea, and was found in the sample having gypsum on the triumphal arch.

The bacterial communities on the standing surfaces and the recently excavated surfaces of the columns are quite different. Proteobacteria and Actinobacteria phyla are mainly found in the standing surfaces of the limestones whereas Firmicutes are dominantly found in the recently excavated surfaces of the limestones, with Proteobacteria and Actinobacteria members. Firmicutes were mainly represented by the genus *Bacillus* that is common inhabitant of soil. The presence of *Bacillus* on the recently excavated stone surfaces is probably due to deposited clay from the nearby surroundings.

The bacterial communities on the deteriorated surfaces (epilithic) and the sound inner cores (endolithic) of the limestones are slightly different. The results showed the presence of an endolithic bacterial community in the inner cores of the limestones, somewhat different from the epilithic bacterial community on the limestone surfaces.

Based on the results of this study, it has been suggested that the excavations should be carried out with preventive conservation measures to prevent further weathering of limestones in open atmospheric conditions. In this context, any accumulation of clays or dust on limestone surfaces should be removed after the excavations to prevent biological growth, however the calcium oxalate layer should be protected. The use of biocides should be avoided because of their harm to the environment and human health. If necessary, environmentally friendly methods could be considered to prevent biocolonization in the future. Biological phenomena should be controlled by changing of the environmental conditions at the site, such as installing drainage systems to keep water away from the stones. A regular maintenance plan should be developed after the conservation interventions. Multi-temporal monitoring of the deterioration patterns on stones should be performed and evaluated.

## REFERENCES

- Adana İl Kültür ve Turizm Müdürlüğü. Anavarza Ören Yeri/Ancient City of Anavarza. <https://adana.ktb.gov.tr/TR-228607/anavarza-oren-yeriancient-city-of-anavarza.html> (Accessed October 10, 2021)
- AFAD 2021, Afet ve Acil Durum Yönetim Başkanlığı (Disaster and Emergency Management Directorate of Turkey). <https://tdth.afad.gov.tr/> (accessed October 10, 2021)
- Balland-Bolou-Bi, C., M. Saheb, N. Bousserhine, S. Abbad-Andalousi, V. Alphonse, S. Nowak, A. Chabas, K. Desboeufs, and A. Verney-Carron. "Effect of microorganism activities in a polluted area on the alteration of limestone used in historical buildings." *Science and Art: A Future For Stone* (2016): 25.
- Beimforde C. Biodeterioration (of Stone). In: Reitner J., Thiel V. (eds) *Encyclopedia of Geobiology. Encyclopedia of Earth Sciences Series*. Springer, Dordrecht (2011). [https://doi.org/10.1007/978-1-4020-9212-1\\_24](https://doi.org/10.1007/978-1-4020-9212-1_24)
- Bionda, D. "RUNSALT—a graphical user interface to the ECOS thermodynamic model for the prediction of the behaviour of salt mixtures under changing climate conditions." (2005).
- Black, C. A. "Methods of soil analysis Part 2, Amer." Society of Agronomy Inc., Publisher Madisson, Wilconsin, USA (1965): 1372-1376.
- Bloomfield, Sally F., Gordon SAB Stewart, Christine ER Dodd, Ian R. Booth, and E. G. M. Power. "The viable but non-culturable phenomenon explained?." *Microbiology* 144, no. 1 (1998): 1-3.
- Bogosian, Gregg, Noelle D. Aardema, Edward V. Bourneuf, Patricia JL Morris, and Julia P. O'Neil. "Recovery of hydrogen peroxide-sensitive culturable cells of *Vibrio vulnificus* gives the appearance of resuscitation from a viable but nonculturable state." *Journal of Bacteriology* 182, no. 18 (2000): 5070-5075.
- Buyruk, Hasan. "Konumu Geçmişi ve Kimliği ile Anavarza." *ODÜ Sosyal Bilimler Araştırmaları Dergisi (ODÜSOBİAD)* 6, no. 3 (2016): 695-710.
- Caneva, Giulia, Maria Pia Nugari, Maria Pia Nugari, and O. Salvadori, eds. *Plant biology for cultural heritage: biodeterioration and conservation*. Getty Publications, 2008.
- Camuffo, Dario. "Physical weathering of stones." *Science of the total environment* 167, no. 1-3 (1995): 1-14.

- CEN 2009. European Standard EN 15801, Conservation of cultural property -Test methods - Determination of water absorption by capillarity. European Standard, European Committee for Standardization (CEN), 2009.
- CEN 2014. European Standard EN 16322, Conservation of cultural property-Test methods - Determination of drying properties. European Standard, European Committee for Standardization (CEN), 2014.
- CEN 2021. European Standard EN 17652, Cultural heritage - Investigation and monitoring of archaeological deposits for preservation in situ (under approval), European Standard, European Committee for Standardization (CEN), 2021.
- Charola, A. Elena. "Salts in the deterioration of porous materials: an overview." *Journal of the American institute for conservation* 39, no. 3 (2000): 327-343.
- Charola, A. Elena, and Christine Bläuer. "Salts in masonry: an overview of the problem." *Restoration of Buildings and Monuments* 21, no. 4-6 (2015): 119-135.
- Crispim, César A., and C. C. Gaylarde. "Cyanobacteria and biodeterioration of cultural heritage: a review." *Microbial ecology* 49, no. 1 (2005): 1-9.
- Costerton, J. William, Zbigniew Lewandowski, Douglas E. Caldwell, Darren R. Korber, and Hilary M. Lappin-Scott. "Microbial biofilms." *Annual review of microbiology* 49, no. 1 (1995): 711-745.
- Ciferri, Orio, Piero Tiano, and Giorgio Mastromei. "Of Microbes and Art." *The role of microbial communities in the Degradation and Protection of Cultural Heritage*, New York: Kluwer Academic/Plenum Publishers (2000).
- Coelho, Catarina, Nuno Mesquita, Inês Costa, Fabiana Soares, João Trovão, Helena Freitas, António Portugal, and Igor Tiago. "Bacterial and Archaeal Structural Diversity in Several Biodeterioration Patterns on the Limestone Walls of the Old Cathedral of Coimbra." *Microorganisms* 9, no. 4 (2021): 709.
- Daffonchio, Daniele, Sara Borin, Elisabetta Zanardini, Pamela Abbruscato, Marco Realini, Clara Urzì, and Claudia Sorlini. "Molecular tools applied to the study of deteriorated artworks." In *Of Microbes and Art*, pp. 21-38. Springer, Boston, MA, 2000.
- Dehio, Christoph, Christa Lanz, Rainer Pohl, Peter Behrens, Delphine Bermond, Yves Piémont, Klaus Pelz, and Anna Sander. "Bartonella schoenbuchii sp. nov., isolated from the blood of wild roe deer." *International journal of systematic and evolutionary microbiology* 51, no. 4 (2001): 1557-1565.
- Del Monte, Marco, and Cristina Sabbioni. "Weddellite on limestone in the Venice [Italy] environment." *Environmental science & technology* 17, no. 9 (1983): 518-522.

- Demas, Martha. "‘Site unseen’: the case for reburial of archaeological sites." *Conservation and management of Archaeological Sites* 6, no. 3-4 (2004): 137-154.
- Price, Clifford A., and Eric Doehne. "Stone conservation: an overview of current research.", Getty Publications, Los Angeles, California (2011).
- Dornieden, Th, A. A. Gorbushina, and W. E. Krumbein. "Biodecay of cultural heritage as a space/time-related ecological situation—an evaluation of a series of studies." *International biodeterioration & biodegradation* 46, no. 4 (2000): 261-270.
- Ergeç, Rifat. "Anazarbus Antik Kenti ve Nekropolü." *Publications de l'Institut Français d'Études Anatoliennes* 13, no. 1 (2001): 389-410.
- Ertunç, Handan. "Kozan ilçesinin beşeri ve ekonomik coğrafyası: Nüfus, yerleşme ve ekonomik özellikleri" Master's Thesis, Sosyal Bilimler Enstitüsü, İstanbul Üniversitesi, İstanbul, Turkey, 1991.
- Ettenauer, Jörg D., Valme Jurado, Guadalupe Pinar, Ana Z. Miller, Markus Santner, Cesareo Saiz-Jimenez, and Katja Sterflinger. "Halophilic microorganisms are responsible for the rosy discolouration of saline environments in three historical buildings with mural paintings." *PLoS One* 9, no. 8 (2014): e103844.
- Ettenauer, Jörg D., Guadalupe Piñar, Ksenija Lopandic, Bernhard Spangl, Günther Ellersdorfer, Christian Voitl, and Katja Sterflinger. "Microbes on building materials—evaluation of DNA extraction protocols as common basis for molecular analysis." *Science of the total environment* 439 (2012): 44-53.
- Fitzner, Bernd, Kurt Heinriches, and Ralf Kownatzki. "Weathering forms at natural stone monuments: Classification, mapping and evaluation." *Internationale Zeitschrift für Bauinstandsetzen= International journal for restoration of buildings and monuments* 3, no. 2 (1997): 105-124.
- Fitzner, Bernd. "Damage diagnosis on stone monuments-in situ investigation and laboratory studies." In *Proceedings of the International Symposium of the Conservation of the Bangudae Petroglyph*, vol. 7, pp. 29-71. 2002.
- Gadd, Geoffrey M. "Geomycology: biogeochemical transformations of rocks, minerals, metals and radionuclides by fungi, bioweathering and bioremediation." *Mycological research* 111, no. 1 (2007): 3-49.
- Gauri, K. Lal, and Jayanta K. Bandyopadhyay. *Carbonate stone: chemical behavior, durability and conservation*. Wiley, New York, 1999.
- Gaylarde, Christine C., and LH Glyn Morton. "Deteriogenic biofilms on buildings and their control: a review." *Biofouling* 14, no. 1 (1999): 59-74.

- Gaylarde, Christine C., César Hernández Rodríguez, Yendi E. Navarro-Noya, and B. Otto Ortega-Morales. "Microbial biofilms on the sandstone monuments of the Angkor Wat complex, Cambodia." *Current microbiology* 64, no. 2 (2012): 85-92.
- Gertrude Bell Archive, Newcastle University.  
[http://gertrudebell.ncl.ac.uk/search\\_photos\\_results.php?search\\_photos=anavarza&start=0](http://gertrudebell.ncl.ac.uk/search_photos_results.php?search_photos=anavarza&start=0) (Accessed November 22, 2019)
- Google Earth 2020, <https://earth.google.com> (accessed March 30, 2020)
- Gorbushina, Anna A., and William J. Broughton. "Microbiology of the atmosphere-rock interface: how biological interactions and physical stresses modulate a sophisticated microbial ecosystem." *Annual review of microbiology* 63 (2009): 431-450.
- Goudie, Andrew, and Heather A. Viles. *Salt weathering hazard*. Wiley, 1997.
- Gough, Michael. "Anazarbus." *Anatolian Studies* (1952): 85-150.
- Gök, Nagihan. "Adana İli Kozan İlçesi'nde Tarihi Çevre Koruma Önerisi." Yüksek Lisans Tezi, Fen Bilimleri Enstitüsü, İstanbul Teknik Üniversitesi, 2006.
- Graue, B., S. Siegesmund, P. Oyhantcabal, Rudolf Naumann, T. Licha, and K. Simon. "The effect of air pollution on stone decay: the decay of the Drachenfels trachyte in industrial, urban, and rural environments—a case study of the Cologne, Altenberg and Xanten cathedrals." *Environmental Earth Sciences* 69, no. 4 (2013): 1095-1124.
- Guillitte, Olivier. "Bioreceptivity: a new concept for building ecology studies." *Science of the total environment* 167, no. 1-3 (1995): 215-220.
- Hançer, Elmon. "Kilikya Ermeni Prensligi'nin İkinci Başkenti Anavarza." *Adalya* 19 (2016): 277-312.
- Herz, Norman, and Ervan G. Garrison. *Geological methods for archaeology*. Oxford University Press, 1997.
- ICOMOS 1964. *International Charter for the Conservation and Restoration of Monuments and Sites (The Venice Charter)*, IInd International Congress of Architects and Technicians of Historic Monuments, Venice, 1964.
- ICOMOS 1931. *The Athens Charter for the Restoration of Historic Monuments*, Adopted at the First International Congress of Architects and Technicians of Historic Monuments, Athens, 1931.
- Imperi, Francesco, Giulia Caneva, Laura Cancellieri, Maria A. Ricci, Armida Sodo, and Paolo Visca. "The bacterial aetiology of rosy discoloration of ancient wall paintings." *Environmental Microbiology* 9, no. 11 (2007): 2894-2902.

- Kaya, İlker and Yetiş, Ayşegül D. "Bazı Tarihi Yerleşimlere Ait Çevresel Faktörlerin CBS Destekli Analizi; Kilikya Bölgesi Örneği." *Bitlis Eren Üniversitesi Fen Bilimleri Dergisi*, 9(3), (2020): 1337-1350.
- Kemmling, A., M. Kämper, C. Flies, O. Schieweck, and M. Hoppert. "Biofilms and extracellular matrices on geomaterials." *Environmental Geology* 46, no. 3 (2004): 429-435.
- Kühnel R.A., "Driving forces of rock degradation." In: *Proceedings 5th International Symposium on the Protection and Conservation of the Cultural Heritage of the Mediterranean Cities*. Sevilla, Spain. Galán E, Zezza F. (eds). Balkema, Rotterdam, pp 11–17. 2002.
- Laiz, L., A. Z. Miller, V. Jurado, E. Akatova, S. Sanchez-Moral, J. M. Gonzalez, A. Dionísio, M. F. Macedo, and C. Saiz-Jimenez. "Isolation of five *Rubrobacter* strains from biodeteriorated monuments." *Naturwissenschaften* 96, no. 1 (2009): 71-79.
- Lee, Chan Hee, and Jeong Eun Yi. "Weathering damage evaluation of rock properties in the Bunhwangsa temple stone pagoda, Gyeongju, Republic of Korea." *Environmental Geology* 52, no. 6 (2007): 1193-1205.
- Li, Qiang, Bingjian Zhang, Zhang He, and Xiaoru Yang. "Distribution and diversity of bacteria and fungi colonization in stone monuments analyzed by high-throughput sequencing." *PloS one* 11, no. 9 (2016): e0163287.
- Van der Klugt, L. J. A. R and Koek, J.A.G., *De kwaliteit van voegen in metselwerk*, SBRpublication 299, 80-81 (1994).
- Locke, W. J. "Recommendations of the Madrid Conference (1904)." *The Architectural Journal: Journal of the Royal Institute of British Architects (RIBA)* Vol. XI. Third Series, point 2 (1904). [http://www.getty.edu/conservation/publications\\_resources/research\\_resource/s/charters/charter01.html](http://www.getty.edu/conservation/publications_resources/research_resource/s/charters/charter01.html) Retrieved from May 15, 2019
- Lubelli, B., R. P. J. Van Hees, and H. J. P. Brocken. "Experimental research on hygroscopic behaviour of porous specimens contaminated with salts." *Construction and Building Materials* 18, no. 5 (2004): 339-348.
- Maravelaki-Kalaitzaki, P., and G. Biscontin. "Origin, characteristics and morphology of weathering crusts on Istria stone in Venice." *Atmospheric Environment* 33, no. 11 (1999): 1699-1709.
- Martino, Patrick D. "What about biofilms on the surface of stone monuments?." In *The open conference proceedings journal*, vol. 7, no. 1. 2016.
- McNamara, Christopher J., and Ralph Mitchell. "Microbial deterioration of historic stone." *Frontiers in Ecology and the Environment* 3, no. 8 (2005): 445-451.

- McNamara, Christopher J., Thomas D. Perry, Kristen A. Bearce, Guillermo Hernandez-Duque, and Ralph Mitchell. "Epilithic and endolithic bacterial communities in limestone from a Maya archaeological site." *Microbial Ecology* 51, no. 1 (2006): 51-64.
- MDCS Homepage. <https://mdcs.monumentenkenis.nl/> (accessed March 18, 2020)
- MGM 2021. Meteoroloji Genel Müdürlüğü (Turkish State Meteorological Service). <https://www.mgm.gov.tr/veridegerlendirme/il-ve-ilceler-istatistik.aspx?k=H&m=ADANA> (accessed October 10, 2021)
- MTA 2021. Maden Tetkik Arama Genel Müdürlüğü (General Directorate of Mineral Research and Exploration). <http://yerbilimleri.mta.gov.tr/anasayfa.aspx> (accessed October 10, 2021)
- Mihajlovski, Agnes, Alexandre Gabarre, Damien Seyer, Faisal Bousta, and Patrick Di Martino. "Bacterial diversity on rock surface of the ruined part of a French historic monument: the Chaalis abbey." *International Biodeterioration & Biodegradation* 120 (2017): 161-169.
- Mishra, A. K., K. L. Garg, and Kamal K. Jain. "Microbiological deterioration of stone--an overview." *Conservation, preservation and restoration: traditions, trends and techniques* (1995): 217-228.
- Oren, Aharon. "Microbial diversity and microbial abundance in salt-saturated brines: why are the waters of hypersaline lakes red?." *Natural Resources and Environmental Issues* 15, no. 1 (2009): 49.
- Palumbo, Gaetano. "Threats and Challenges to the Archaeological Heritage in the Mediterranean (2000)." *Archaeological Sites: Conservation and Management*: 186.
- Pinhassi, Jarone, and Tom Berman. "Differential growth response of colony-forming  $\alpha$ - and  $\gamma$ -proteobacteria in dilution culture and nutrient addition experiments from Lake Kinneret (Israel), the eastern Mediterranean Sea, and the Gulf of Eilat." *Applied and Environmental Microbiology* 69, no. 1 (2003): 199-211.
- Pinheiro, Ana Catarina, Nuno Mesquita, João Trovão, Fabiana Soares, Igor Tiago, Catarina Coelho, Hugo Paiva de Carvalho et al. "Limestone biodeterioration: A review on the Portuguese cultural heritage scenario." *Journal of cultural heritage* 36 (2019): 275-285.
- Piñar, Guadalupe, Katrin Ripka, Johannes Weber, and Katja Sterflinger. "The microbiota of a sub-surface monument the medieval chapel of St. Virgil (Vienna, Austria)." *International Biodeterioration & Biodegradation* 63, no. 7 (2009): 851-859.
- Press, Frank, and Raymond, Siever. *Understanding Earth*. 3rd Ed., New York: W.H. Freeman and Company, 2002.



- Price, C. A. "Stone Conservation" An Overview of Current Research. Getty Conservation Institute. Los Angeles, California. (1996). [http://hdl.handle.net/10020/gci\\_pubs/stone\\_conservation](http://hdl.handle.net/10020/gci_pubs/stone_conservation)
- Price, C. A. An expert chemical model for determining the environmental conditions needed to prevent salt damage in porous materials. European Commission Research Report No 11, (Protection and Conservation of European Cultural Heritage). Archetype Publications, London, 2000.
- RILEM 1984. CPC 11.3 Absorption of water by concrete by immersion under vacuum. RILEM Recommendations for the Testing and Use of Constructions Materials, 36-37. 1984.
- Perez-Rodriguez, J. L., A. Duran, M. A. Centeno, J. M. Martinez-Blanes, and M. D. Robador. "Thermal analysis of monument patina containing hydrated calcium oxalates." *Thermochimica acta* 512, no. 1-2 (2011): 5-12.
- Saarela, Maria, Hanna-Leena Alakomi, Maija-Liisa Suihko, Liisa Maunuksela, Laura Raaska, and Tiina Mattila-Sandholm. "Heterotrophic microorganisms in air and biofilm samples from Roman catacombs, with special emphasis on actinobacteria and fungi." *International Biodeterioration & Biodegradation* 54, no. 1 (2004): 27-37.
- Sabbioni, C. "Mechanisms of air pollution damage to stone." *The effects of air pollution on the built environment* 2 (2003): 63-88.
- Sand, Wolfgang. "Microbial mechanisms of deterioration of inorganic substrates—a general mechanistic overview." *International Biodeterioration & Biodegradation* 40, no. 2-4 (1997): 183-190.
- Schaffer, Robert John. *The weathering of natural building stones*. Special Report No:18, Building Research Establishment, Watford, 1932.
- Scherer, George W. "Internal stress and cracking in stone and masonry." In *Measuring, monitoring and modeling concrete properties*, pp. 633-641. Springer, Dordrecht, 2006.
- Scheerer, Stefanie, Otto Ortega-Morales, and Christine Gaylarde. "Microbial deterioration of stone monuments—an updated overview." *Advances in applied microbiology* 66 (2009): 97-139.
- Schröer, Laurenz, Tim De Kock, Veerle Cnudde, and Nico Boon. "Differential colonization of microbial communities inhabiting Lede stone in the urban and rural environment." *Science of the Total Environment* 733 (2020): 139339.
- Schröer, Laurenz, Nico Boon, Tim De Kock, and Veerle Cnudde. "The capabilities of bacteria and archaea to alter natural building stones—A review." *International Biodeterioration & Biodegradation* 165 (2021): 105329.

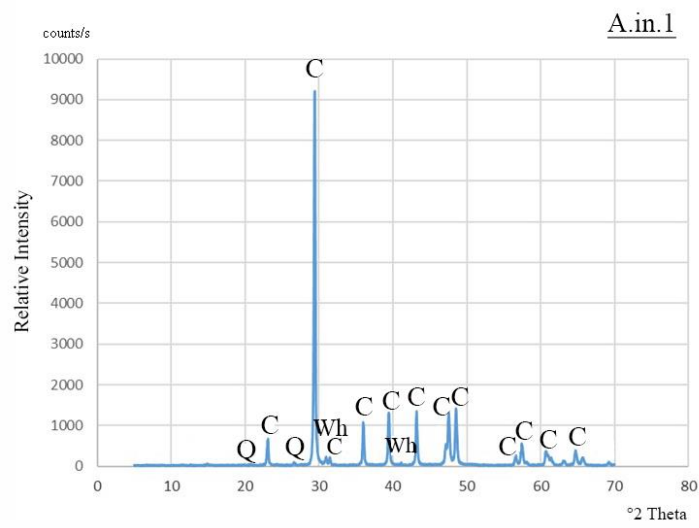
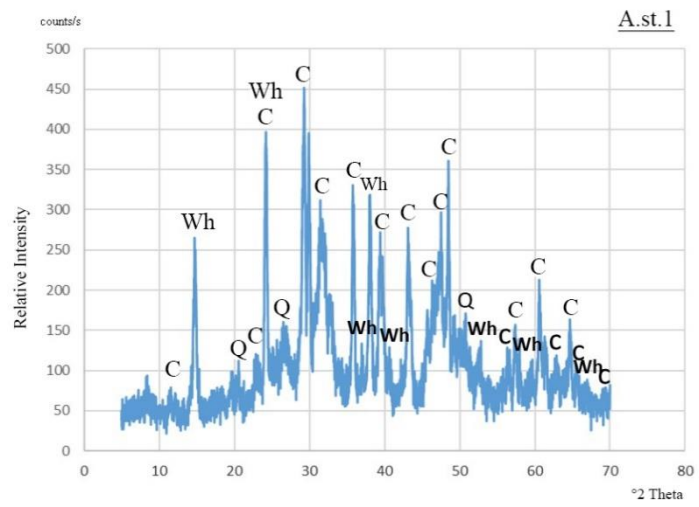
- Skipper, Philip, and Lynda Skipper. "A survey of bacterial colonisation of historic limestone buildings: Lincoln Cathedral and St. Peter at Gowts, United Kingdom." In *Rehab 2014—Proceedings of the International Conference on Preservation, Maintenance and Rehabilitation of Historic Buildings and Structures*, pp. 1003-1012. Green Lines Institute, 2014.
- Snethlage, Rolf. "Leitfaden Steinkonservierung." Fraunhofer IRB, Stuttgart 289 (2005).
- Steiger, Michael, A. Elena Charola, and Katja Sterflinger. "Weathering and deterioration." In *Stone in architecture*, pp. 227-316. Springer, Berlin, Heidelberg, 2011.
- Sterflinger, Katja, and Guadalupe Piñar. "Microbial deterioration of cultural heritage and works of art—tilting at windmills?." *Applied microbiology and biotechnology* 97, no. 22 (2013): 9637-9646.
- Stewart, Eric J. "Growing unculturable bacteria." *Journal of bacteriology* 194, no. 16 (2012): 4151-4160. <https://doi.org/10.1128/JB.00345-12>.
- Stone 2020, Monument Future: Decay and Conservation of Stone, 14th International Congress on the Deterioration and Conservation of Stone, September 7th – 12th, 2020, Göttingen, Germany, <http://stone2020.uni-goettingen.de/>
- Thorn, Colin E., Robert G. Darmody, John C. Dixon, and Peter Schlyter. "Weathering rates of buried machine-polished rock disks, Kärkevagge, Swedish Lapland." *Earth Surface Processes and Landforms: The Journal of the British Geomorphological Research Group* 27, no. 8 (2002): 831-845.
- Tiano, Piero. "Biodegradation of cultural heritage: decay mechanisms and control methods." In Seminar article, new university of Lisbon, Department of Conservation and Restoration, pp. 7-12. 2002.
- Török, Ákos. "Oolitic limestone in a polluted atmospheric environment in Budapest: weathering phenomena and alterations in physical properties." *Geological Society, London, Special Publications* 205, no. 1 (2002): 363-379.
- UNESCO 1956, Recommendation on International Principles Applicable to Archaeological Excavations, UNESCO, 1956.
- Urzi, Clara E., Wolfgang E. Krumbein, and Thomas Warscheid. "On the question of biogenic colour changes of Mediterranean monuments (coating, crust, microstromatolite, patina, scialbatura, skin, rock varnish)." In *La conservation des monuments dans le bassin méditerranéen. Actes du 2ème symposium international. Genève, 19-21 novembre 1991= The conservation of monuments in the Mediterranean Basin. Proceedings of the 2nd international symposium. Genève, 19-21 Novembre 1991*, pp. 397-420. 1992.

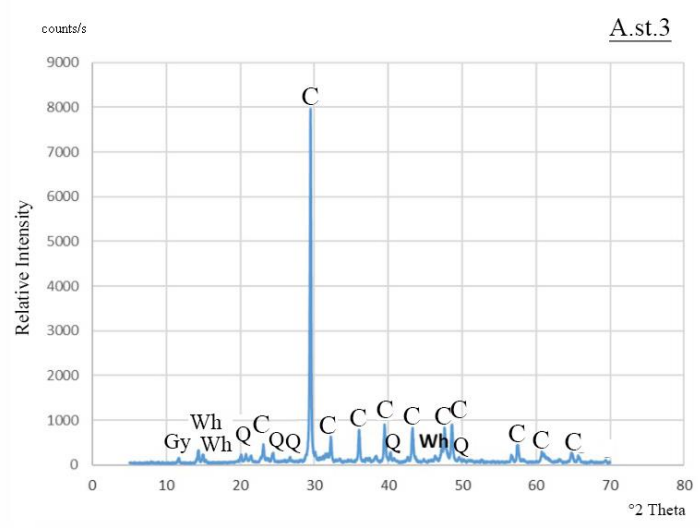
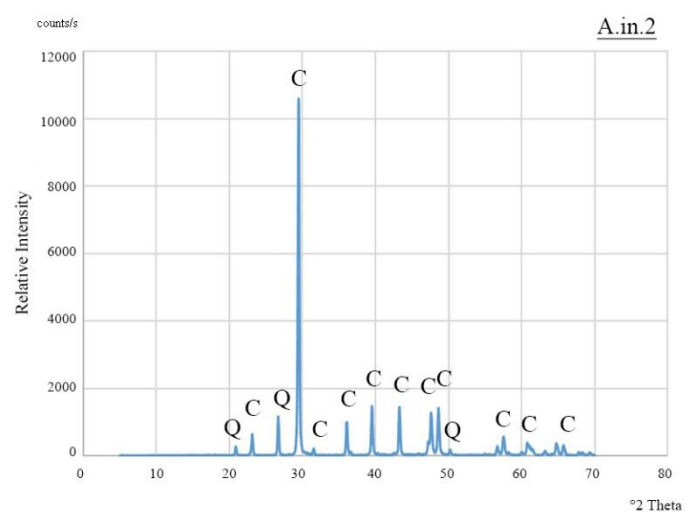
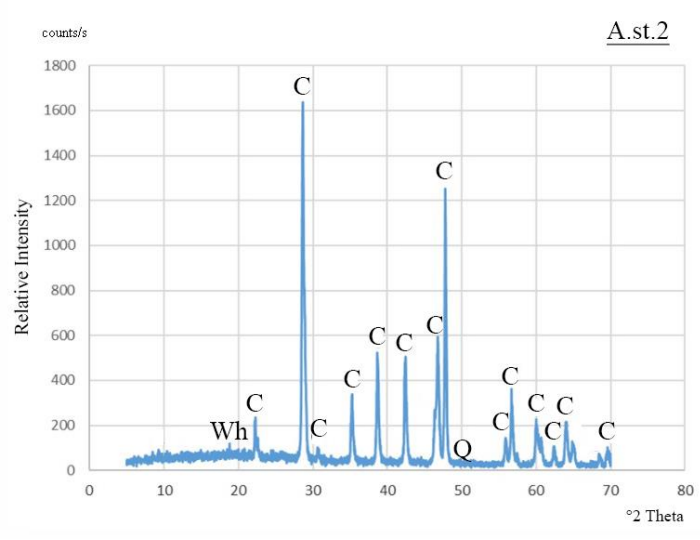
- Urzi, Clara. and De Leo, Filomena. "Biodeterioration of Cultural Heritage in Italy: State of Art", ARIADNE 8 Advanced Research Workshops: Bio-degradation of Cultural Heritage, Prag. 2001.
- Viles, H. A. "Durability and conservation of stone: coping with complexity." *Quarterly Journal of Engineering Geology and Hydrogeology* 46, no. 4 (2013): 367-375.
- Wang, Quanyu, Marianne Odlyha, and Neil S. Cohen. "Thermal analyses of selected soil samples from the tombs at the Tianma-Qucun site, Shanxi, China." *Thermochimica acta* 365, no. 1-2 (2000): 189-195.
- Warscheid, Th, and Joanna Braams. "Biodeterioration of stone: a review." *International Biodeterioration & Biodegradation* 46, no. 4 (2000): 343-368.
- Yüceer, Hülya, F. Fatih Gülşen, Rozelin Aydın, and Selen Güler. "The Ancient City of Anazarbos and Its Significance as a World Heritage Site." *Archaeologies* (2021): 1-36. Zanardini, E., P. Abbruscato, N. Ghedini, M. Realini, and C. Sorlini. "Influence of atmospheric pollutants on the biodeterioration of stone." *International Biodeterioration & Biodegradation* 45, no. 1-2 (2000): 35-42.
- Zanardini, Elisabetta, Eric May, Robert Inkpen, Francesca Cappitelli, J. Colin Murrell, and Kevin J. Purdy. "Diversity of archaeal and bacterial communities on exfoliated sandstone from Portchester Castle (UK)." *International Biodeterioration & Biodegradation* 109 (2016): 78-87.
- Zurita, Y. Peraza, G. Cultrone, P. Sánchez Castillo, E. Sebastián, and F. C. Bolívar. "Microalgae associated with deteriorated stonework of the fountain of Bibatauín in Granada, Spain." *International Biodeterioration & Biodegradation* 55, no. 1 (2005): 55-61.

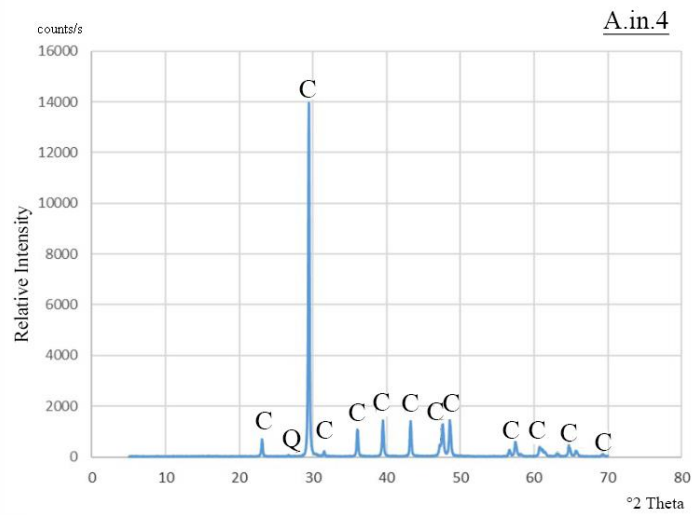
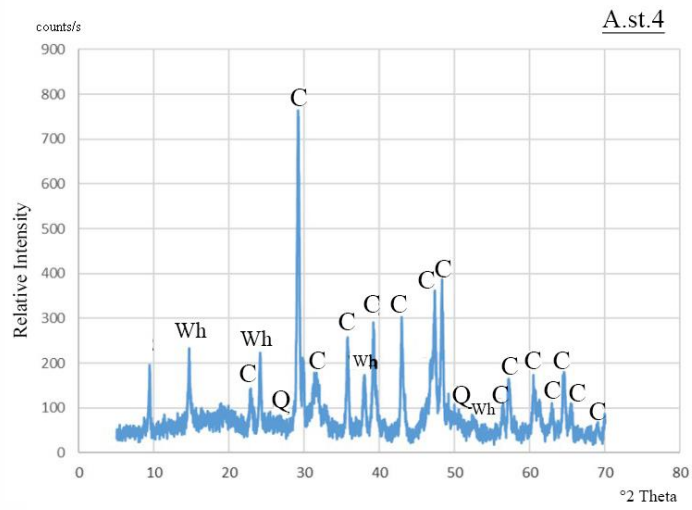
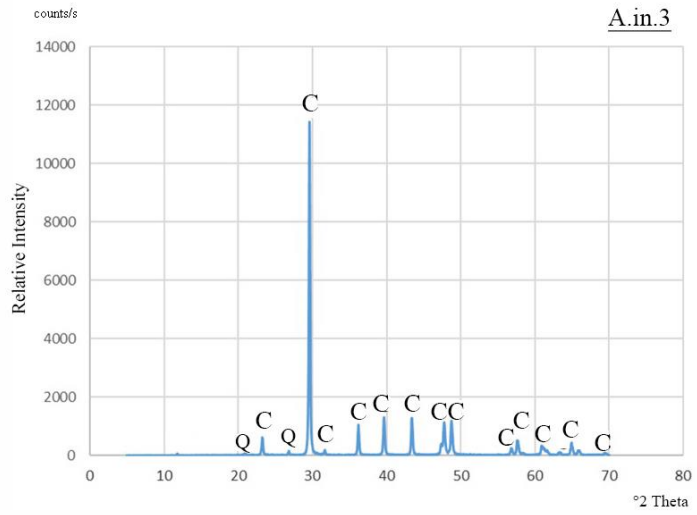
# APPENDICES

## APPENDIX A

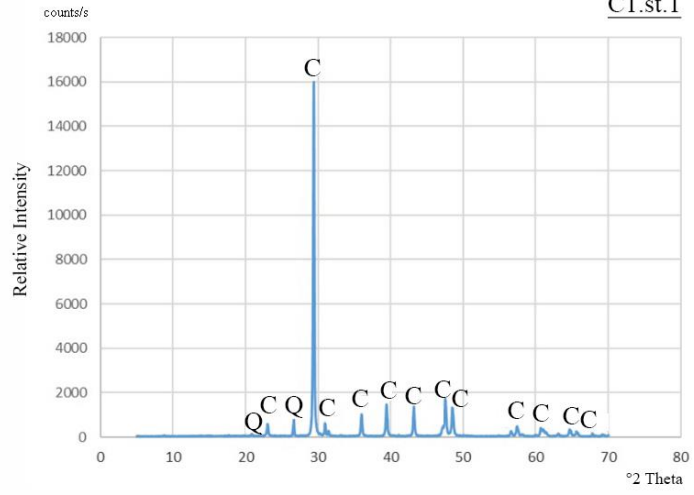
### MINERALOGICAL COMPOSITIONS OF LIMESTONES (XRD PATTERNS)



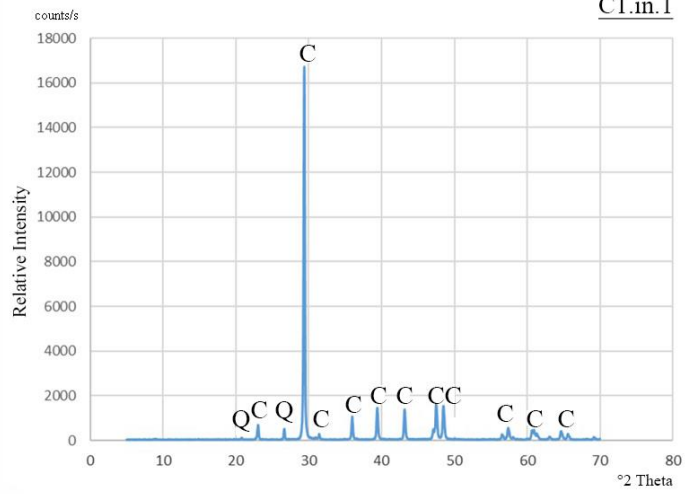




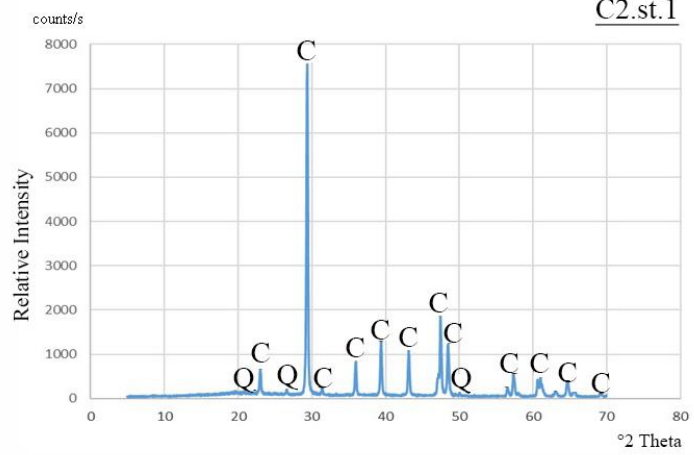
C1.st.1



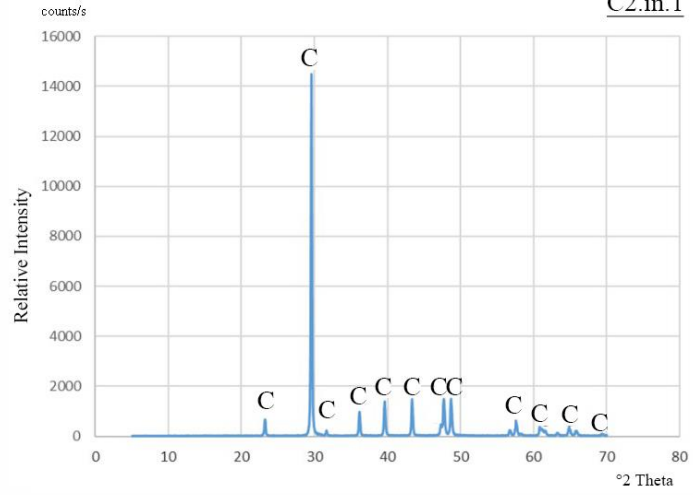
C1.in.1



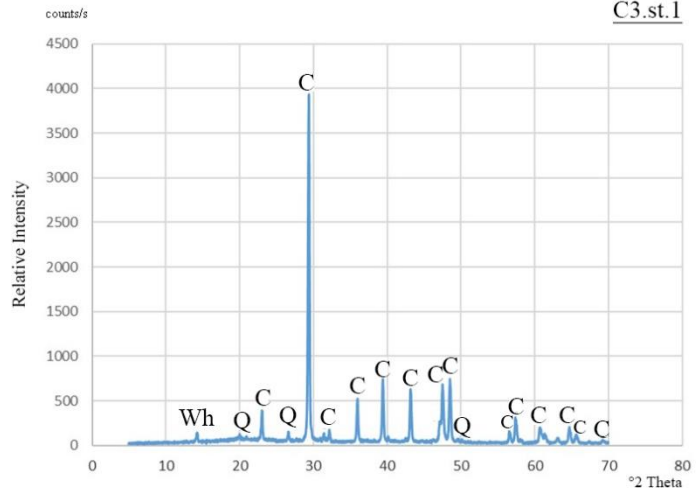
C2.st.1



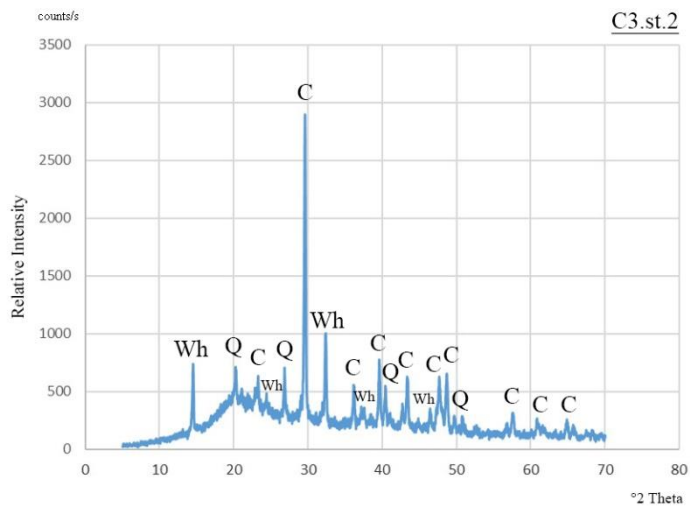
C2.in.1



C3.st.1

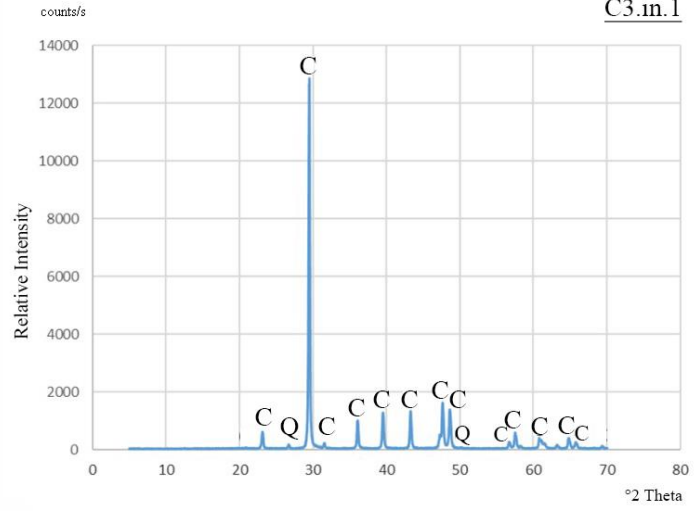


C3.st.2

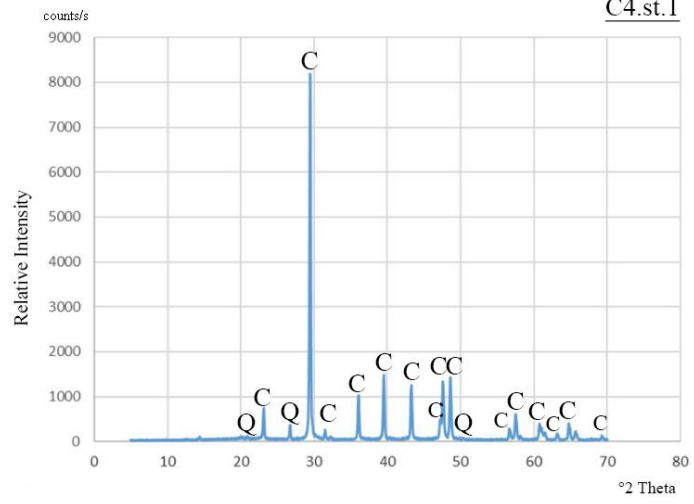




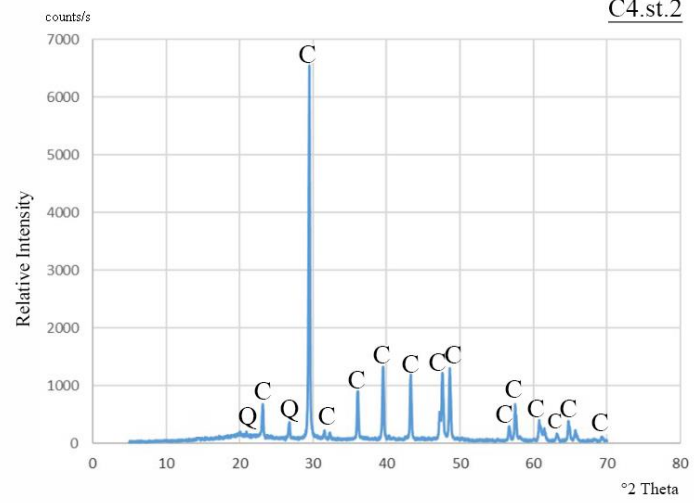
C3.in.1



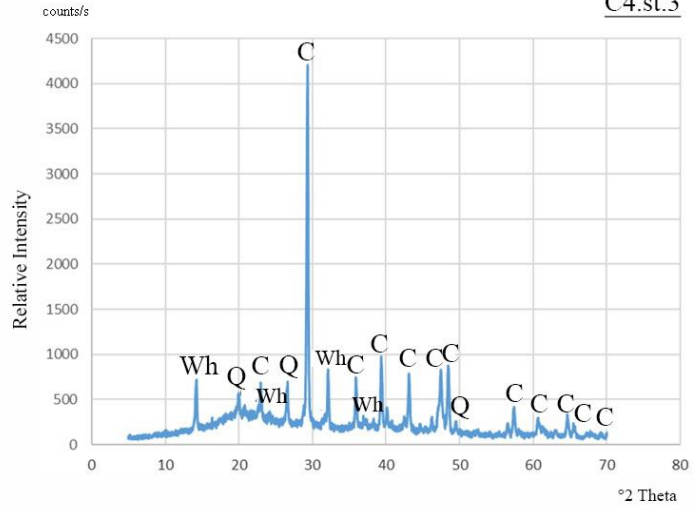
C4.st.1



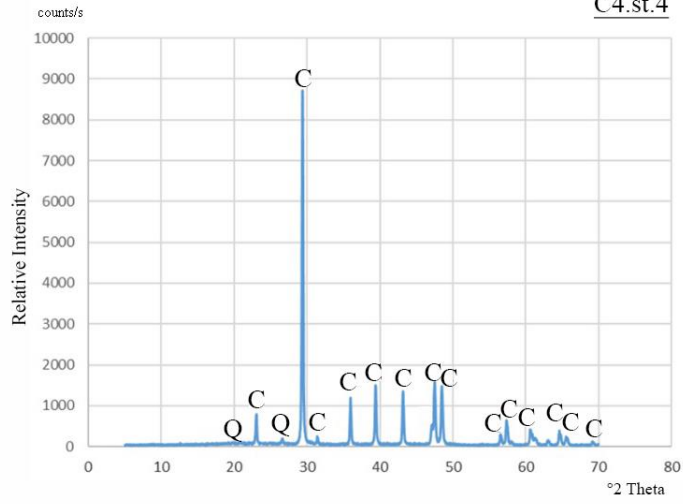
C4.st.2



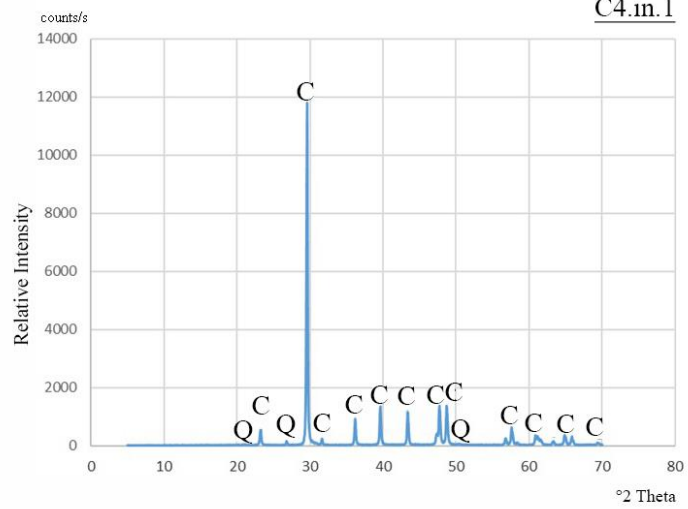
C4.st.3

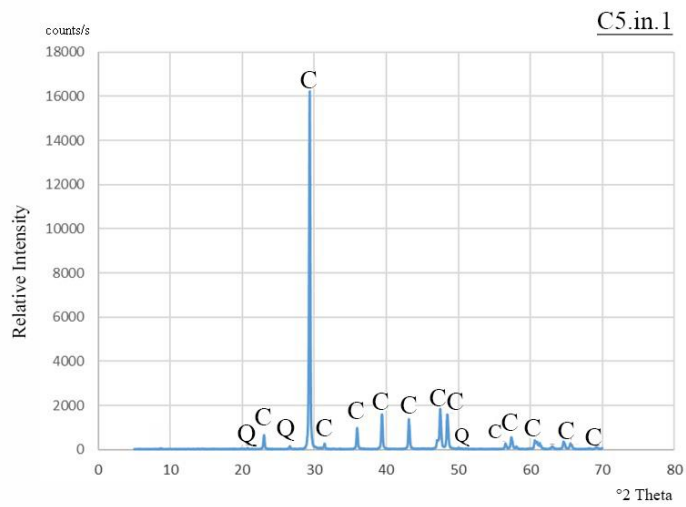
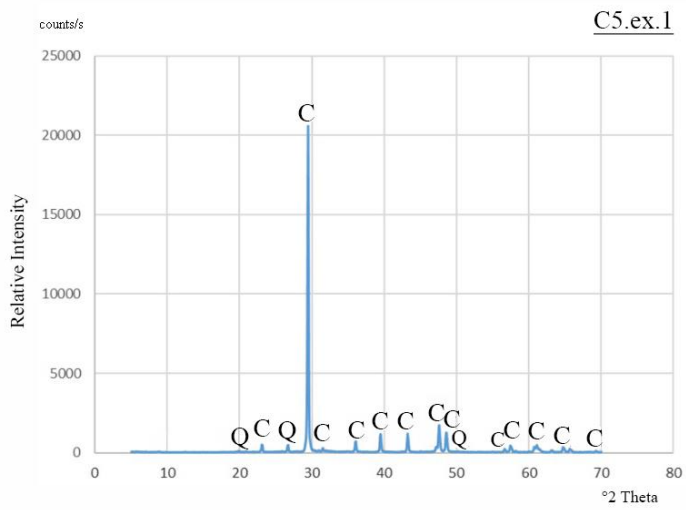
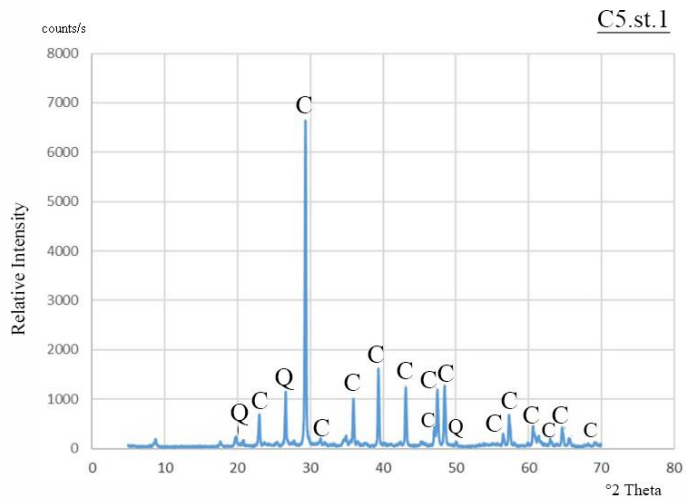


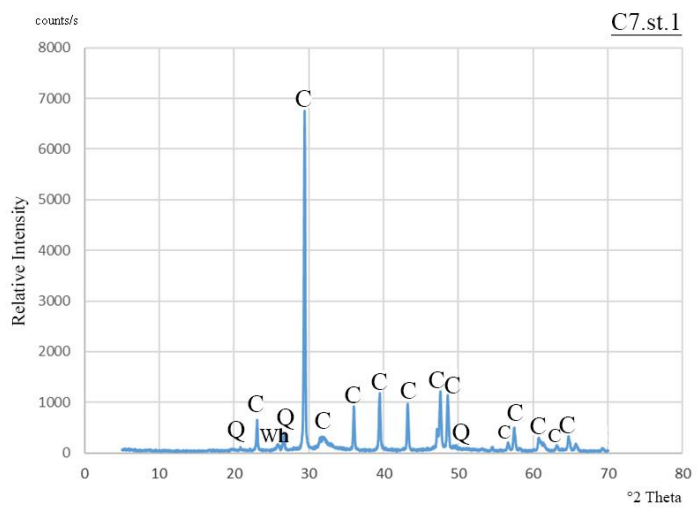
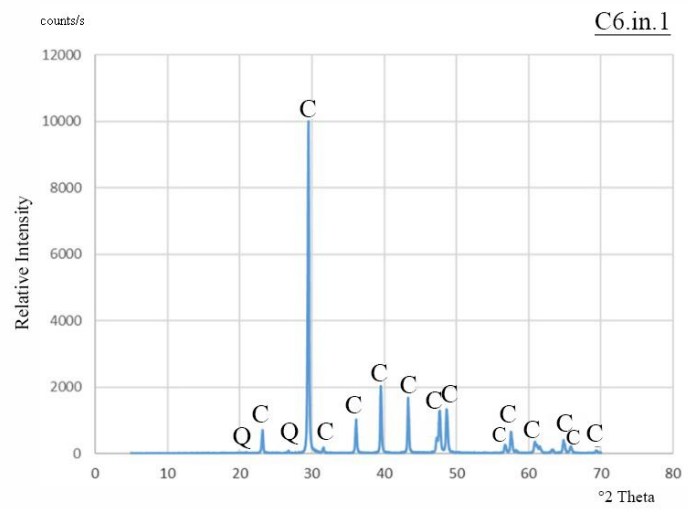
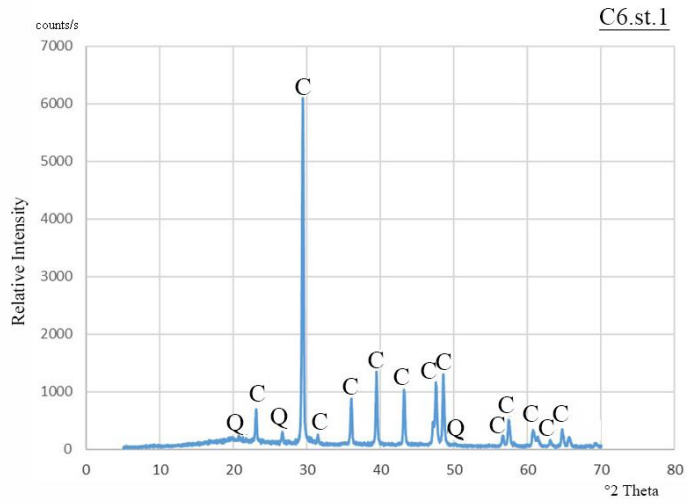
C4.st.4

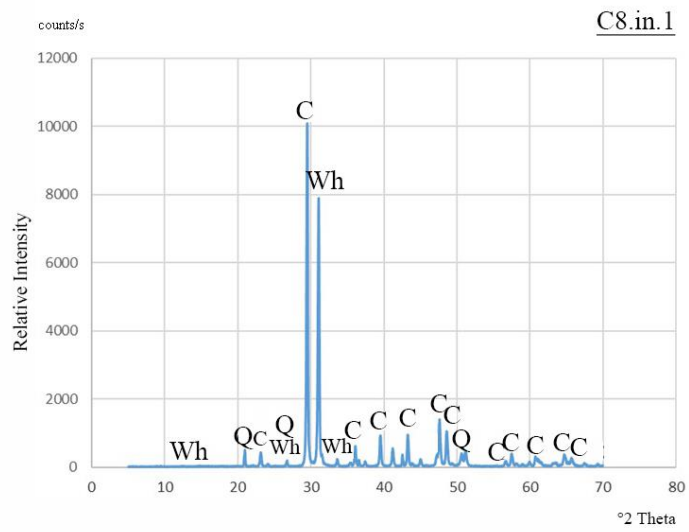
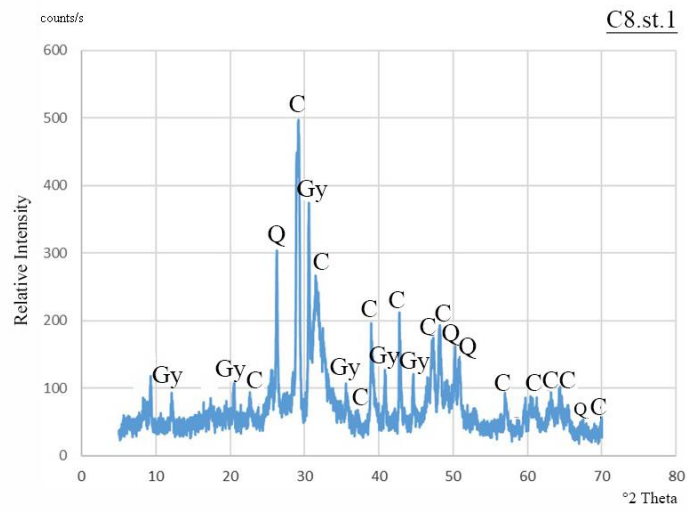
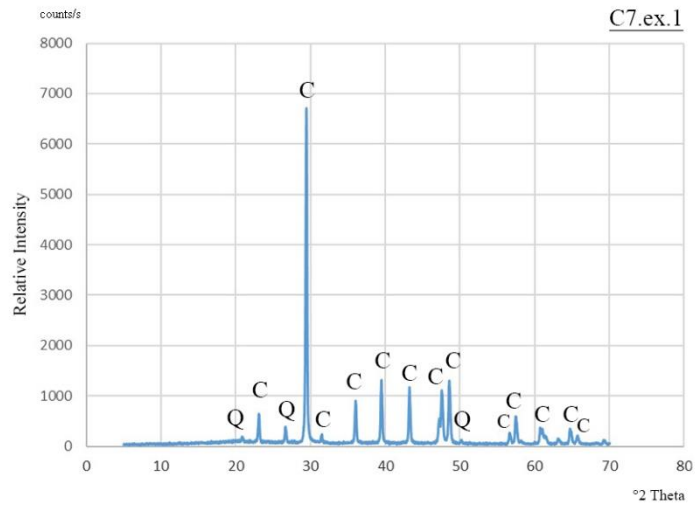


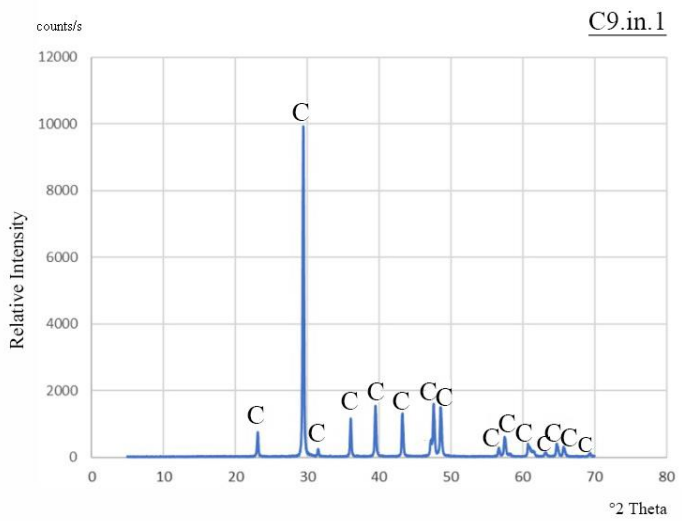
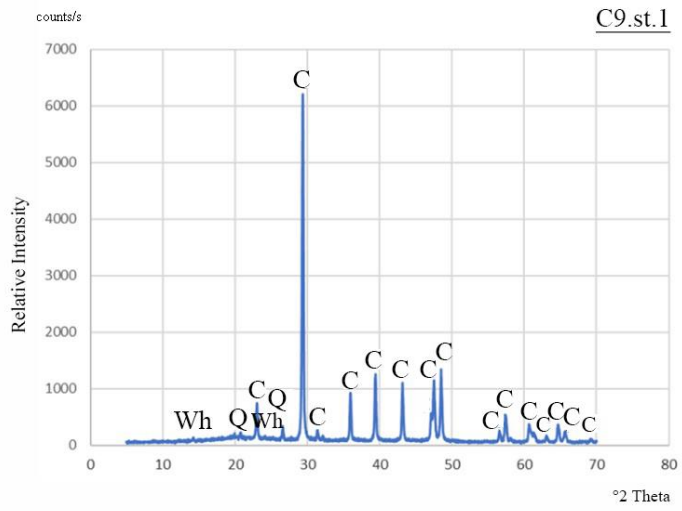
C4.in.1







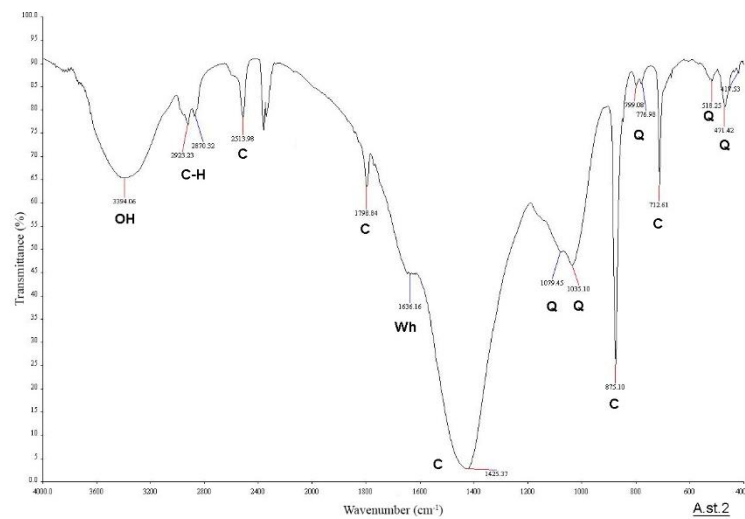
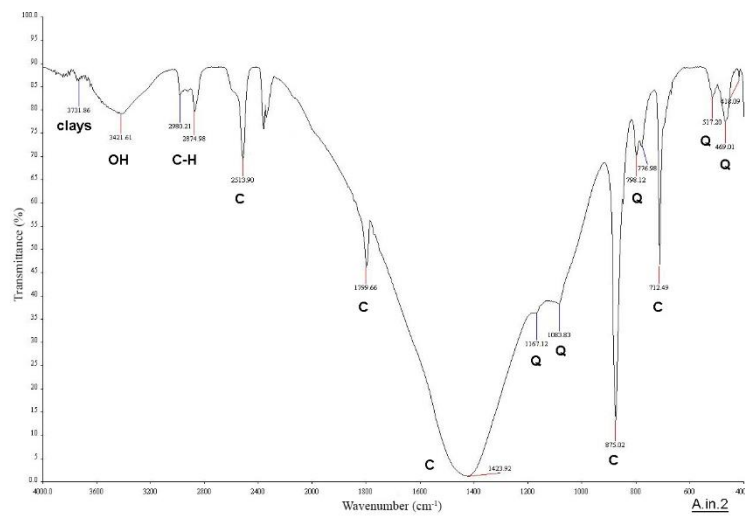
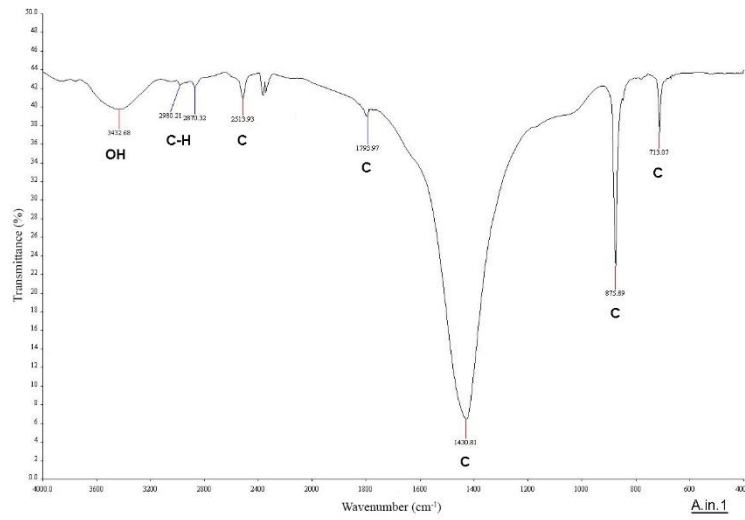


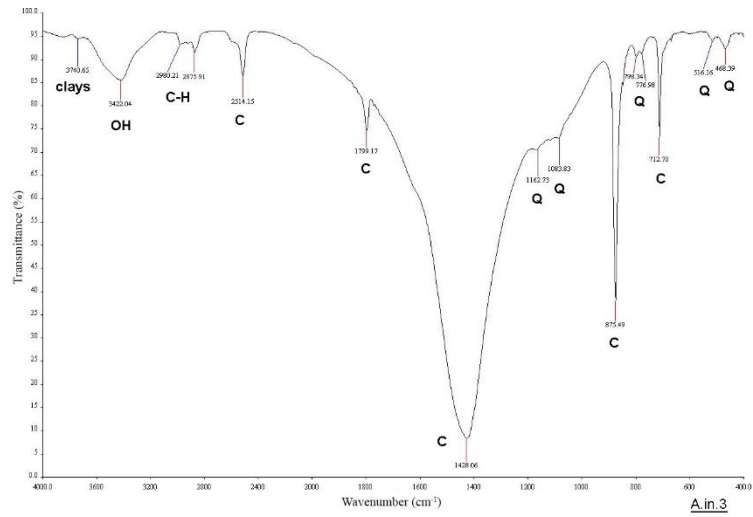


# APPENDIX B

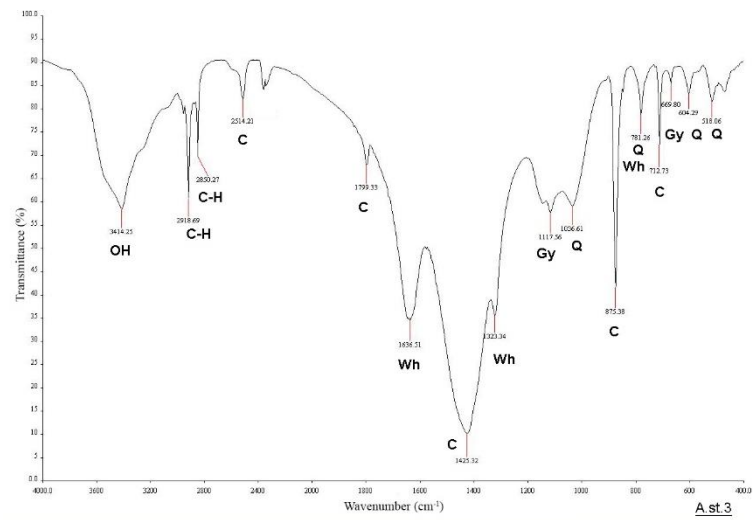
## MINERALOGICAL COMPOSITIONS OF LIMESTONES

### (FT-IR SPECTRUMS)

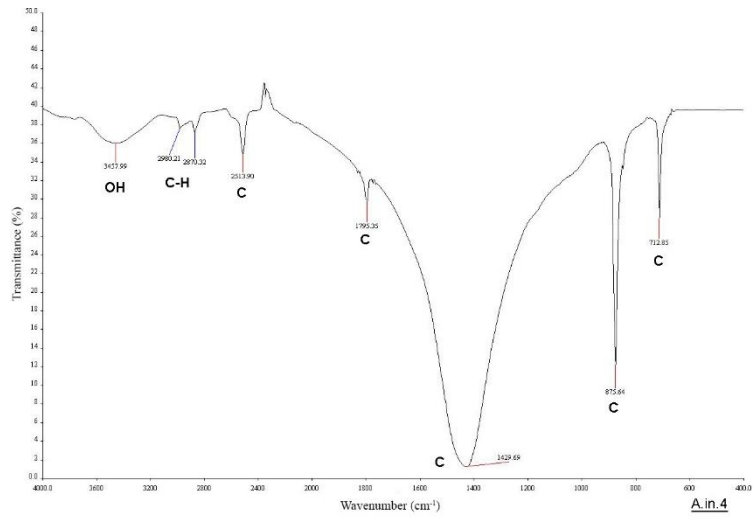




A.in.3

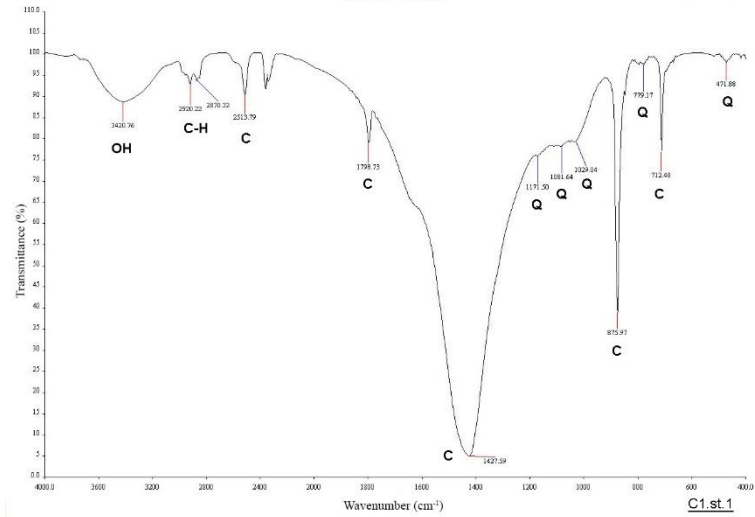
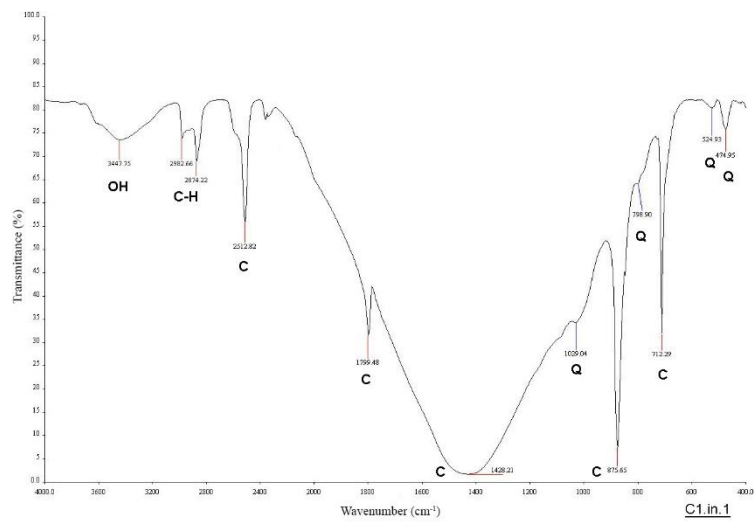
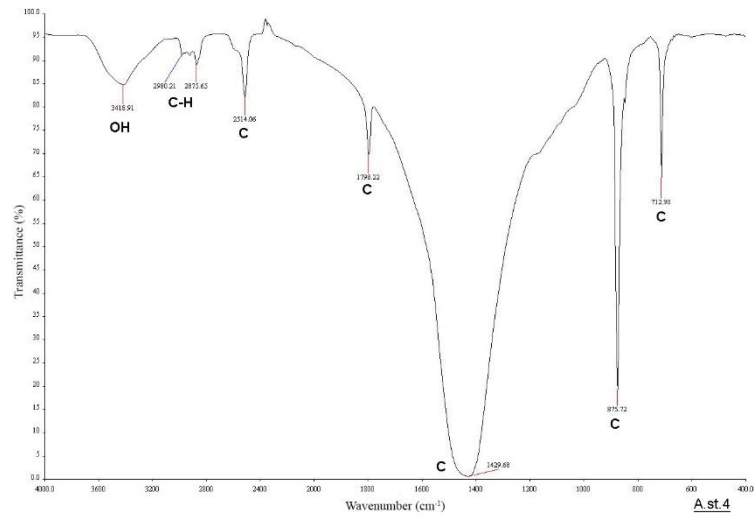


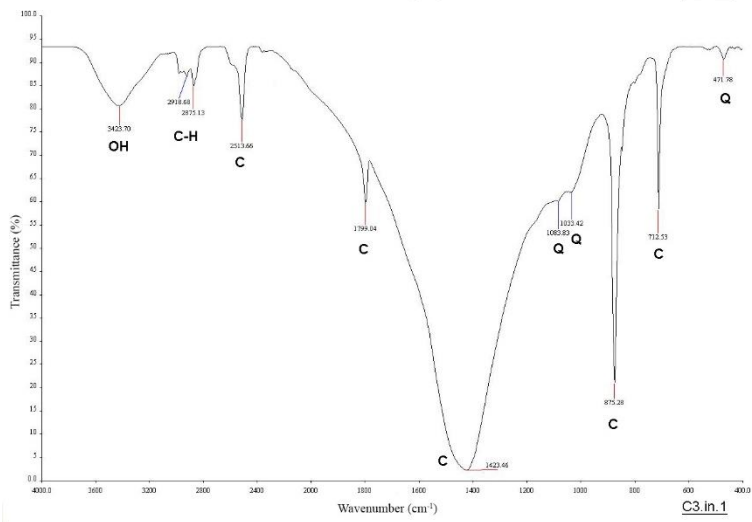
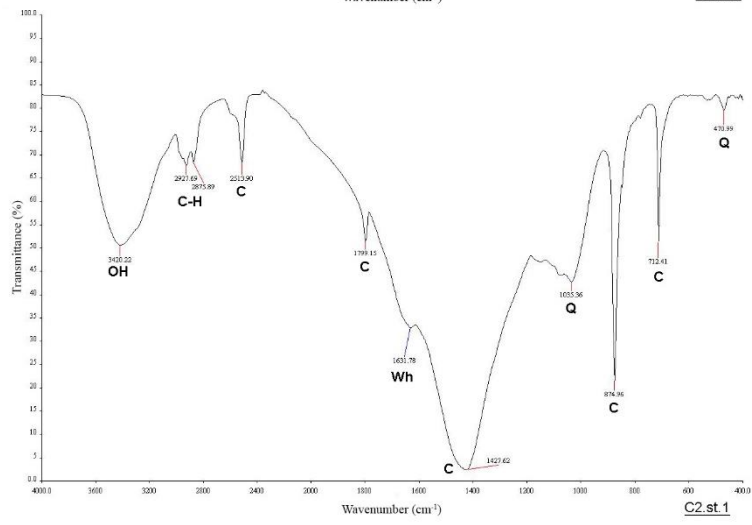
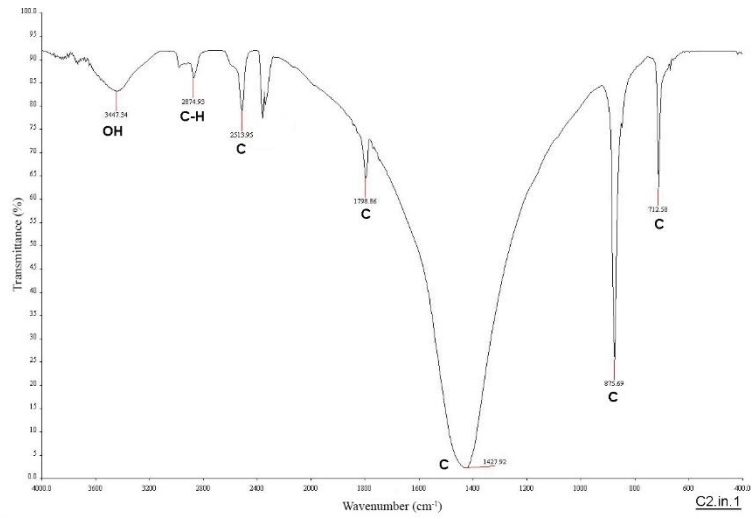
A.st.3

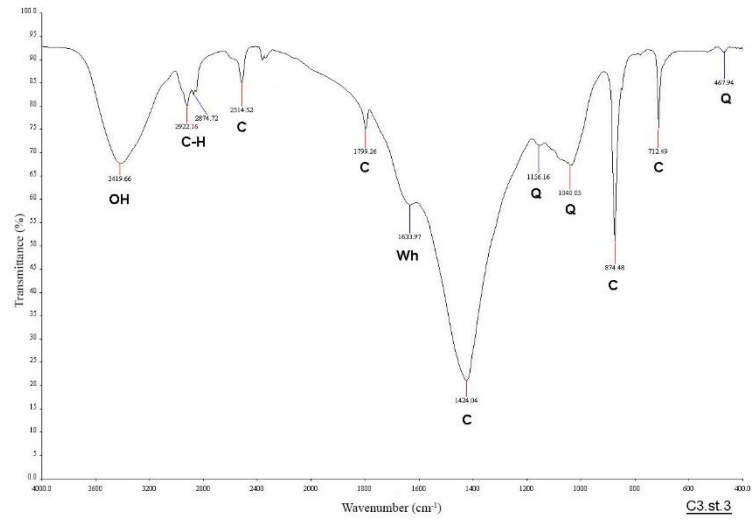
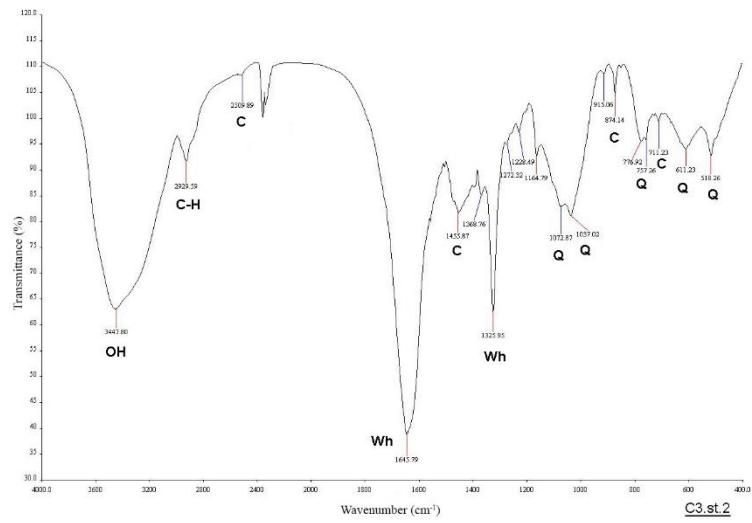
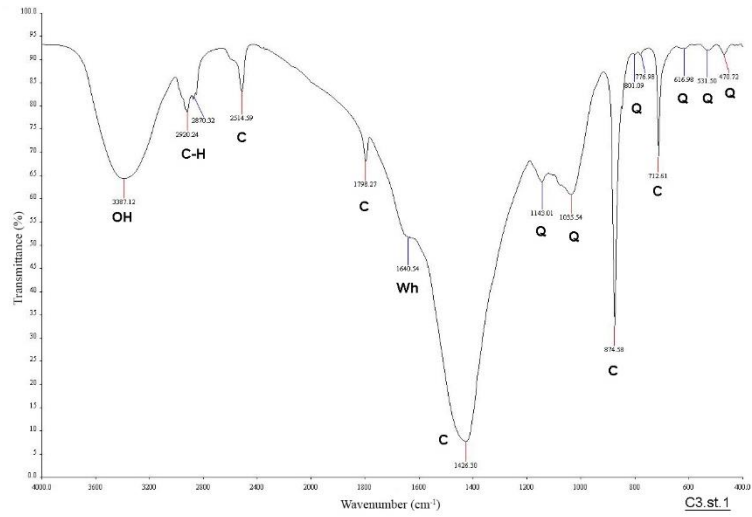


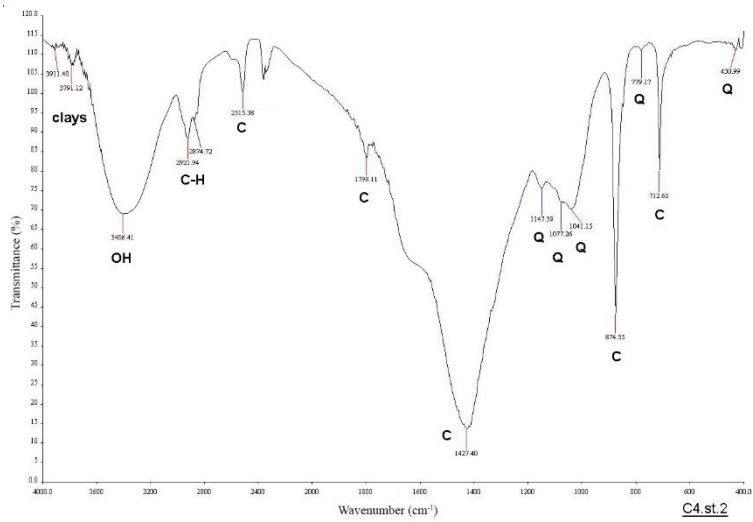
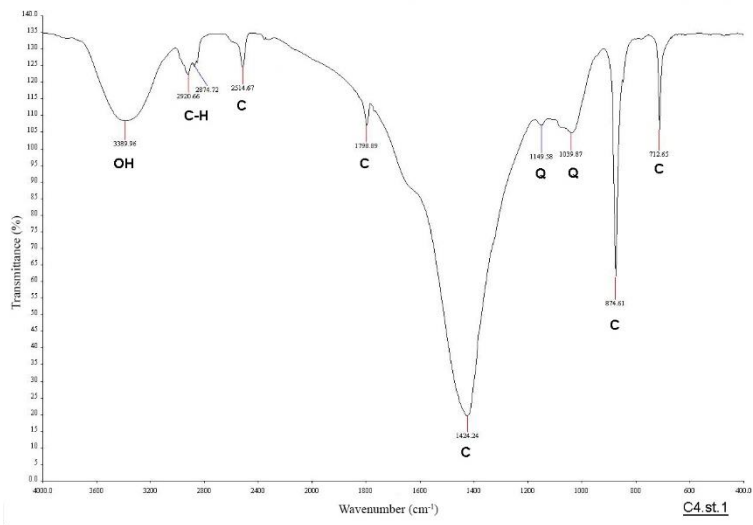
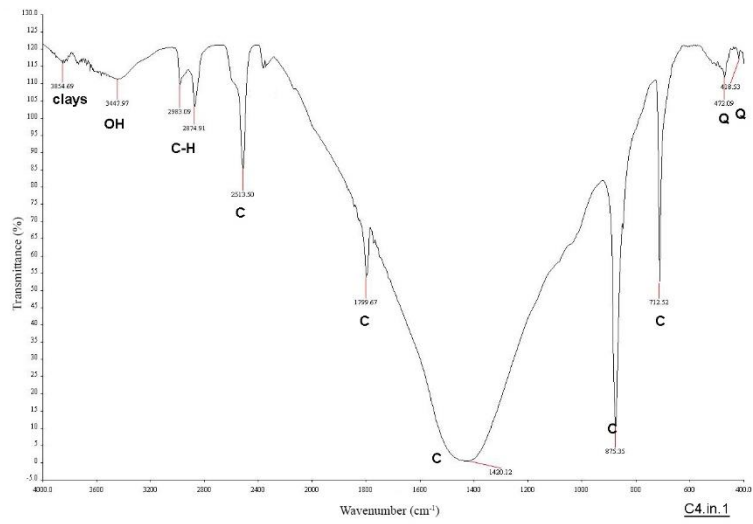
A.in.4

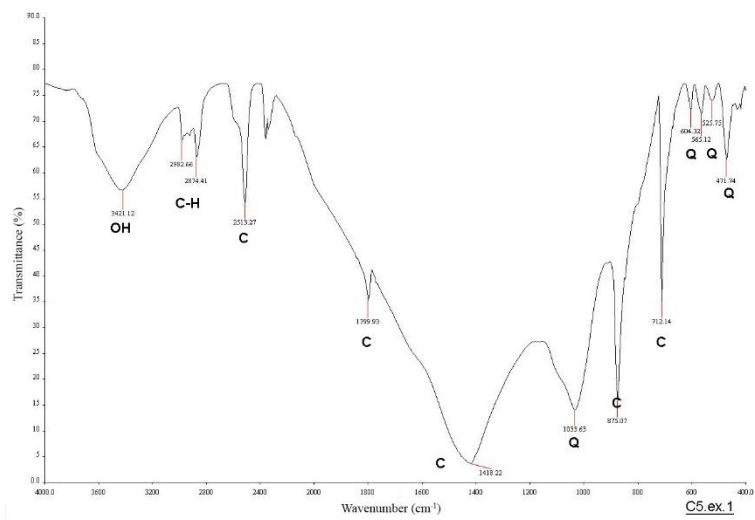
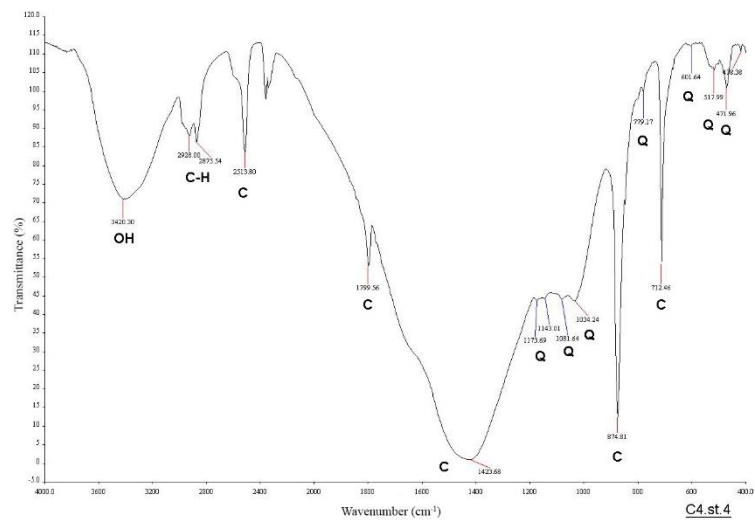
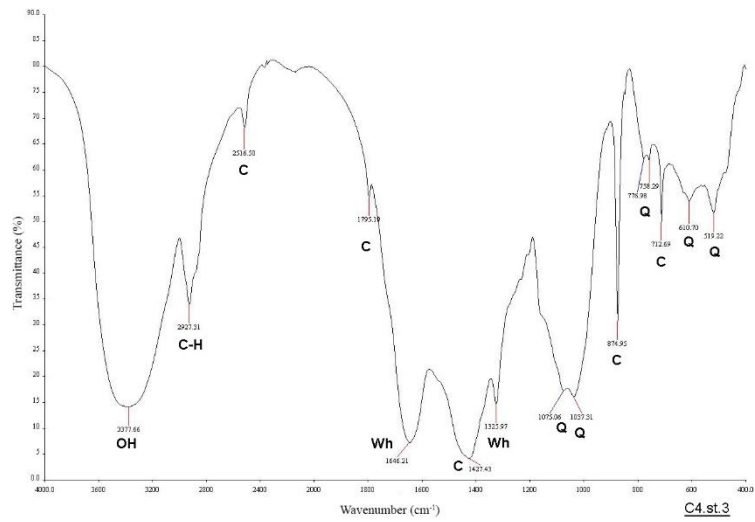


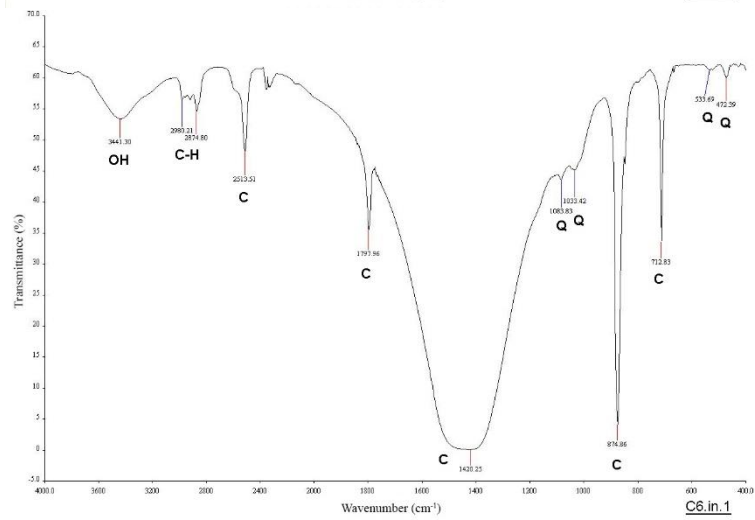
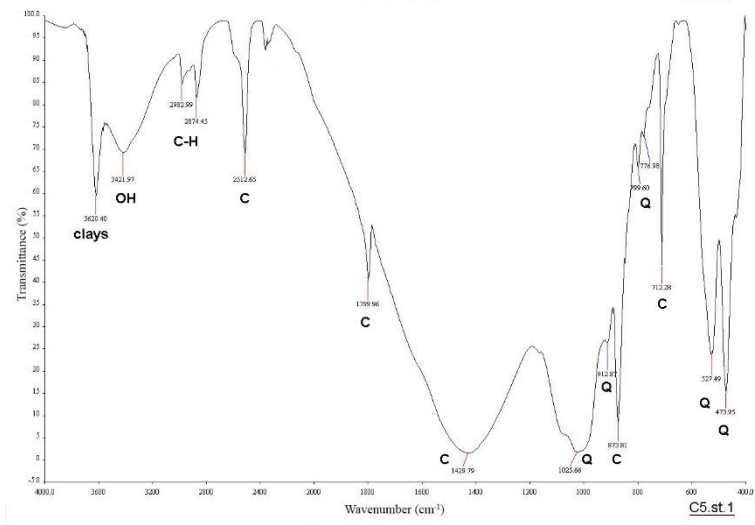
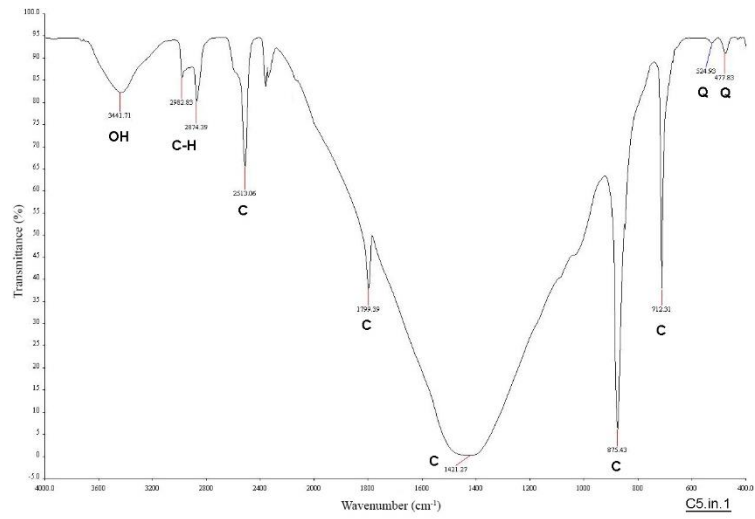


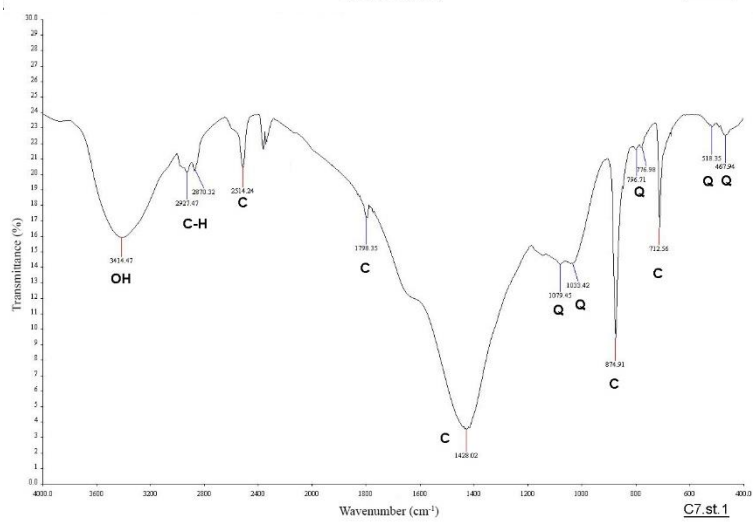
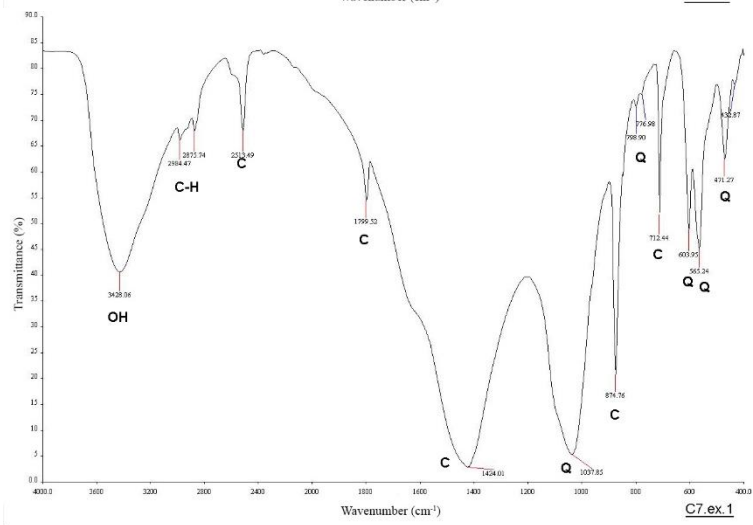
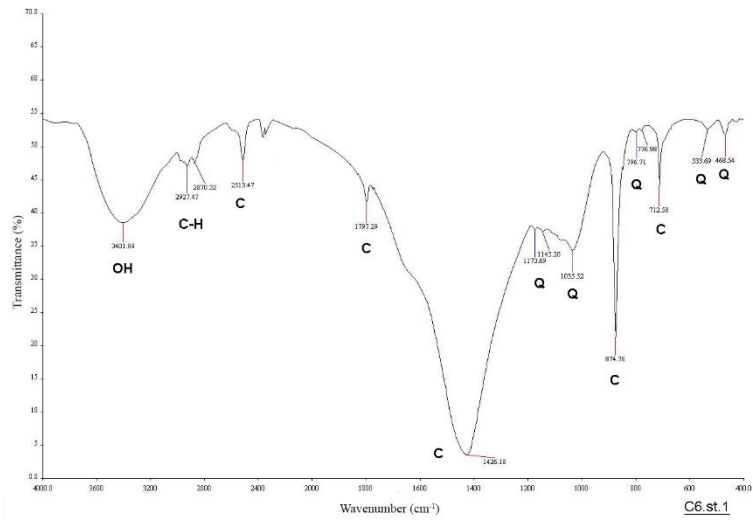


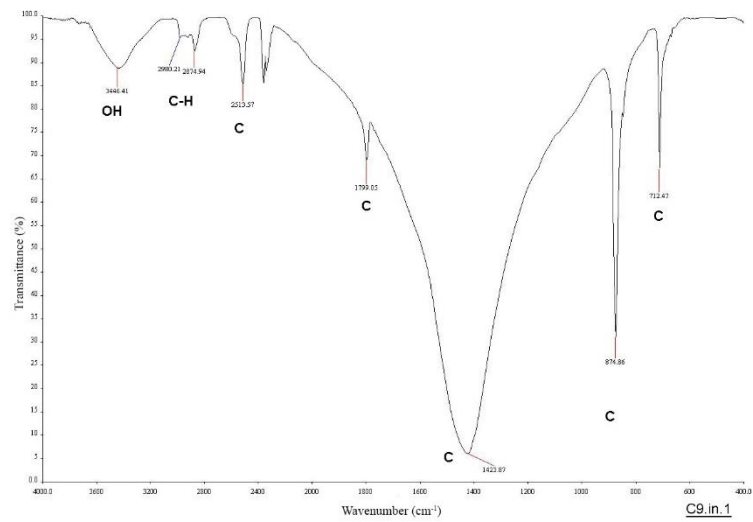
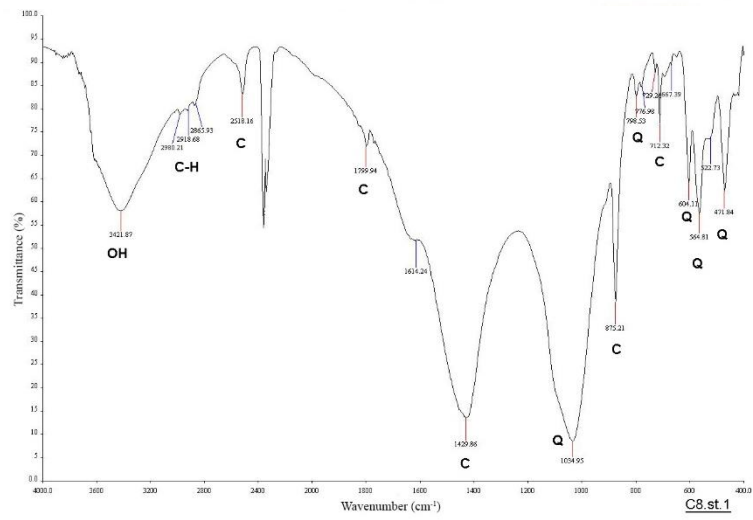
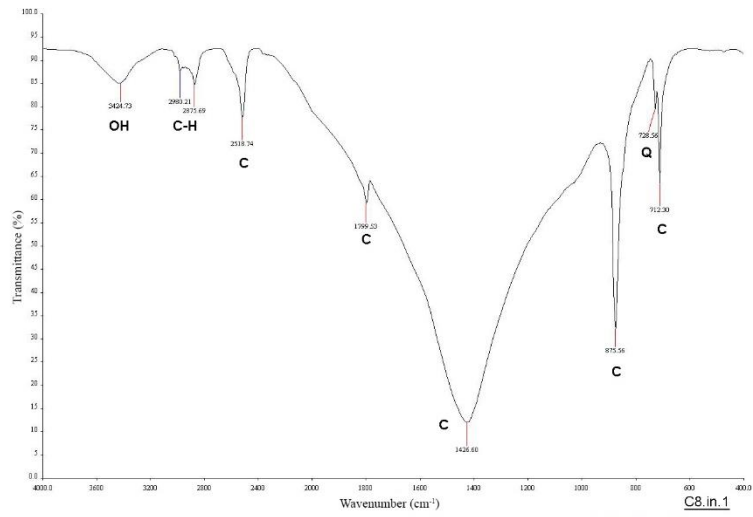




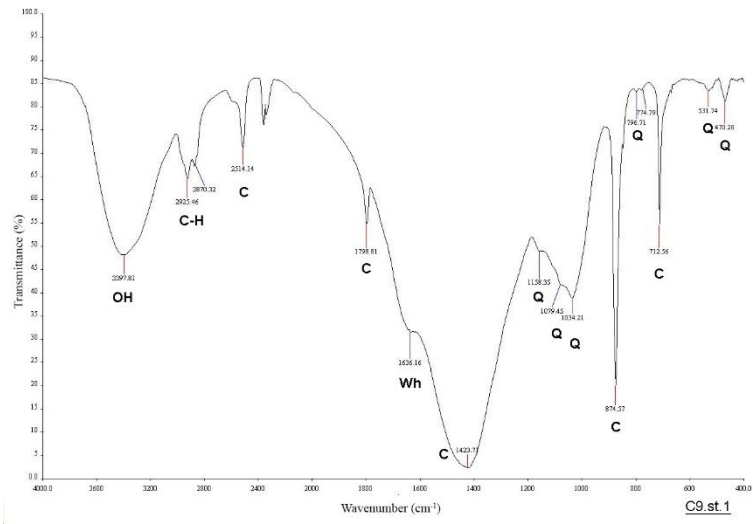






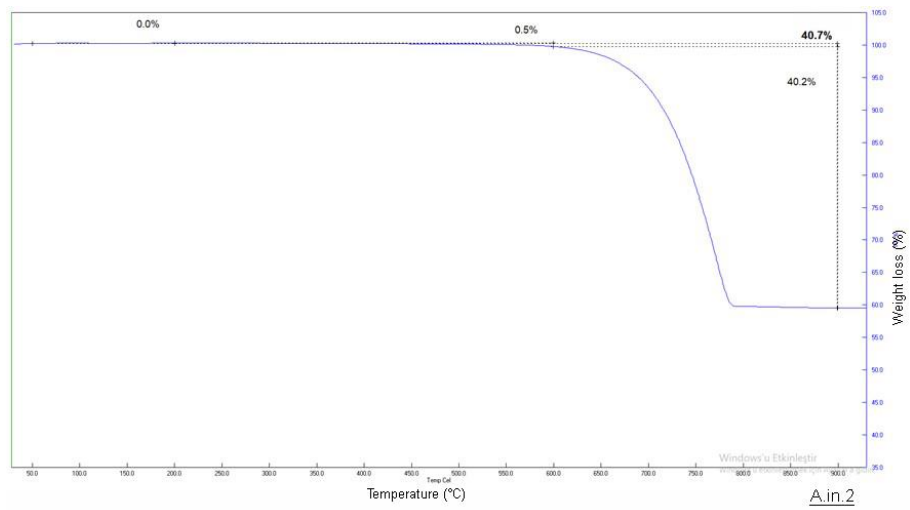
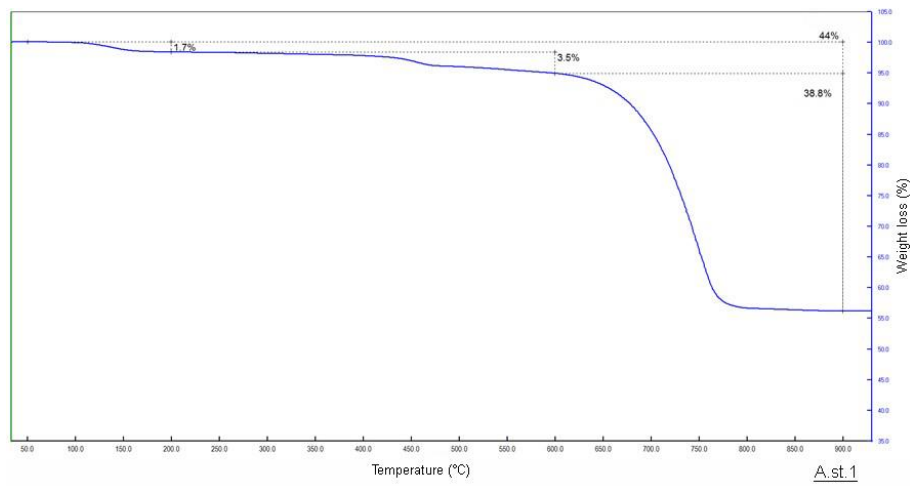
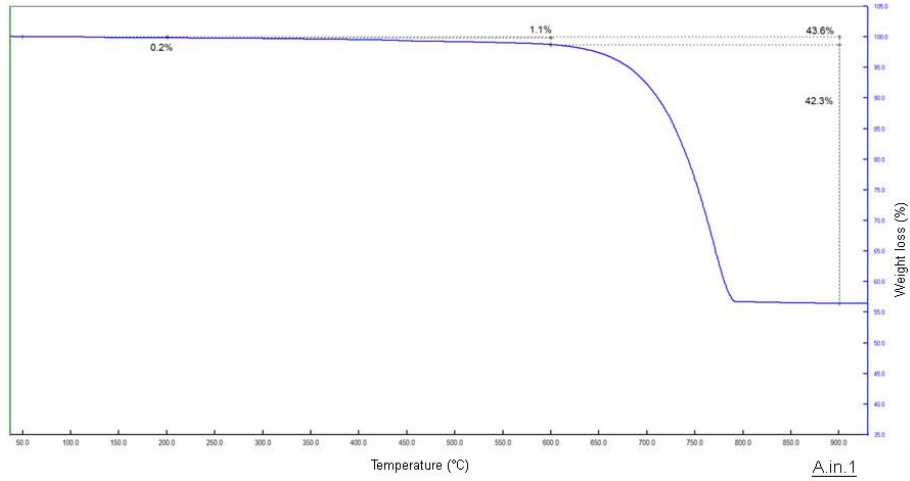


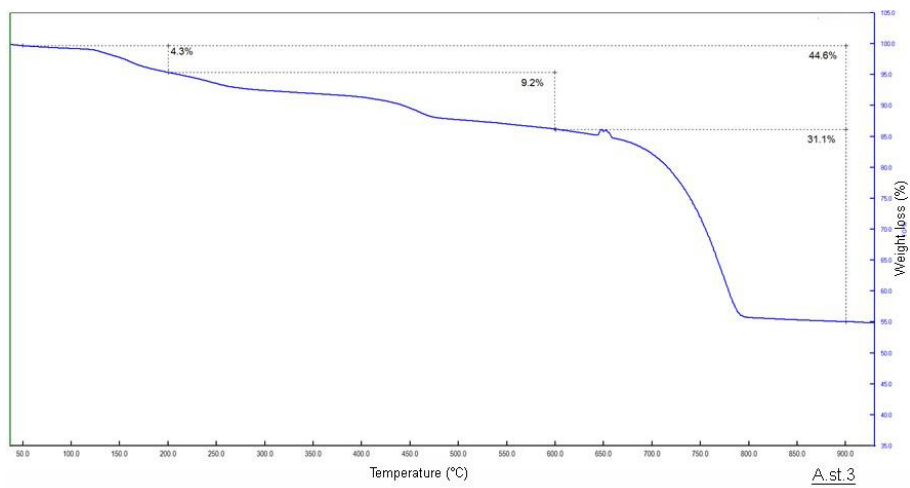
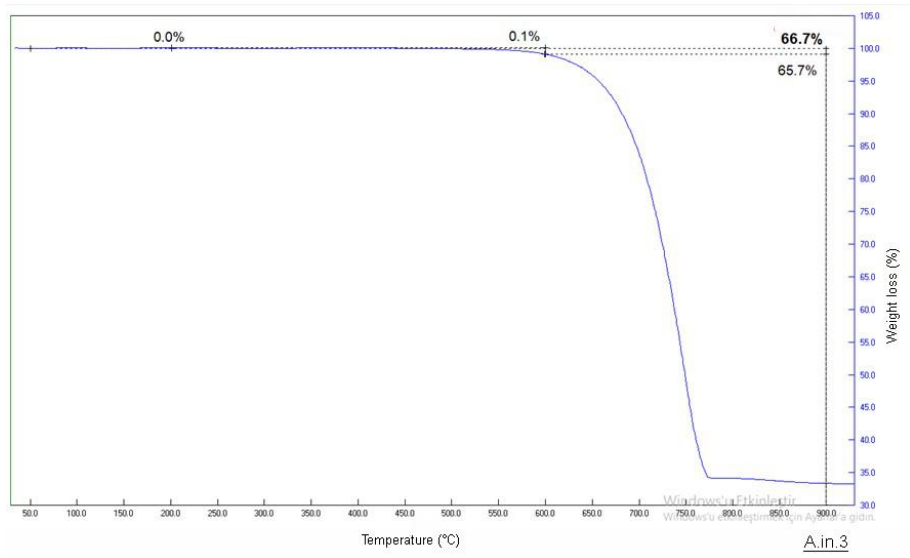
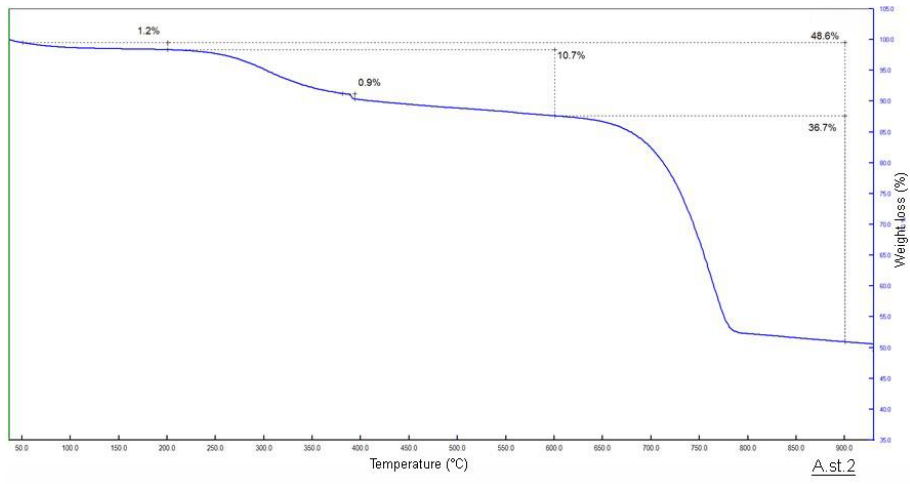


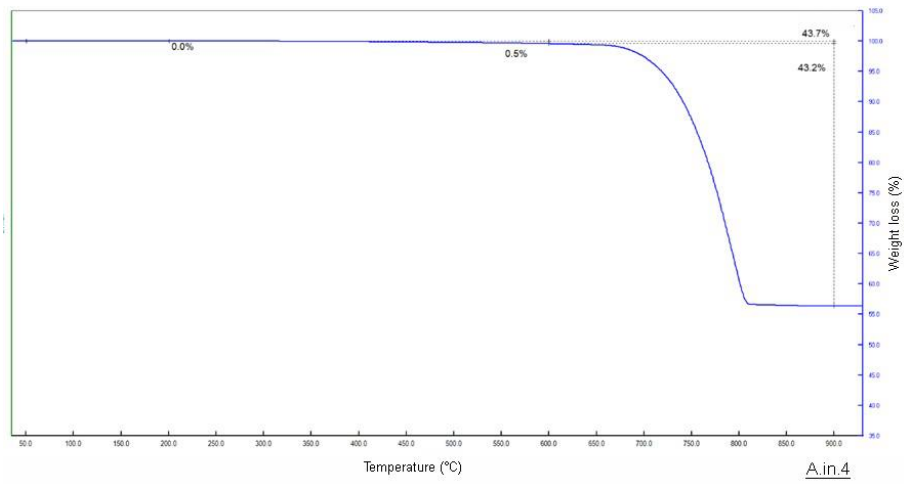


# APPENDIX C

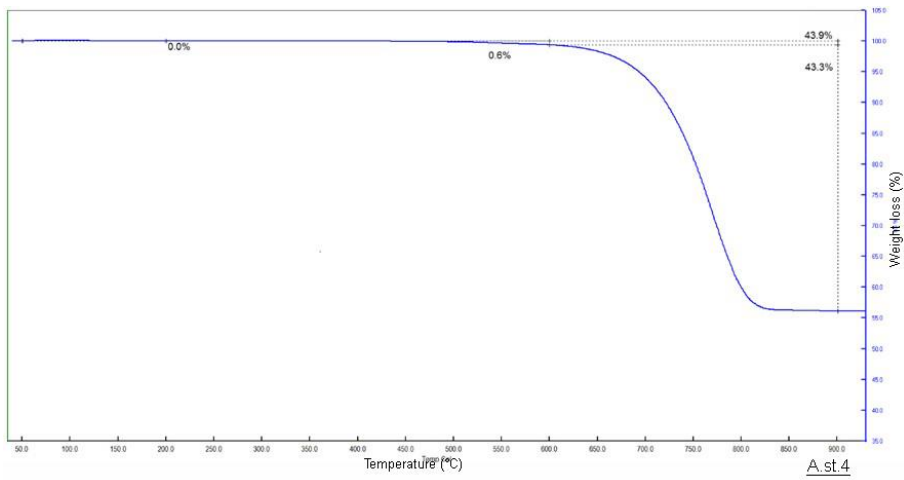
## CHEMICAL COMPOSITIONS OF LIMESTONES (TGA CURVES)



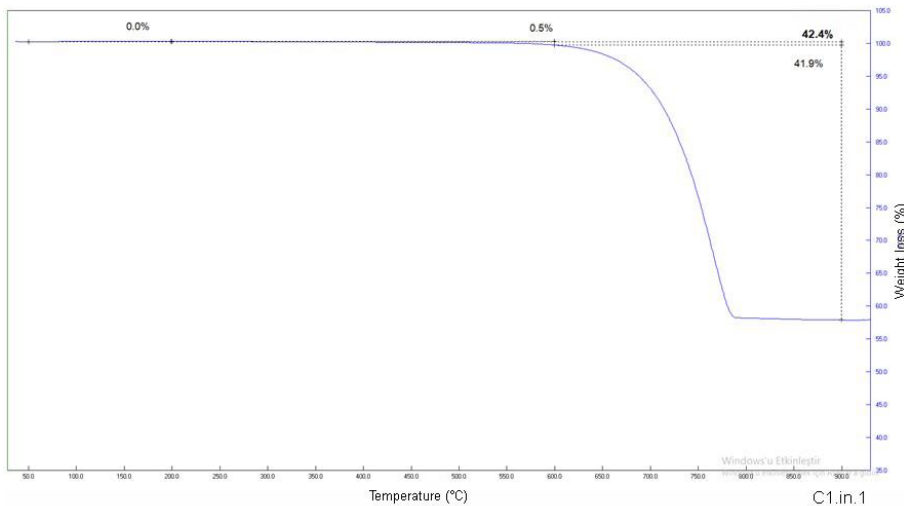




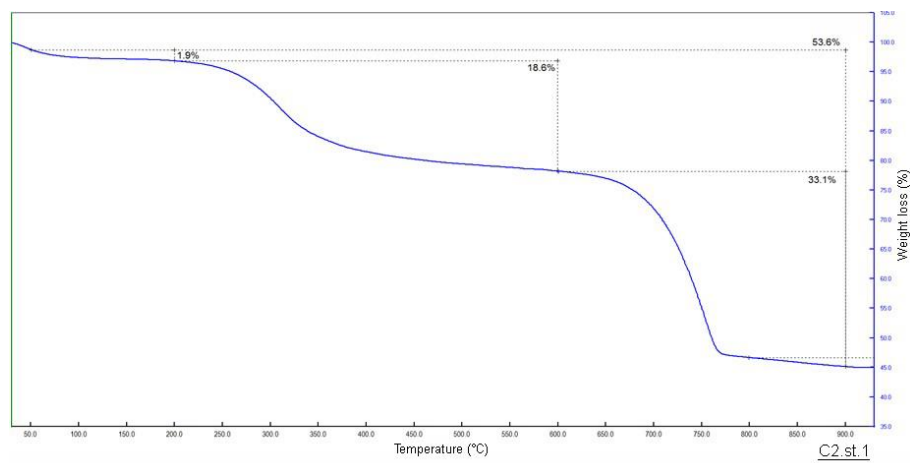
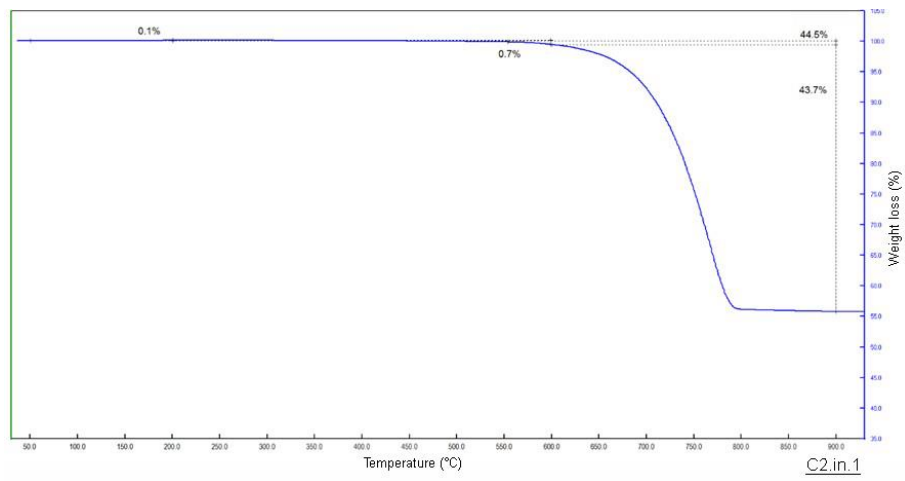
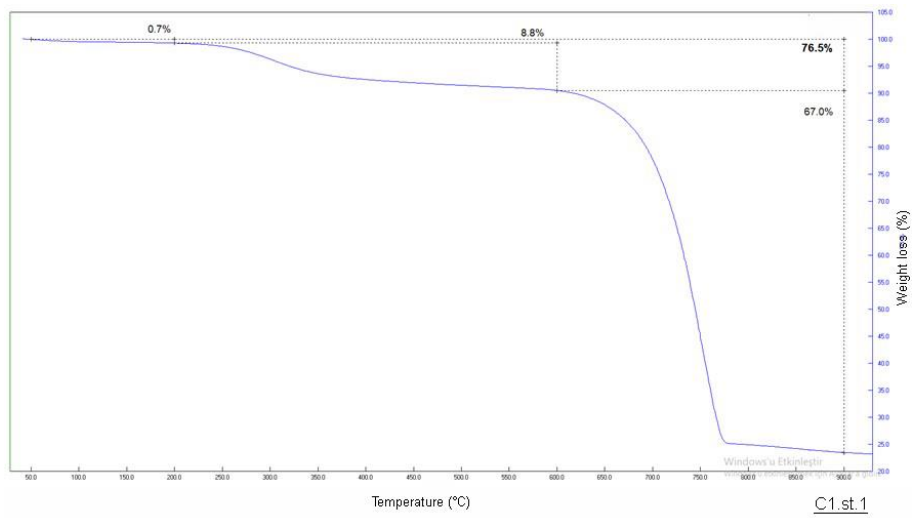
A.in.4

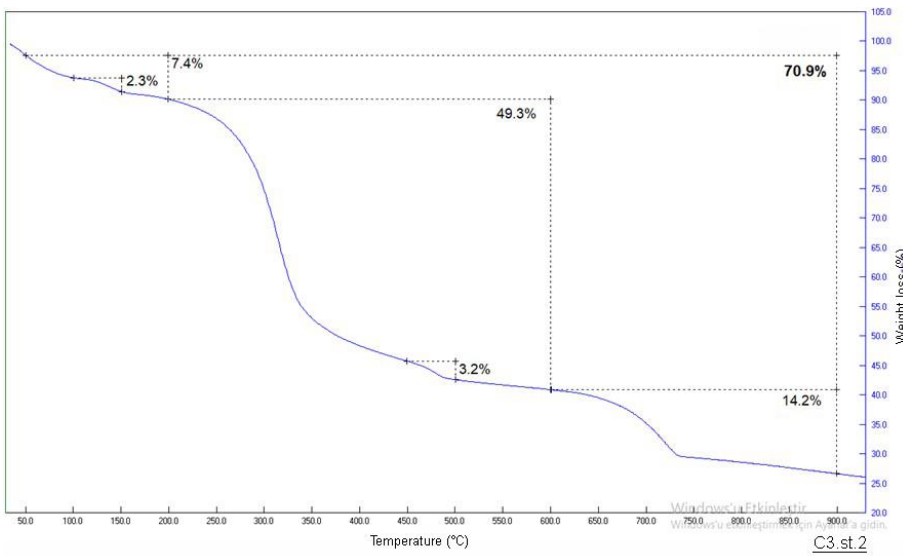
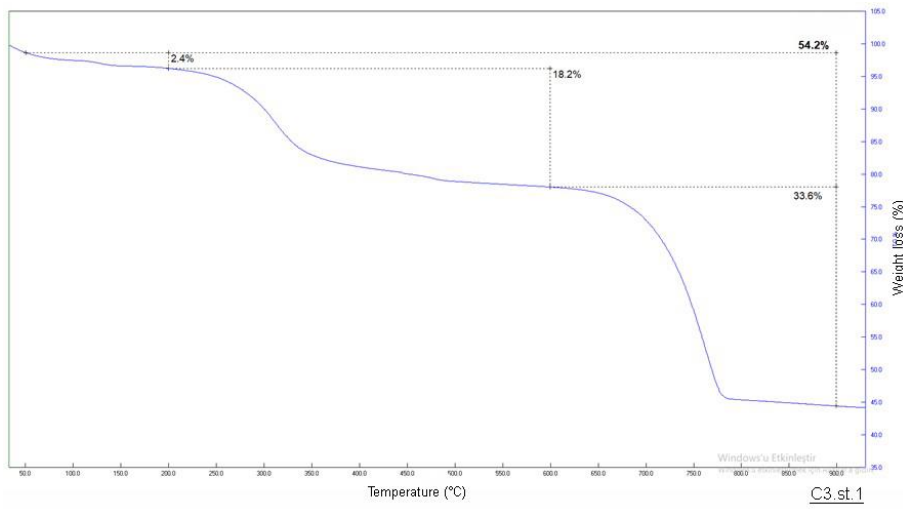
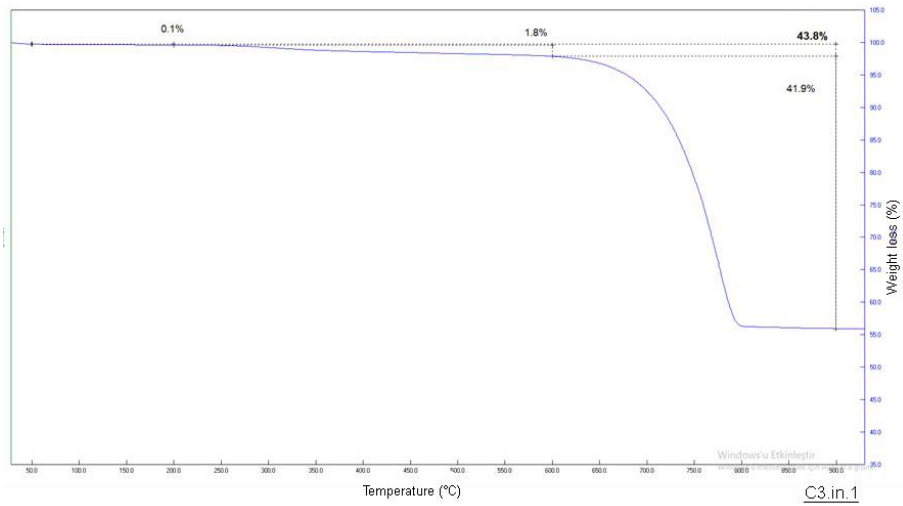


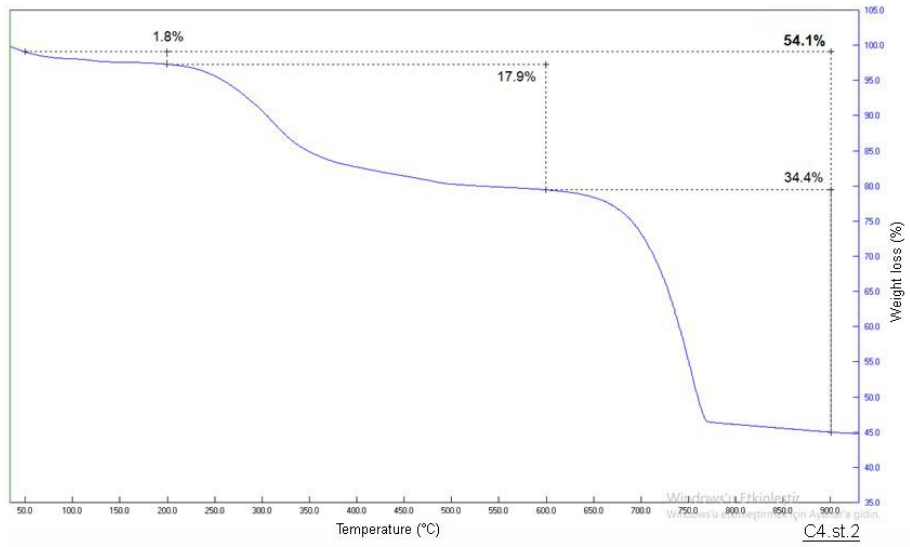
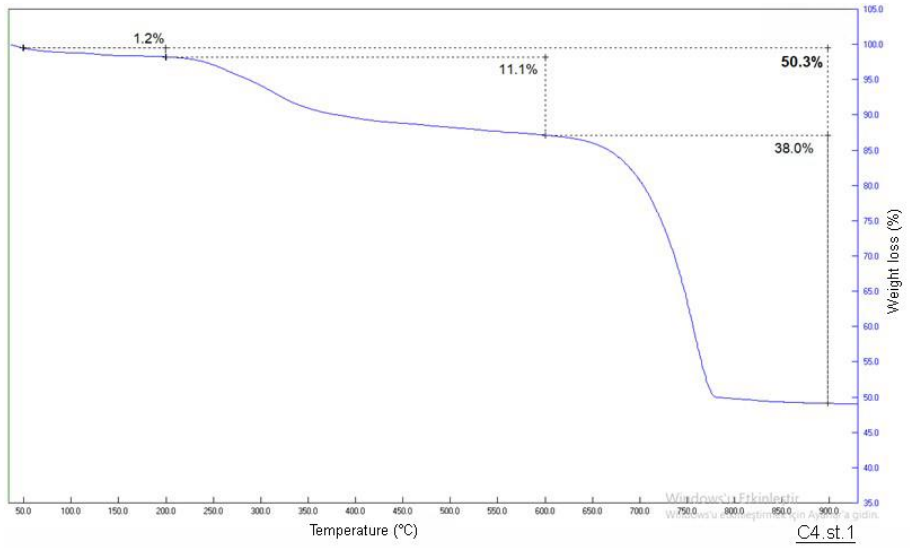
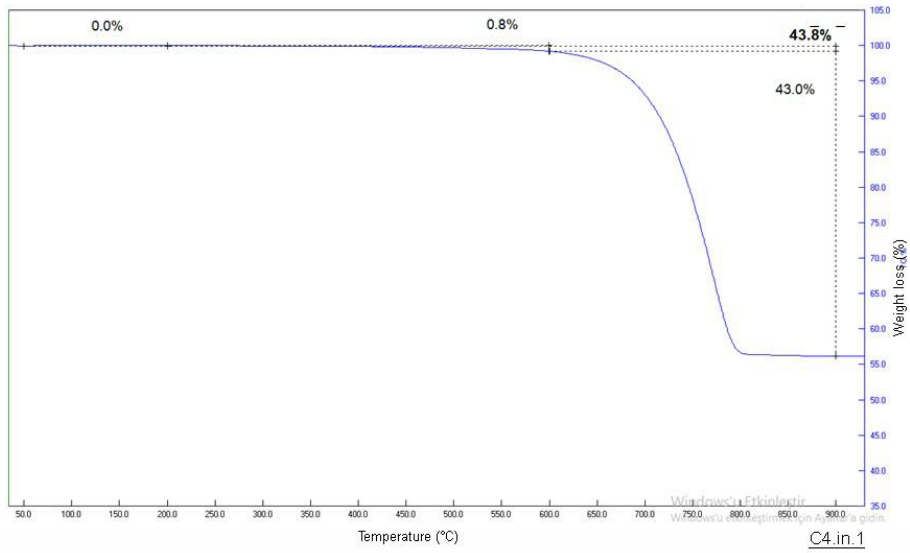
A.st.4

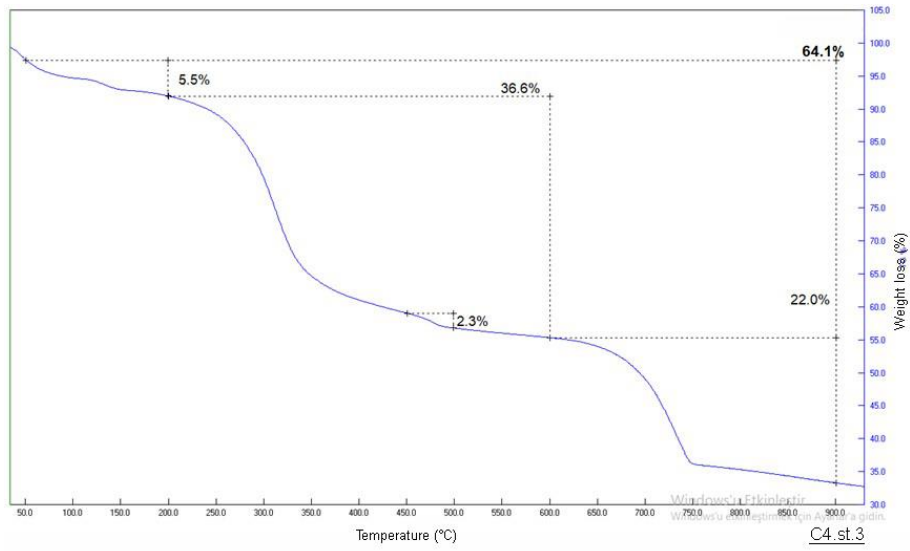


C1.in.1

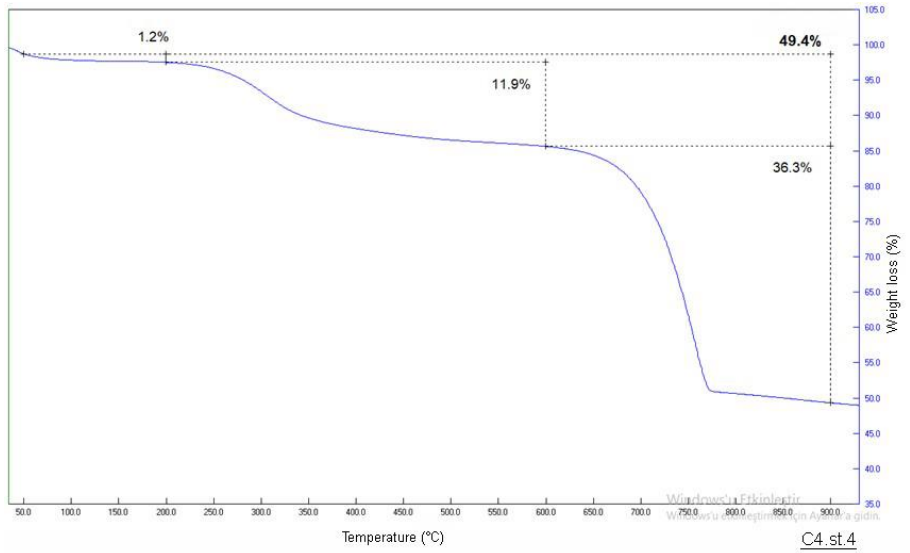




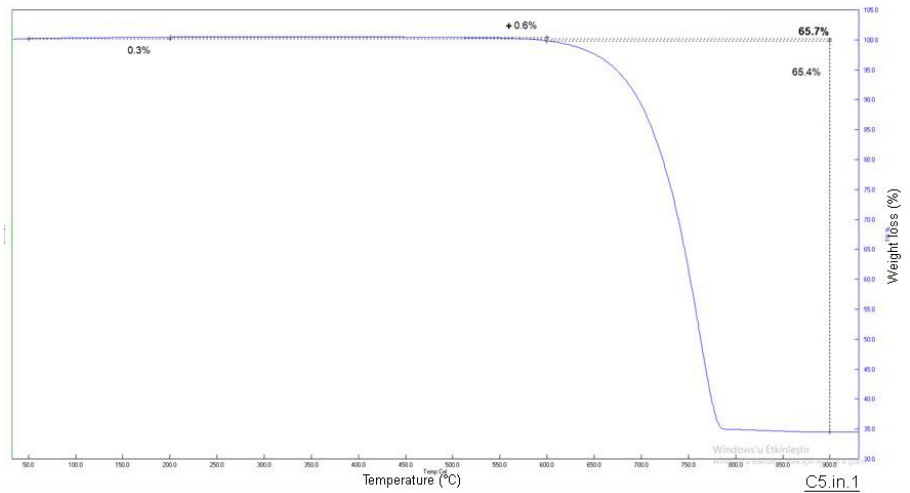




C4.st.3

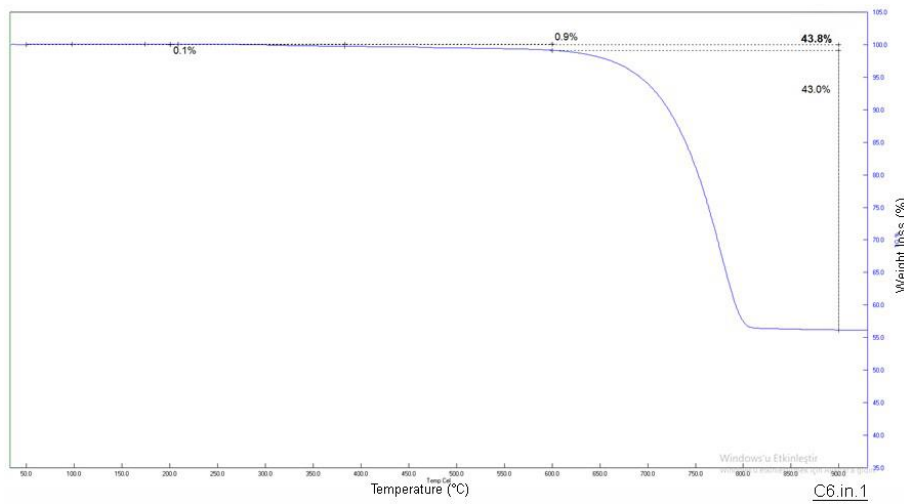
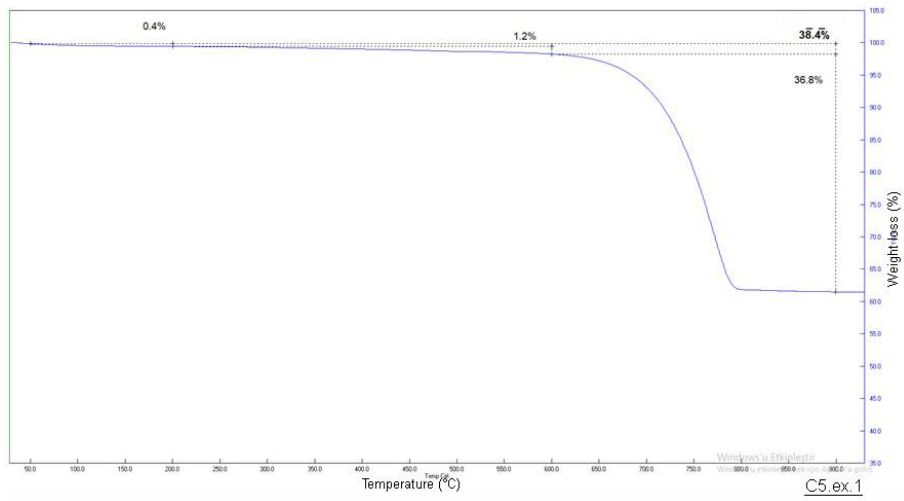
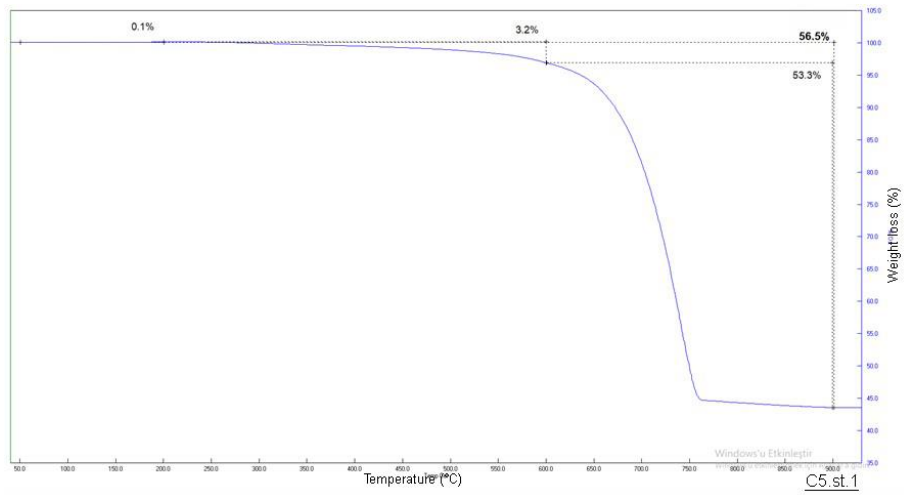


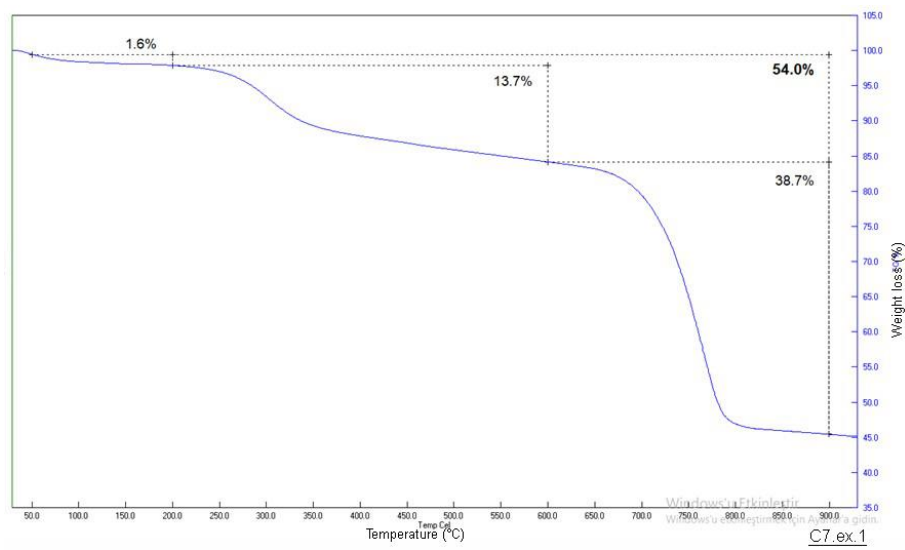
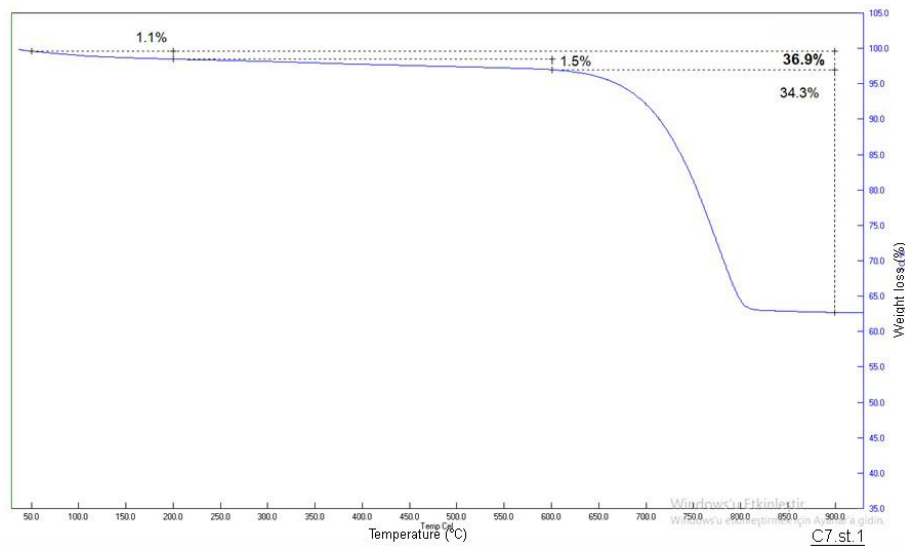
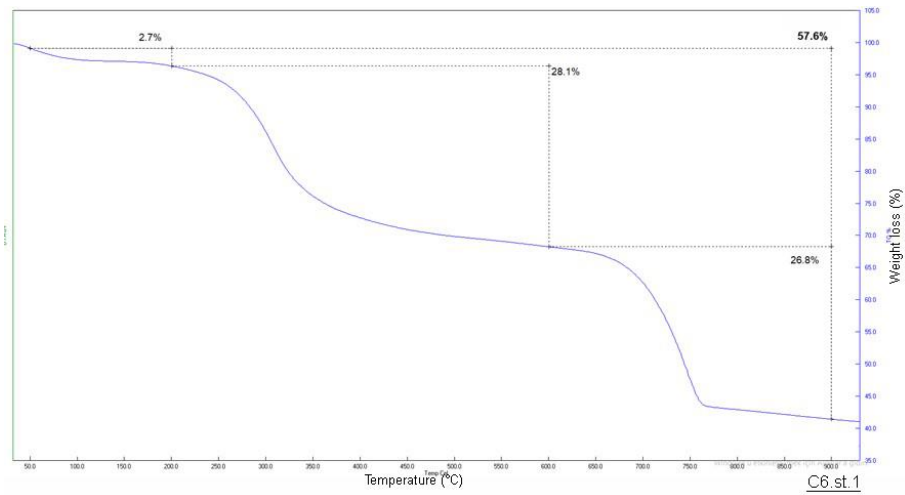
C4.st.4

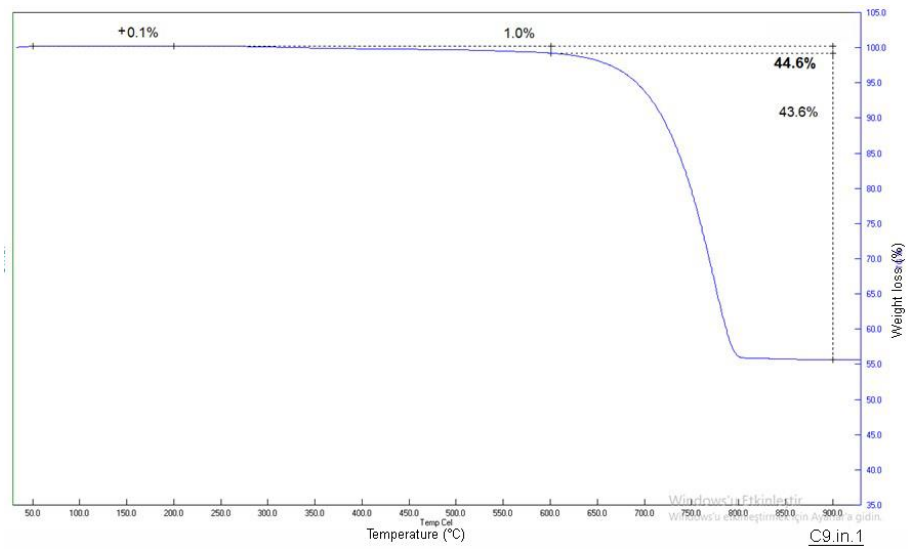
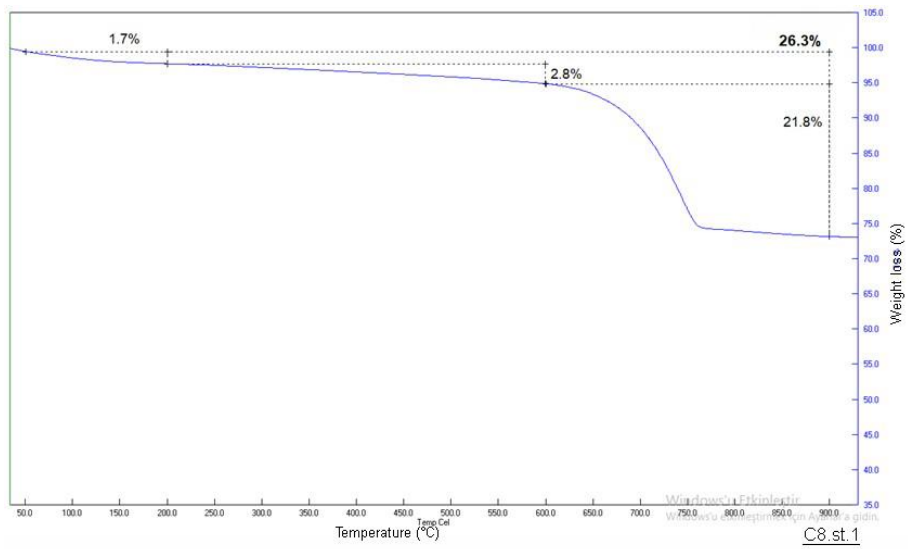
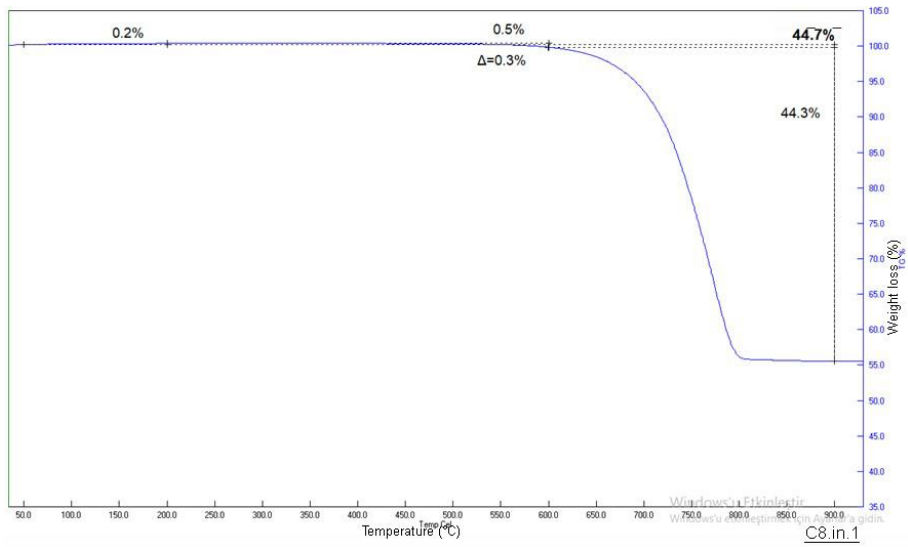


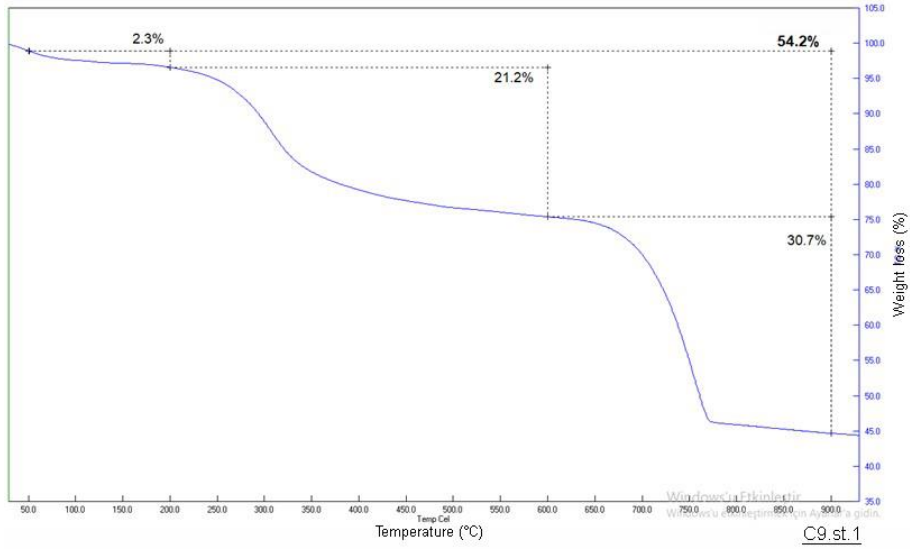
C5.in.1











## APPENDIX D

### SOLUBLE SALTS OF STONES (IC RESULTS)

sample name	height (cm)	depth (cm)	HMC (%)	Anions (micromol/g)			Cations (micromol/g)				
				Chlorine (Cl)	Nitrate (NO <sub>3</sub> <sup>-</sup> )	Sulphate (SO <sub>4</sub> <sup>2-</sup> )	Sodium (Na)	Ammonium (NH <sub>4</sub> <sup>+</sup> )	Potassium (K)	Magnesium (Mg)	Calcium (Ca)
A.st.1	150	0-1	0,31	0,654105	n.a.	1,712664	2,593342	n.a.	4,037675	1,77432627	12,16068
A.st.1	150	1-2	0,16								
A.ex.1	50	0-1	0,38								
A.ex.1	50	1-2	0,21								
A.ex.1	50	2-5	0,81								
A.st.2	120	0-1	0,46	3,623389	3,10775	23,44032	2,043951	n.a.	2,792598	2,89323185	28,21582
A.st.2	120	1-2	0,46								
A.st.3	120	0-1	1,45	15,27081	19,57892	32,49202	7,621	n.a.	13,9304	n.a.	61,44823
A.st.3	120	1-2	0,89								
C1.st.1	60	0-1	0,11	0,518574	n.a.	n.a.	0,728677	n.a.	0,781498	1,21353631	15,02944
C1.st.1	60	1-2	0,18								
C1.st.1	60	2-5	0,53								
C2.st.1	75	0-1	0,17	n.a.	n.a.	n.a.	0,372933	n.a.	n.a.	0,98395392	30,11639
C2.st.1	75	1-2	0,12								
C2.st.1	75	2-5	0,16								
C3.st.1	120	0-1	0,25	n.a.	n.a.	n.a.	n.a.	n.a.	n.a.	0,60481382	24,90656
C3.st.1	120	1-2	0,13								
C4.st.1	120	0-1	0,57								
C4.st.1	120	1-2	0,10								
C4.st.1	120	2-5	0,25								
C4.ex.1	50	0-1	0,19								
C5.st.1	100	0-1	0,29	0,50842	n.a.	0,771298	0,669278	0,84649925	1,851246	0,63340876	24,83895
C5.st.1	100	1-2	0,79								
C5.st.1	100	2-5	1,49								
C5.ex.1	25	0-1	0,81								
C5.ex.1	25	1-2	0,27								
C6.st.1	100	0-1	0,71	0,704031	n.a.	1,44522	1,233246	n.a.	n.a.	2,60152232	19,59406
C6.st.1	100	1-2	0,17								
C6.ex.1	25	0-1	0,16								
C6.ex.1	25	1-2	0,69								
C7.st.1	100	0-1	0,20	1,141511	n.a.	0,587117	0,743908	1,06352902	0,816794	1,29808681	22,4758
C7.st.1	100	1-2	0,79								
C7.ex.1	50	0-1	0,15								
C7.ex.1	50	1-2	1,09								
C8.st.1	100	0-1	0,52	0,723211	0,613467	0,691679	0,75	0,51554964	1,669395	1,7270109	15,46395
C8.st.1	100	1-2	0,26								
C8.ex.1	50	0-1	0,22								
C8.ex.1	50	1-2	0,23								
C8.ex.1	50	2-5	0,65								
C9.st.1	75	0-1	0,39	0,749584	0,549944	1,424807	0,774369	n.a.	0,735715	2,46903929	24,76173
C9.st.1	75	1-2	0,41								

**APPENDIX E**  
**SOLUBLE SALTS OF STONES**  
**(CONDUCTIVITY RESULTS)**

Sample	Conductivity of the solutions (%)
A.so.1	0,58
A.so.2	0,865
C2.so.1	0,605
C4.so.1	0,545
C5.so.1	0,505
C6.so.1	0,425
C7.so.1	0,425
C8.so.1	0,47
C9.so.1	0,38

**APPENDIX F**

**CHEMICAL COMPOSITIONS OF SOILS**

**(EDS RESULTS)**

SAMPLE	Na <sub>2</sub> O	MgO	Al <sub>2</sub> O <sub>3</sub>	SiO <sub>2</sub>	P <sub>2</sub> O <sub>5</sub>	SO <sub>3</sub>	K <sub>2</sub> O	FeO	CaO
A.so.1	0,50	3,63	13,69	44,17	1,37	0,25	2,77	5,78	27,83
A.so.2	0,39	3,19	9,99	32,51	1,62	0,37	2,50	4,03	45,39
C2.so.1	0,53	3,37	13,26	45,05	1,97	0,26	2,96	5,58	27,03
C4.so.1	0,59	3,65	15,31	47,15	1,76	0,27	3,10	6,48	21,69
C5.so.1	0,60	3,53	13,48	42,45	1,47	0,17	2,64	6,14	29,54
C6.so.1	0,57	3,58	14,69	48,21	2,19	0,11	3,16	5,94	21,56
C7.so.1	0,49	3,49	13,97	49,99	2,61	0,37	2,95	6,29	19,83
C8.so.1	0,40	3,90	12,80	41,34	1,22	0,17	2,47	5,62	32,08
C9.so.1	0,46	3,55	14,83	48,77	1,94	0,09	3,15	6,14	21,05

## APPENDIX G

### MICROBIOLOGY RESULTS

Sample code	Bacteria Phylum
C8.st.1	Proteobacteria, Actinobacteria, Firmicutes, Bacteroidetes, others
C2.st.2	Proteobacteria, Actinobacteria, Cyanobacteria, others
C2.in.2	Proteobacteria, Actinobacteria, Firmicutes, others
C9.st.1	Proteobacteria, Actinobacteria, Bacteroidetes, Cyanobacteria, Acidobacteria, others
C7.st.1	Proteobacteria, Actinobacteria, Bacteroidetes, Acidobacteria, others
C7.ex.1	Proteobacteria, Actinobacteria, Firmicutes, Bacteroidetes, others
C5.ex.1	Proteobacteria, Actinobacteria, Firmicutes, Bacteroidetes, others
A.st.1	Proteobacteria, Actinobacteria, Bacteroidetes, others
A.st.3	Proteobacteria, Actinobacteria, Firmicutes, Bacteroidetes, Rhodothermaeota, Euryarchaeota, others
C1.st.1	Proteobacteria, Actinobacteria, Cyanobacteria, Bacteroidetes, Deinococcus-Thermus, others
C5.st.1	Proteobacteria, Actinobacteria, Bacteroidetes, others
C6.in.1	Proteobacteria, Actinobacteria, others
C6.st.1	Proteobacteria, Actinobacteria, Bacteroidetes, Acidobacteria, others
C3.st.2	Proteobacteria, Actinobacteria, Bacteroidetes, others
C3.st.3	Proteobacteria, Actinobacteria, Bacteroidetes, Acidobacteria, others



Sample code	Bacteria Classes
C8.st.1	Actinobacteria, Chitinophagia, Bacilli, Gammaproteobacteria, others
C2.st.2	Actinobacteria, Alphaproteobacteria, Oscillatoriophycidae, Nostocales, Chroococcidiopsidales, Oscillatoriophycidae, others
C2.in.2	Actinobacteria, Rubrobacteria, Alphaproteobacteria, Acidimicrobia, others
C9.st.1	Actinobacteria, Oscillatoriophycidae, Rubrobacteria, Alphaproteobacteria, Blastocatellia, Acidimicrobia, Cytophagia, others
C7.st.1	Actinobacteria, Blastocatellia, Rubrobacteria, Alphaproteobacteria, others
C7.ex.1	Actinobacteria, Bacilli, Alphaproteobacteria, Gammaproteobacteria, others
C5.ex.1	Actinobacteria, Bacilli, Alphaproteobacteria, Cytophagia, Flavobacteria, Clostridia, Gammaproteobacteria, others
A.st.1	Actinobacteria, Cytophagia, Alphaproteobacteria, others
A.st.3	Stenosarchaea grubu, Actinobacteria, Rubrobacteria, Bacilli, Rhodothermia, Flavobacteria, others
C1.st.1	Actinobacteria, Rubrobacteria, Deinococci, Alphaproteobacteria, Cytophagia, Chroococcidiopsidales, others
C5.st.1	Actinobacteria, Rubrobacteria, Alphaproteobacteria, others
C6.in.1	Actinobacteria, Thermoleophilia, Rubrobacteria, Alphaproteobacteria, others
C6.st.1	Actinobacteria, Blastocatellia, Cytophagia, Alphaproteobacteria, Deinococci, Chroococcidiopsidales, others
C3.st.2	Actinobacteria, Cytophagia, Alphaproteobacteria, others
C3.st.3	Actinobacteria, Rubrobacteria, Blastocatellia, Thermoleophilia, Cytophagia, Alphaproteobacteria, others

Sample code	Bacteria Genera
C8.st.1	Trueperella, Lactobacillus, Sphingomonas, others
C2.st.2	Kineosporia, Crossiella, Rubrobacter, Aliterella Antarctica, Loriellopsis cavernicola, Aerosakkonema, Bartonella, Chelativorans, Rubellimicrobium, Acidisoma, Sphingobium, Sphingomonas, others
C2.in.2	Illumatobacter, Blastococcus, Geodermatophilus, Klenkia, Janibacter, Arthrobacter, Nocardioides, Rubrobacter, Bacillus, Lactobacillus, Bartonella, Chelativorans, Oceanicella, Blastomonas, Sphingomonas, others
C9.st.1	Blastocatella, Brevitalea, Illumatobacter, Actinoplanes, Kribbella, Microlunatus, Pseudonocardia, Gaiella, Rubrobacter, Adhaeribacter, Aerosakkonema, Enterovirga, Rubellimicrobium, Acidisphaera, Sphingobium, Sphingomonas, others
C7.st.1	Aridibacter, Blastocatella, Kineosporia, Marmoricola, Crossiella, Rubrobacter, Flavisolibacter, Chelatococcus, Chelativorans, Rubellimicrobium, Craurococcus, Sphingomonas, others
C7.ex.1	Blastococcus, Modestobacter, Knoellia, Arthrobacter, Pseudarthrobacter, Rubrobacter, Bacillus, Lactobacillus, Bartonella, others
C5.ex.1	Lawsonella, Lactobacillus, Bartonella, Sphingobium, Vibrio, others
A.st.1	Blastococcus, Kineococcus, Kineosporia, Actinoplanes, Actinomycetospora, Hymenobacter, Rubellimicrobium, Acidisoma, Acidisphaera, Sphingobium, Sphingomonas, others
A.st.3	Halococcaceae, Frankia, Motilibacter, Modestobacter, Allokutzneria, Rubrobacter, Salinimicrobium, Bartonella, Rubrivirga, others
C1.st.1	Blastococcus, Kineosporia, Nakamurella, Microlunatus, Actinomycetospora, Rubrobacter, Hymenobacter, Aliterella Antarctica, Deinococcus, Bartonella, Alsobacter, Rubellimicrobium, others
C5.st.1	Rubrobacter, Bartonella, others
C6.in.1	Cryptosporangium, Kineococcus, Kineosporia, Pseudarthrobacter, Marmoricola, Crossiella, Gaiella, Rubrobacter, Solirubrobacter, Methylobacterium, Chelativorans, Rubellimicrobium, Acidicaldus, Craurococcus, Sphingomonas, others
C6.st.1	Blastocatella, Blastococcus, Kineococcus, Kineosporia, Nakamurella, Actinoalloteichus, Crossiella, Hymenobacter, Aliterella Antarctica, Rubellimicrobium, Acidicaldus, Craurococcus, Sphingomonas, others
C3.st.2	Kineococcus, Actinoplanes, Actinoalloteichus, Hymenobacter, Phenylbacterium, Methylobacterium, Rubellimicrobium, Acidisoma, Acidisphaera, Sphingobium, Sphingomonas, others
C3.st.3	Blastocatella, Kineococcus, Kribbella, Nocardioides, Pseudonocardia, Rubrobacter, Solirubrobacter, Hymenobacter, Rubellimicrobium, Acidicaldus, Acidisoma, Roseomonas, Sphingomonas, others

# VITA

**Surname, Name:** İpekci, Emre

## **Education:**

**Ph.D.**, Architectural Restoration, Izmir Institute of Technology, Izmir, Turkey (2021)

Thesis: Evaluation of stone deterioration problems of Anavarza Archaeological Site for the purpose of conservation

**Research grant**, YUDAB - International Research Scholarships for Research Assistants, Delft University of Technology (TU Delft), the Netherlands, 2020-2021.

Project: Investigation of the role of salts in the decay of the limestones from the archeological site of Anavarza

**Research grant**, TUBITAK 1001 - the Scientific and Technological Research Projects Funding Program, Turkey, 2018-2020.

Project: Investigation of biodegradation in stone material in the Ancient City of Anavarza (Anzarbos)

**M.Sc.**, Architectural Restoration, Izmir Institute of Technology, Izmir, Turkey (2016)

Thesis: Plaster characteristics of Çinili Hamam built by Mimar Sinan in İstanbul

**Exchange student**, Università degli Studi di Napoli Federico II, Napoli, Italy (2015)

**B.Arch.**, Architecture, Uludag University, Bursa, Turkey (2013)

## **Work Experience:**

**Research Assistant**, Department of Conservation and Restoration of Cultural Heritage, Faculty of Architecture, Izmir Institute of Technology, Izmir, Turkey (Jan 2015-Dec 2021)

**Researcher**, Department of Architectural Engineering + Technology, Faculty of Architecture and the Built Environment, TU Delft, Delft, the Netherlands (Feb 2020-Feb 2021)

**Architect**, Leo Design, Bursa, Turkey (Sept 2011-Jan 2014)